

The University of Maine

DigitalCommons@UMaine

Electronic Theses and Dissertations

Fogler Library

Summer 8-23-2019

Exploring Different Peripheral Nociceptive Input Underlying Ongoing and Movement Evoked Cancer-Induced Bone Pain

Joshua Havelin

University of Maine, joshua.havelin@maine.edu

Follow this and additional works at: <https://digitalcommons.library.umaine.edu/etd>

Recommended Citation

Havelin, Joshua, "Exploring Different Peripheral Nociceptive Input Underlying Ongoing and Movement Evoked Cancer-Induced Bone Pain" (2019). *Electronic Theses and Dissertations*. 3098.

<https://digitalcommons.library.umaine.edu/etd/3098>

This Open-Access Thesis is brought to you for free and open access by DigitalCommons@UMaine. It has been accepted for inclusion in Electronic Theses and Dissertations by an authorized administrator of DigitalCommons@UMaine. For more information, please contact um.library.technical.services@maine.edu.

**EXPLORING DIFFERENT PERIPHERAL NOCICEPTIVE INPUT UNDERLYING
ONGOING AND MOVEMENT EVOKED CANCER-INDUCED BONE PAIN**

By

Joshua Havelin

B.S. University of New England, 2011

A DISSERTATION

Submitted in Partial Fulfillment of the

Requirements for the Degree of

Doctor of Philosophy

(in Biomedical Sciences)

The Graduate School

The University of Maine

August 2019

Advisory Committee:

Tamara King Deeny, Associate Professor, University of New England, Advisor

Ian Meng, Professor, University of New England

Derek Molliver, Associate Professor, University of New England

Robert Burgess, Professor, The Jackson Laboratory

Edward Bilsky, Provost/Chief Academic Officer, Pacific Northwestern University

Copyright 2019 Joshua Havelin

All Rights Reserved

**EXPLORING DIFFERENT PERIPHERAL NOCICEPTIVE INPUT UNDERLYING
ONGOING AND MOVEMENT EVOKED CANCER-INDUCED BONE PAIN**

By Joshua Havelin

Dissertation Advisor: Dr. Tamara King Deeny

An Abstract of the Dissertation Presented
in Partial Fulfillment of the Requirements for the
Degree of Doctor of Philosophy
(in Biomedical Sciences)
August 2019

Cancer-induced bone pain is reported to be one of the most detrimental aspects of the disease, often broadly categorized into two separate pain phenomena. Patients experience ongoing pain, a dull achy persistent background pain that worsens as disease progresses which is currently treated with around the clock mu opioid receptor (MOR) agonists such as morphine. Patients also report transient episodes of severe pain that is spontaneous but often triggered by movement that “breaks through” around the clock medication. Breakthrough pain is treated with additional rapid onset MOR agonists that are hindered by dose-limiting side effects and often misalign with treatment for patients. The failure of current medications to effectively treat patients and undesirable side effects of MOR agonists highlights the need to develop novel treatments. We examined the hypothesis that ongoing pain and breakthrough pain are mitigated by unique populations of sensory afferents.

Utilizing a rat model of cancer-induced bone pain (CIBP) that implants MATBIII adenocarcinoma cells into the tibia of Fischer rats, we demonstrate that IB4-binding fibers play a critical role in transducing breakthrough pain, whereas TRPV1 expressing fibers do not. Limitations of the chemo-ablative approach used to target these neurons directed work to a

mouse model of CIBP that relies on implantation of Lewis lung carcinoma cells into the femur of C57BL/6 mice. Utilizing Nav1.8-Cre and MrgD-Cre-ERT2 mouse lines, targeted expression of the light sensitive proton pump ArchT allowed for the inhibition of neurons in animals with CIBP. Using conditioned place preference to pain relief, we demonstrate that inhibition of Nav1.8 fibers relieves ongoing pain, and silencing MrgD fibers in tumor-bearing animals results in conditioned place preference. We also describe a potential approach to measure breakthrough pain in the mouse, but did not characterize it. This work provides evidence to target these populations of sensory neurons to develop treatments in an effort to reduce and treat cancer-induced ongoing and breakthrough pain. The implication of non-peptidergic neurons to convey components of cancer-induced bone pain is a novel finding and distinguishes them for a unique role in CIBP from other work in the pain field.

DEDICATION

To my family and friends, all of you who have advised, trained, guided, entertained, supported, tolerated and listened to me complain over the past 5-10 years. First and foremost, my loving and patient fiancé Dr. Jennifer Cormier who began this adventure with me, and has always encouraged me to be a “glass half full” kind of person. Rather than my normal demeanor of “this glass is half full of poison”. It has been an indescribable pleasure to share the past 7 years with you and grow as individuals together, hopefully now I can divert my attention to wedding planning. My parents, Anne and George Havelin for teaching me to finish the things you start, and although I ignore your advice sometimes, there are likely no two-other people on earth who know me better and push me to do the things I often times don’t want to. Hopefully from now on phone calls on my drive home can be more focused on planning fishing trips rather than being frustrated with school. My brother Zachary Havelin for never giving up on me and being, an albeit at times, a disagreeable distraction, the best guide I’ve had while adventuring through the wonderful state of Maine. My friend, mentor, fellow outdoorsmen, and perhaps one-day colleague, Dr. Alexander Skorput for being a constant point of reference and advice in the woods, on the water, and in the lab for 10 years. Cheers to looking forward to more adventures in the future. Lastly, my committee members for being a continual source of inspiration, supportive wealth of knowledge and direction, and serving as examples of the kind, patient, caring, and welcoming adult and professional I would like to be.

ACKNOWLEDGEMENTS

Foremost, I would like to thank my advisor and mentor, Dr. Tamara King Deeny, for the continuous patience and support over the past 7 to 8 years, to help me grow both in the lab and as a person, and to help drive home the lesson to be kind and understanding, always. Dr. Derek Molliver for entertaining, although sometimes crushing, my wild ideas and questions with hard facts and citable references. My only regret is not taking you up on the boogey boarding in San Diego. Dr. Ian Meng who has been a continual source of inspiration in supporting the growth of people around us as individuals, and for going outside of his comfort zone and going trap shooting with my mother, brother and I. Dr. Robert Burgess for being a steadfast pillar, and discussing at length why dropping out within the first two semesters of my time in the GSBSE program could potentially be a short sighted choice, and for giving me all the right reasons to stay. Of my committee members, lastly, but by far not the least, Dr. Edward Bilsky and his family for being the starting point for my adventure in neuroscience and pain research, and for being a mentor both professionally and personally for over a decade. I would by no means be where I am today had you not accepted me into your lab as an undergraduate, and overlooked the naiveties and “energetic” nights of my younger years.

This work has been supported by the University of Maine, Graduate School of Biomedical Science and Engineering; UMaine’s INBRE program; NIHP20GM103643 (Ian Meng and Tamara King).

I would like to thank a number of members of the University of New England’s research team and group. Firstly, an immensely large thank you for the tremendous amount of help and imaging guidance to Pete Caradonna. Who would have thought we’d end up here after *that* night during your freshman year? Denise Giuvelis for always being a reliable friend and

colleague to discuss reasons why mice do and don't behave the way we want them to, and running plans. Ivy Berquist for keeping me up to date and in-line with animal care, and sharing some great beers over the past several years. Jamie Vaughn for helping me learn as much as I could about maintaining multiple colonies of mice, and running samples in the capacity of the genotyping core. Ramaz Geguchadze and Diana Goode for teaching me the tedious art of dissecting mouse dorsal root ganglia. Neal Mecum for always, always, being ready to share a beer and a complaint or two about research and all of its glaring shortcomings, while acknowledging all the reasons we both keep coming back for more punishment. I look forward to the days when we can talk more about fishing and brewing than day-to-day life in the lab. Lastly, a very large thank you to my very good friend Chad Lyons for humoring me, and others in my presence, about how life goes on and the ways it will improve after school. Thank you all over the past 11 years for keeping me around!

TABLE OF CONTENTS

DEDICATION	iii
ACKNOWLEDGEMENTS	iv
LIST OF TABLES	xi
LIST OF FIGURES	xii
LIST OF ABBREVIATIONS.....	xiv
Chapter	
1. INTRODUCTION TO CANCER-INDUCED BONE PAIN	1
1. Introduction.....	1
1.1. Preface, Etiology of Cancer-induced Bone Pain.....	1
1.2. Contributions of Preclinical Models to the Neurobiology of Bone Pain.....	9
1.2.1. Introduction	9
1.2.2. Overview of the Pain Pathway	10
1.2.3. Initiation of Pain Signals from the Bone and Joint	15
1.2.4. Site of Injury or Pathology.....	19
1.2.5. Sensitization	22
1.2.6. Descending Pain Modulation	25
1.2.7. Conclusion	26
1.3. Preclinical Models of Cancer-induced Bone Pain	27
1.4. Known Mechanisms Driving Cancer-induced Bone Pain	32
2. MEDIATION OF MOVEMENT-INDUCED BREAKTHROUGH CANCER PAIN BY IB4-BINDING	
NOCICEPTORS IN RATS.....	41
2.1. Abstract	41
2.2. Introduction.....	42

2.3. Materials and Methods	44
2.3.1. Animal Care	44
2.3.2. Cell Line Maintenance	44
2.3.3. Surgical Procedures and Drug Treatment	44
2.3.4. Behavioral Measures	50
2.3.5. Radiograph Analysis of Disease Progression	53
2.3.6. Statistical Analysis	54
2.4. Results	56
2.4.1 Tumor-induced Bone Loss, Tactile Hypersensitivity, and Impaired Limb Use	56
2.4.2. Movement-induced Pain Induces CPA That Breaks Through Morphine Infusion	57
2.4.3. Blockade of Sensory Afferent Input from Tibia Prevents, But Does Not Reverse Movement-induced BTP	59
2.4.4. Spinal Capsaicin Eliminates TRPV1, SP, CGRP Immunofluorescence and IB4-SAP Diminishes IB4 Immunofluorescence in the Spinal Cord Dorsal Horn	61
2.4.5. Functional Blockade of IB4-binding, not TRPV1-expressing Fibers Blocks BTP	63
2.4.6. Ablation of IB4 or TRPV1-expressing Fibers Did Not Alter Tumor-induced Bone Remodeling	66
2.5. Discussion	66
2.5.1. Reverse Translation of BT Pain	67
2.5.2. Potential Role of Peripheral and Central Sensitization	68

2.5.3. Mechanistic Difference Between Initiation and Maintenance of BTP	68
2.5.4. Separate Roles of TRPV1+ and IB4-Binding Fibers in BT Pain.....	69
2.6. Acknowledgments	72
3. UTILIZING OPTOGENETICS TO INVESTIGATE THE ROLE OF PERIPHERAL NEURONS INVOLVED IN CANCER-INDUCED BONE PAIN IN THE MOUSE	74
3.1. Introduction.....	74
3.1.1 Background of Fiber Types in Cancer-induced Bone Pain	74
3.1.2. Justification of Targeting Subpopulations of Sensory Neurons.....	76
3.1.3. Brief Overview of Utility of Optogenetics in the Study of Pain	82
3.2. Materials and Methods	88
3.2.1. LLC Cell Line Maintenance.....	88
3.2.2. Animal Care and Treatment	88
3.2.3. Transgenic Mouse Lines and Crosses	88
3.2.4. Genotyping of Mouse Lines.....	90
3.2.5. Surgical Procedures and Manipulations.....	91
3.2.6. Behavioral Assays and Observations.....	98
3.2.7. Tissue Collection and Immunohistochemical Staining for Verification of MrgD ^{CRE-ERT2} Mouse Line.....	105
3.2.8. Statistical Analysis and Graphing	106
3.3. Results	109
3.3.1. Classical Cancer-induced Measures of Pain	109
3.3.2. DAMGO Induced Pain Relief, and Failure of Deltorphin II to Relieve Ongoing Pain	113
3.3.3. Evaluation of Tdtomato Expression in MrgD ^{CRE-ERT2} Mouse Line.....	115

3.3.4. Evaluation of Delivery and Activation of Undiluted AAV2/8 ArchT Viral Vector in MrgD-tdtomato Positive Cells.....	116
3.3.5. Fiber Optic Implant Quality Assurance and Surgical Implant Challenges.....	117
3.3.6. Successful Optogenetic Blockade of AITC Induced Nocifensive Behaviors in Nav1.8 and MrgD Expressing Fibers.....	117
3.3.7. ArchT Expression in Animals from Nav1.8 and MrgD cre Mouse Lines.....	119
3.3.8. ArchT Induced Silencing of Nav1.8 Fibers Relieves Cancer-induced Ongoing Pain, and ArchT Induced Silencing of MrgD Fibers in Animals with Cancer Induces CPP	120
3.3.9. Failure to Induce CPA to Hind Limb Movement in Cancer Treated Animals, and Alternative Behavioral Measures Affected by Hind Limb Movement.....	122
3.4. Discussion	126
3.4.1. Classical Measures of CIBP	127
3.4.2. Efficacy of MOR Agonist to Alleviate Ongoing CIBP	128
3.4.3. Efficacy of Virally Delivered ArchT to Block AITC Induced Nociceptive Behaviors.....	129
3.4.4. The Role of Subsets of Nociceptive Fibers in Cancer-induced Ongoing Pain	131
3.4.5. Inability to Establish CPA to Hind Limb Movement in the Mouse and Potential Alternative Measures of Hind Limb Movement-induced Pain.....	136
3.5. Conclusion	138
4. DISCUSSION OF FINDINGS	139
4.1. Summary of Results	139
4.2. Major Findings.....	140

4.3. Limitations and Lingering Questions	148
4.4. Future Directions	151
4.5. Concluding Remarks	153
BIBLIOGRAPHY.....	154
BIOGRAPHY OF THE AUTHOR.....	178

LIST OF TABLES

Table 1.1. Nomenclature Commonly Used for Peptidergic and Non-peptidergic Fibers 12

Table 2.1. Numbers of Sections Analyzed for Staining Intensity..... 50

Table 2.2. Statistical Analysis Results for ANOVA 55

Table 3.1. Statistical Analysis of Results 108

LIST OF FIGURES

Figure 2.1.	Tumor-induced Bone Remodeling, Referred Pain and Impaired Limb Use	56
Figure 2.2.	Hindpaw Movement Induces Breakthrough Pain in the Presence of Morphine	58
Figure 2.3.	Movement-induced Breakthrough Pain is Prevented, but not Reversed, by Saphenous Lidocaine	60
Figure 2.4.	Capsaicin Eliminates TRPV1, SP and CGRP Immunofluorescent Staining and IB4-SAP Diminishes Immunofluorescence in the Spin Dorsal Horn	62
Figure 2.5.	Tactile Hypersensitivity and Movement-induced Breakthrough Pain is Dependent on IB4 Positive Fibers.....	65
Figure 2.6.	Tumor-induced Bone Loss is Observed in all Tumor-bearing Rats Irrespective of Treatment.....	66
Figure 3.1.	Verification of Fiber Optic Output and Implant Placement	97
Figure 3.2.	Potential Overlap in the Mrgprd (MrgD) and Trpa1 (TRPA1) Expressing Cells In the DRG.....	100
Figure 3.3.	Representative Images of Condition Place Preference (CPP) Boxes and CPP Paradigm.....	103
Figure 3.4.	Radiographic Images Demonstrating Tumor Induced Bone Loss	110
Figure 3.5.	Classical Measures of Cancer-induced Bone Pain.....	111
Figure 3.6.	Additional Measures of Cancer-induced Behavioral Changes in Female Mice over 5 minutes Observation Period	113
Figure 3.7.	Pharmacologically Induced Pain Relief of Cancer-induced Pain by MOR Agonist DAMGO but not DOR Agonist Deltorphin II.....	114
Figure 3.8.	Representative Immunohistochemical Screening of MrgD-tdtomato Animals.....	115

Figure 3.9. Successful Transfection of MrgD Cell Bodies with ArchT-eGFP Flex Virus and Trafficking to Afferent Terminals in the Spinal Cord Dorsal Horn	116
Figure 3.10. Activation of Virally Delivered ArchT in Both Nav1.8 and MrgD Afferents Blocks AITC-Induced Nocifensive Behaviors	118
Figure 3.11. Expression Patterns of Cre-activated ArchT-eGFP from Ai40D Transgenic Mice ..	120
Figure 3.12. ArchT Induced Silencing of Nav1.8 Fibers Causes Relief of Ongoing Pain and ArchT Induced Silencing of MrgD Fibers in Cancer Animals Results in CPP	122
Figure 3.13. Failure of Hind Limb Movement to Induce CPA in Cancer Afflicted C57BL/6 Wild Type Mice	124
Figure 3.14 Hind Limb Movement Induced Decrease in Distance Travelled and Rearing Behavior	125
Figure 3.15 Altered Locomotor Behaviors from Cancer and Movement of the Cancer Afflicted Hind Limb	126
Figure 3.16 Demonstrable Overlap inRNAseq Data of Sensory Neurons	133

LIST OF ABBREVIATIONS

- ADP:** adenosine diphosphate
- Arch:** archaerhodopsin from *Halorubrum sodomense*
- ArchT:** archaerhodopsin from *Halorubrum* strain TP009
- ATF3:** activated transcription factor 3
- ATP:** adenosine triphosphate
- BDNF:** brain derived neurotrophic factor
- BTP:** breakthrough pain
- C-LTMRs:** c fiber – low threshold mechanoreceptors
- CGRP:** calcitonin gene-related peptide
- CIBP:** cancer-induced bone pain
- CPP:** conditioned place preference
- DOR:** delta opioid receptor
- DRG:** dorsal root ganglia
- ED50:** effective dose to reach 50% of desired effect
- eGFP:** enhanced green fluorescent protein
- GABA:** gamma-aminobutyric acid
- GDNF:** glial cell-line derived neurotrophic factor
- GFPA:** glial fibrillary acidic protein
- GPCR:** G protein coupled receptor
- i.v.:** intravenous
- IASP:** International association for the study of pain

IB4: isolectin B4

IGF: Insulin-like growth factor

IHC: immunohistochemical

IL1-Beta: interleukin-beta 1

IL6: interleukin 6

LLC: Lewis lung carcinoma

LMA: locomotor assay

MOR: Mu opioid receptor

mPGES-1: microsomal prostaglandin E synthase -1

MrgD: mas-related G-coupled protein sub family D

Nav1.8: voltage gated sodium channel 1.8

NGF: nerve growth factor

NK-1: neurokinin receptor 1

NSAIDS: nonsteroidal anti-inflammatory drugs

OPG: osteoprotegerin

P2X3: purinergic receptor P2X3

p38-MAPK: p38 mitogen activated protein kinases

PBS: phosphate buffered saline

PBSTx: PBS containing 0.1% triton detergent

pERK: phosphorylated extracellular receptor kinase

PFA: paraformaldehyde

PGE2: prostaglandin E2

RANK-L: RANK-ligand

RANK: receptor activator of nuclear factor kappa B

RNA: ribonucleic acid

RTX: resiniferotoxin

RVM: rostroventromedial medulla

s.c.: subcutaneous

SP: substance P

TG: trigeminal ganglia

TH: tyrosine hydroxylase

TNF-alpha: tumor necrosis factor alpha

VEGF: vascular growth factor

CHAPTER 1

INTRODUCTION TO CANCER-INDUCED BONE PAIN

1. Introduction

1.1. Preface, Etiology of Cancer-Induced Bone Pain

It is well known and established that common cancers such as breast, prostate and lung have a propensity to metastasize to the bone (Coleman 2006, Lozano-Ondoua, Symons-Liguori et al. 2013, Kane, Hoskin et al. 2015). It is estimated that nearly 70% of patients that die as a result of their cancer have bone metastasis, with the most common sites of cancer metastasis being the vertebrae, pelvis long bones and ribs (Kane, Hoskin et al. 2015). Estimates place the incidence of patients suffering from cancer or a history of cancer in America at 14.5 million in 2015 and nearly 32.6 million worldwide in 2012 (Smith and Saiki 2015). Reports also suggest that nearly all patients with myeloma, more than half with metastatic breast and prostate cancer and a third of patients with lung cancer develop metastasis to the bone (Gul, Sendur et al. 2016).

Upon metastasis these lines of cancer often have differential effects on the bone following their establishment and development of unique tumor microenvironments (Mantyh 2014, Mantyh 2014). The origin of these tumors induces varying, but characterized effects on the bone. For example, metastases of lung origin lean towards bone degradation or osteolytic lesions, breast cancer metastases typically induce a range of maladaptive bone remodeling that results in osteolytic lesions as well as maladaptive osteoblastic lesions (Mantyh 2006)). Metastases of prostate origin typically have maladaptive bone deposition and remodeling, or osteoblastic lesions (Mantyh 2006). The maladaptive bone remodeling that occurs in patients is often, but not always accompanied by pain that originates from the sites of metastasis and bone

remodeling (Mantyh 2014, Mantyh 2014, Kane, Hoskin et al. 2015). Nearly two-thirds of patients with metastasis have been reported to experience severe pain (Mantyh 2006). While more broadly, 34% of patients who are hospitalized with cancer and 45% of patients enrolled in in-home care report pain (Scarpi, Calistri et al. 2014). In fact, pain originating from a site of tumor growth or metastasis is typically one of the first symptoms that draws patients to the clinic and nearly half of patients with cancer report moderate to severe pain (Halvorson, Kubota et al. 2005, Kane, Hoskin et al. 2015, Paice 2018).

Pain is often reported by patients to be one of the worst or most feared consequences of these ailments (Paice 2018, Paice 2018). Despite improvements in pain management and improved understanding of CIBP, patients continue to suffer from inadequate pain management (Paice 2018, Paice 2018). From the perspective of the field as well as patients, this is worsened by the increased survival time of patients, due to improvements in cancer treatments, patients live longer with these maladaptive bone pathologies (Lozano-Ondoua, Hanlon et al. 2013, Lozano-Ondoua, Symons-Liguori et al. 2013, Kane, Hoskin et al. 2015, Paice 2018, Paice 2018). Patients' reports typically describe two separate pain phenotypes, that as the disease progresses are both treated with the same class of analgesics. The first and more prominent pain phenotype is a dull-achy type of pain from the site of remodeling/metastasis that is constant and worsens as the disease progresses and/or time goes on. Due to the description of the pain and its nature, this is referred to as ongoing pain.

This is treated in accordance with the World Health Organization's "Ladder" of analgesia that begins with non-steroidal anti-inflammatory drugs (NSAIDs) to treat the pain patients experience. This is escalated in response to the worsening of pain reported by the patient, to adding adjuvant treatments in addition to NSAIDs, followed by "weak" opioids such as tramadol, codeine and buprenorphine, but ultimately escalates to around the clock mu opioid receptor

(MOR) agonists such as morphine (Sabino and Mantyh 2005, Mantyh 2006, Kane, Hoskin et al. 2015). The last step on the ladder allows for additional administration of adjuvant drugs to manage fear and anxiety, however this may introduce complications with chronic opioid regimens (Bruera and Paice 2015, Kane, Hoskin et al. 2015) .

This escalation occurs in an attempt to mitigate background pain to a level that can allow patients to still retain a positive quality of life. However, some patients' doses are escalated to a point where the treatments (high doses of MOR agonists) detrimentally affect the patient's quality of life themselves. Proper management of this requires a skilled and vigilant team of medical professionals to adequately titrate and prescribe analgesics (Bruera and Paice 2015). In addition to this, patients often have to be prescribed additional compensatory compounds, such as laxatives early in analgesic prescription to manage the more prominent side-effects of opioid therapy such as constipation (Bruera and Paice 2015). Treating patients afflicted with CIBP can be difficult even after following well described practices, requiring multiple visits to titrate dosing as well as identifying tolerable MOR agonist agents (Bruera and Paice 2015, Smith and Saiki 2015). Another challenge is adequate education of clinicians in successful pain management. Reports suggest that clinicians in the most optimal position to manage a patient's pain, receive inadequate training to do so (Smith and Saiki 2015). Even while practices exist and continue to improve, estimates still place nearly 50% of patients with under managed pain (Smith and Saiki 2015). Development of tolerance to MOR agonists that patients likely develop also leads to escalation of doses of treatments. While not directly assessing the outcomes in patients with CIBP, there is mounting evidence that MOR agonists themselves do not effectively treat vary forms of chronic pain (Morrone, Scuteri et al. 2017). Following in the footsteps of the larger pain research community, these limitations of MOR agonists drives those of us working to find better treatments for advanced and difficult pain types, and to question if

it is responsible to continue to rely so heavily on treatment of pain with chronic regimens of MOR agonists. This is further complicated at this point in time by the opioid overuse epidemic, which correlative studies suggest has directly affected patients suffering from CIBP, resulting in decreased prescriptions for patients who have no alternative to manage their pain (Paice 2018).

Some clinical reports argue that treatment of ongoing pain with MOR agonists are sufficient and ample at reducing pain and improving quality of life, while it is widely accepted that a better alternative is necessary for patients (Mantyh 2006, Schmidt 2015, Mercadante and Bruera 2016). Best clinical practice aims to treat each individual patient while maintaining open dialogue to allow changes in treatment dependent on the needs of the individual (Bruera and Paice 2015). One practice used in the clinic known as “opioid switching”, a practice that nearly 80% of patients will require, involves the rotation or switching between different MOR agonists to achieve therapeutic levels of pain relief while minimizing side-effects (Bruera and Paice 2015, Mercadante and Bruera 2016). Some work suggests that this practice can reduce, but not eliminate adverse side effects in as many as 50-90% of patients (Mercadante and Bruera 2016). This is not completely understood, and attempts to underpin a genetic correlation have provided no target single nucleotide polymorphisms supporting a cause for the exacerbated pain from CIBP, or the need to switch certain individuals from one MOR agonist to another (Scarpi, Calistri et al. 2014). This leads to a best practice of tailoring dosing regimens and therapies to fit the needs of the individual rather than treating patients as a whole, another detail highlighting why CIBP is “one of the most difficult chronic pains to treat” (Mantyh 2014, Mantyh 2014). These limitations of the current approach to treating patients with CIBP highlight why research continues to attempt to find alternatives to MOR agonists to treat intense pain.

In addition, and perhaps alternatively to MOR agonists, patients are treated with radiotherapy, and agents that actively block cancer-induced bone remodeling to stay ongoing

pain from sites of pathological bone remodeling, which have varying degrees of success (Kane, Hoskin et al. 2015). Bisphosphonates have been demonstrated to bind to bone and actively block osteoclast induced bone destruction through osteoclast induced cell death (Drake, Clarke et al. 2008, Mantyh 2014, Mantyh 2014). Osteoprotegerin (OPG) and denosumab both target and block the receptor activator of nuclear factor kappa B (RANK) and RANK-ligand (RANKL) pathway that induces osteoclast activation. This approach has been demonstrated to effectively block pathological osteoclast induced bone-remodeling, which by blocking bone remodeling resolves some aspects of pain from sites of metastasis, but these treatments have restrictive side-effects of their own (Mantyh 2014, Mantyh 2014, Gul, Sendur et al. 2016).

Studies indicate that these compounds reduce skeletal pain and delay skeletal related events such as hypercalcemia and fracture, some of the factors that are believed to induce pain from the bone, but have room for improvement (Coleman 2008, Mantyh 2014, Mantyh 2014). While effective at reducing pathological bone resorption in a number of skeletal diseases, bisphosphonates have been associated with several undesirable side-effects that can lead to discontinued use. The first being gastrointestinal disturbance including erosive esophagitis if taken improperly, and potentially nausea, dyspepsia, abdominal pain and gastritis (Kennel and Drake 2009). Initial exposure to bisphosphonates may also induce temporary fever, however this occurrence reduces after multiple exposures and is believed to be temporary (Kennel and Drake 2009). Severe suppression of bone turn over and the requirement for adequate vitamin D and calcium supplementation are also considerations for patients undergoing chronic bisphosphonate therapy (Kennel and Drake 2009). Lastly and perhaps most apparent are the associated risks of renal dysfunction and osteonecrosis of the jaw, resulting in special considerations to be taken if use in patients is required (Coleman 2008, Kennel and Drake 2009).

While preclinical evidence of Anti-nerve growth factor (NGF) antibodies provide evidence that the treatment blocks measures of ongoing bone pain in both models of CIBP and osteoporosis, they fail to stop bone remodeling (Halvorson, Kubota et al. 2005, Jimenez-Andrade, Bloom et al. 2010, Bloom, Jimenez-Andrade et al. 2011, Suzuki, Millicamps et al. 2018). At least one clinical trial investigating the effects of anti-NGF monoclonal antibody suggest positive effects on CIBP, as well as other studies suggesting the same in osteoarthritis and lower back pain (Sopata, Katz et al. 2015, Chang, Hsu et al. 2016). Several studies that included anti-NGF treatment suggested a connection between long term use of anti-NGF treatment, with or without NSAID co-administration, and rapid joint destruction, resulting in a temporary hold on clinical studies utilizing this approach (Chang, Hsu et al. 2016). However, this ban has since been lifted due to the potential for benefit in the clinical population with considerations and radiologic intervention, but no clinically/FDA approved anti-NGF agent is currently available (Chang, Hsu et al. 2016).

In addition to ongoing pain, many patients with skeletal metastasis experience pain that “breaks through” around the clock medication, typically opioids, managing their ongoing pain. Due to its etiology this pain phenomenon is referred to as “breakthrough pain” (BTP). Estimates put the percentages of patients who experience BTP while already experiencing ongoing pain at 40-80%, however confounds in reports exist as to whether or not proper definition of BTP has been used in some studies examining the pain type (Mercadante 2015). While BTP can occur spontaneously, it is much more often triggered, and likely more readily documented, in response to movement. Unavoidable movements such as getting out of bed in the morning or performing necessary tasks often can be enough to trigger a BTP episode. Equally as detrimental but likely more stressful, unexpected and involuntary movements such as coughing or sneezing can result in initiation of a BTP experience (Mercadante 2015). It is reported that

these BTP experiences can occur as many as 4 times a day, rate as high as 7.4/10 on the pain intensity scale and last 30-60 minutes (Mercadante 2015, Mercadante 2018). Due to the unpredictable nature of BTP, patients often have to choose between pursuing activities, (i.e. maintaining a positive quality of life) or avoiding activities that might produce pain (Mercadante 2015).

It is in part due to the unexpected nature of this pain type and the need to take analgesic regimens in response to the start of the pain, that current treatments fall on the patient to dose in response to sensation of pain. If you can imagine, this is not an ideal method of effectively treating intense pain and improving the quality of life of patients. Due to the pharmacokinetics of treatment methods (dosing in response to pain initiation), this often results in patients missing the window to adequately treat their most severe pain (Kane, Hoskin et al. 2015). By clinical definition BTP must be a pain experience that breaks through onboard opioid treatments, originally described in 1990 (Portenoy and Hagen 1990, Mercadante 2015). Although this is the well-accepted clinical and preclinical definition, until recently many clinical based reports have not accurately adhered to this criteria, making the description of and evaluation of treatment of BTP in past reports to some extent murky (Mercadante 2015). Recent reports address and acknowledge this limitation and highlight the need for more stringent inclusion/exclusion criteria in clinical reports (Mercadante 2011, Mercadante 2015). Previous treatments of BTP involved dosing oral morphine at levels proportional to those being used to manage patients' ongoing background pain, with little to no scientific evidence to support this approach (Mercadante 2011, Mercadante 2015). While intravenous morphine with doses of between 6 and 12 mg, (also proportional to daily regimens of background medication) demonstrate rapid pain relief, it is confounded by the propensity of cognitive failure and

feasibility of intravenous delivery, which most patients cannot comply with (Mercadante 2011, Mercadante 2012, Sousa, de Santana Neto et al. 2014, Mercadante 2015).

Due to the relatively slow pharmacokinetics of oral morphine treatment, analgesic application has shifted towards more rapid MOR agonist formulations (Mercadante 2015). The current mainstay to treat BTP is with rapid onset opioids, with varying methods of delivery, which have reportedly better outcomes for patients, however efficacy of these require ideal patient responsiveness (Mercadante 2015). Transmucosal fentanyl and lozenges, lollipops and other means to rapidly and dose-dependently deliver additional MOR agonists are available to patients (Mercadante 2015). A recent report attempted to compare new analgesics used to treat BTP to the traditional oral morphine, finding that reported and well conducted clinical experiments suggest that out of the available treatments, the most effective agents are fentanyl products, although admitting oral morphine has its place for treatment of predictive episodic BTP (Mercadante 2018).

Relying on additional MOR agonists to treat BTP is limited in a number of ways. The first hurdle in treatment likely lies with the nature of dosing in response to the sensation of pain, as previously mentioned, which can result in patients misaligning therapy with their pain experience (Kane, Hoskin et al. 2015). In this sense, a medication with alternative mechanisms of action to MOR agonists that would allow for around the clock dosing would be ideal. Alternative mechanisms to MOR agonists are needed as evidence reports that even at high doses of MOR agonists, patients with advanced disease and pain, continue to experience BTP, demonstrating that MOR agonists fail to effectively treat BTP (Bennett 2010, Havelin, Imbert et al. 2017). One possible explanation to this is that the sensory fibers transducing BTP may be mechanistically or inherently different from those that respond to MOR agonists and successfully manage ongoing pain (Havelin, Imbert et al. 2017). Due to the regimens patients

are already on, there is the realistic limitation of dosing to effect due to the adverse and potentially life threatening side effects of MOR agonists. Side effects such as nausea, constipation, somnolence, dizziness and risk of falls, mental confusion and potential respiratory depression, all limit the improvement of quality of life these patients experience despite any benefits to pain relief they may experience (Bruera and Paice 2015, Kane, Hoskin et al. 2015, Mercadante 2015).

A non-opioid option with opioid sparing effects would greatly benefit the quality of life of these patients. These limitations and current failures of treatments demonstrate that at the level of the patient we have not developed a treatment that sufficiently manages CIBP or a treatment that simultaneously allows them to return to the quality of life they desire. To develop such a class or agent of analgesics, the field has relied heavily on animal models of CIBP that allow us to isolate the site where CIBP is generated and therefore study the effects of tumor modulation of local tissue and neuroanatomical changes induced by this chronic pain in a controlled manner.

1.2. Contributions of Preclinical Models to the Neurobiology of Bone Pain

The section below is work that is published as a review article in Osteoporosis Reports (Havelin and King 2018). It has been slightly modified for this dissertation.

1.2.1. Introduction

Ultimately a most optimal treatment may be a dual acting therapy that has alternate molecular targets that treat pain while also slowing the growth of cancer. Preclinical studies over the past 20 years have implicated a number of molecular targets, as well as some agents to target them, however few if any of these have made it to the clinic to positively impact patient's

quality of life. These will be discussed in Chapter 1.3 after a brief explanation of preclinical models and pain signaling to emphasize contributions preclinical models have made to our understanding of mechanisms driving CIBP.

Bone and joint pain can occur in response to numerous conditions including trauma, infection, inflammation, autoimmune disease, genetic driven disease states, joint and bone pathology associated with aging, and cancer. Bone and joint associated pain can be acute (e.g. due to trauma), recurring, or chronic in nature. Indeed, musculoskeletal pain such as osteoarthritis is the most common form of chronic pain and disability worldwide. It is important to recognize that bone and joint pain is very complex, with multiple types of pain as well as multiple etiologies that may require different treatment strategies for complete pain management. Some patients also report development of persistent background pain and/or breakthrough pain episodes that are resistant to currently available medications (Hawker, Stewart et al. 2008, Paice and Ferrell 2011, Hawker and Stanaitis 2014, Mercadante 2015). This indicates a requirement for development of therapies targeting multiple mechanisms underlying the various aspects of bone and joint pain for more comprehensive pain management for these patients. Development of such therapeutic options requires better understanding of mechanisms underlying the multiple aspects of bone and joint pain needed for better care for these patients.

1.2.2. Overview of the Pain Pathway

Signals from events that may damage tissue (e.g. twisted joint, stressful impact) or from actual damaged tissue activate specialized sensory neurons known as nociceptors. Both bone and joint tissue are innervated by these specialized neurons which allow for the transduction of painful stimuli to aid in preventing further damage to tissue and repeating potentially tissue

damaging behaviors (Jimenez-Andrade, Mantyh et al. 2010, Alliston, Hernandez et al. 2017, Eitner, Hofmann et al. 2017, Ivanusic 2017). Multiple classes of nociceptors have been studied to date, differentiated by their cell body and axon size, their myelination patterns, electrophysiological characteristics such as conduction velocity and response thresholds, and the characteristics of stimuli that they respond to (Schaible and Schmidt 1983, Schaible and Schmidt 1983, Cavanaugh, Lee et al. 2009, Woller, Eddinger et al. 2018). Evidence that different classes of sensory neurons contain observable differences in cytochemical markers as well as terminate in different anatomical locations with the spinal cord dorsal horn have existed since the 1980's and 1970s (Hunt and Rossi 1985). Interestingly, the observations that peptide rich and peptide lacking c-fibers have slightly different innervation patterns in the periphery, and the theory that these nociceptors may indeed transmit unique nociceptive signals is not new (Hunt and Rossi 1985). Critical evaluation of these two fiber types by Molliver and colleagues demonstrated unique neurochemical markers between the populations as well as termination patterns in the spinal cord dorsal horn (Molliver, Radeke et al. 1995). Elegant work by Molliver and colleagues demonstrated that throughout development expression patterns of TrkA, the receptor for NGF, is downregulated to a smaller population of neurons that go on to express classic markers of peptidergic fibers (i.e. calcitonin gene-related peptide, [CGRP]) (Molliver, Radeke et al. 1995, Molliver, Wright et al. 1997). Neurons in the dorsal root ganglia that downregulate TrkA begin to express c-Ret, a receptor for glial cell line-derived neurotrophic factor (GDNF) (Molliver, Wright et al. 1997). Additionally, this work demonstrated that while TrkA expressing neurons require NGF for continued survival, c-Ret expressing cells require GDNF, and the two cell populations do not survive in the presence of the others neurotrophic factor (Molliver, Wright et al. 1997). Reports have also suggested that following dissection and growth in-vitro and injury the non-peptidergic population of cells potentially undergo a

phenotypic switch or regression (Wang, Molliver et al. 2011). In-vitro the non-peptidergic cells once again require NGF to survive, and in-vivo following injury they begin to express the transient receptor potential vanilloid 1 (TRPV1) protein, a classical marker of the peptidergic population (Wang, Molliver et al. 2011). Table 1.1 contains some common nomenclature that is used somewhat interchangeably when discussing these two fiber types.

Table 1.1. Nomenclature Commonly Used for Peptidergic and Non-peptidergic Fibers

Nav1.8 expressing fibers (C-fibers) Nociceptors	
Peptidergic Fibers	Non Peptidergic Fibers
Neuropeptides (CGRP-SP)	MrgD, IB4
Mu opioid receptors	No mu opioid receptors
NGF/TrkA	GDNF/cRET

These classic observations have been repeated, supported and expanded upon through the use of modern tools. Recent RNA sequencing data indicate that multiple classes of nociceptors exist (Usoskin, Furlan et al. 2015). Distinct RNA transcription profiles and protein expression in conjunction with behavioral experiments demonstrate specific nociceptive responses from nociceptor populations that have distinct molecular characteristics (Zylka, Rice et al. 2005, Cavanaugh, Lee et al. 2009, Scherrer, Imamachi et al. 2009, King, Qu et al. 2011, Okun, DeFelice et al. 2011, Barabas, Kossyрева et al. 2012, Usoskin, Furlan et al. 2015, Havelin, Imbert et al. 2017). Studies such as these demonstrate that different fiber populations not only exist but convey distinct sensory information depending on modality (thermal, chemical, mechanical) as well as areas of innervation (cutaneous vs deep tissue) as outlined in the labeled line hypothesis of sensory processing (Cavanaugh, Lee et al. 2009, Scherrer, Imamachi et al.

2009, King, Qu et al. 2011, Okun, DeFelice et al. 2011, Barabas, Kossyрева et al. 2012, Havelin, Imbert et al. 2017).

Sensory fibers mediating pain and itch project to the spinal cord, where projections terminate in the superficial lamina of the dorsal horn, lamina I and II (Link, Pulliam et al. , Ma 2010, Abaira and Ginty 2013, Bourane, Duan et al. 2015, Duan, Cheng et al. 2017, Todd 2017). Upon activation by noxious stimulation, terminal endings of the nociceptors release small molecule (eg. glutamate) and peptidergic (e.g. substance P, CGRP) neurotransmitters into the synaptic cleft. Of interest to our work, the two major populations of nociceptors often referred to as the “non-peptidergic” and “peptidergic” have been demonstrated to use these signals. These neurotransmitters act on receptors located on interneurons within the spinal cord as well as projection neurons that project along specialized tracts (e.g. the anterolateral tract) to various regions of the brain such as the thalamus, periaqueductal grey, lateral parabrachial area and regions within the medullary reticular formation (Link, Pulliam et al. , Ma 2010, Abaira and Ginty 2013, Bourane, Duan et al. 2015, Duan, Cheng et al. 2017, Todd 2017). There has been a great deal of progress in gaining a better understanding of the circuitry mediating nociception within the spinal cord (Link, Pulliam et al. , Ma 2010, Abaira and Ginty 2013, Bourane, Duan et al. 2015, Duan, Cheng et al. 2017, Todd 2017).

While some of the second order neurons within superficial dorsal horn of the spinal cord project signals directly to the brain, not all neurons are involved in directly transmitting information to the brain (Todd 2017). Additionally, within lamina I-II, roughly 90-95% neurons in lamina I and nearly all neurons in lamina II are characterized as interneurons (Todd 2017). Interneurons that modulate pain signals intuitively consist of both inhibitory neurons that release gamma-aminonutyric acid (GABA) and glycine, and excitatory interneurons that are predominately glutamatergic (Todd 2017). Various studies examining the role of these

interneurons indicate that they play a key role in processing the incoming signal, with several interneuronal populations responding to multiple modalities of input (e.g. chemical, mechanical, thermal, touch, itch) (Abraira and Ginty 2013, Duan, Cheng et al. 2014, Bonin, Wang et al. 2016, Koch, Acton et al. 2018). Although studies have begun to explore the role of subpopulations of spinal inhibitory and excitatory interneurons in mediating pain, itch and mechanical allodynia, a full understanding of the complex interactions and circuitry is not complete (Koch, Acton et al. 2018). Little is known regarding processing of sensory information from deep tissues such as the joint and the bones. It is very likely that gaining a better understanding of the processing and integration of signals within the spinal cord will be essential in developing improved treatments that address the multiple components of bone and joint pain such as movement-associated pain, breakthrough pain, and persistent background aches and pains.

Of importance, multiple regions within the brain including cortical regions (e.g. anterior cingulate cortex, somatosensory cortex, prefrontal cortex, insula, parietal lobe), the diencephalon (thalamus), and the limbic regions (e.g. amygdala) are implicated in processing the incoming signal and contribute to the perception of pain (Tracey 2017). Notably, these different brain regions may contribute to different components of the complex sensation of pain that includes both sensory and emotional components (Navratilova, Atcherley et al. 2015, Navratilova, Morimura et al. 2016). Clinical and preclinical studies are making important gains in our understanding of how these different brain regions contribute to the affective (unpleasant) and sensory (intensity, location) aspects of pain (Porreca and Navratilova 2017). How these and other regions interact and how they may be altered in the conditions of chronic pain (e.g. arthritis, low back pain) are under investigation (Kuner and Flor 2016, Davis and Seminowicz 2017). Moreover, key changes in brain volume, functional connections, and processing are observed using imaging studies (Mansour, Farmer et al. 2014, Smith, López-Solà et al.). In

patients with chronic back pain, studies have reported diminished cortical grey matter and impaired emotional decision-making (Apkarian, Sosa et al. 2004). These observations are mimicked in a preclinical model of nerve injury in which chronic pain disrupts normal function and anatomy of the prefrontal cortex, partially reversed by different molecules with analgesic properties (Shiers, Pradhan et al. 2018). This observation has been expanded to other chronic pain states including chronic osteoarthritis (Mansour, Farmer et al. 2014, Smith, López-Solà et al. 2017).

1.2.3. Initiation of Pain Signals from the Bone and Joint:

Early studies in the cat demonstrated that the knee joint is innervated by sympathetic fibers as well as sensory afferent fibers, primarily fine myelinated A-delta fibers and unmyelinated (slow conducting C-fibers) sensory afferent neurons (Langford and Schmidt 1983). Both A-delta and C-fibers demonstrated responses to mechanical stimulation at higher thresholds compared to other tissues such as skin, with some fibers that respond only to stimulation in the noxious range (Schaible and Schmidt 1983). Electrophysiological studies characterizing movement-induced activation of sensory fibers innervating the joint further classified these fibers into 4 subtypes: fibers activated by non-noxious movement; fibers activated both by non-noxious and noxious movement; fibers activated only by noxious movement, and fibers that failed to respond to movement (Schaible and Schmidt 1983).

These data led to the conclusion that the sensory afferent fibers innervating the joint contribute to deep pressure sensation and nociception, and likely signal that the joint is about to leave the normal working range (Schaible and Schmidt 1983). Subsequent electrophysiological characterization of the A-delta and C-fibers innervating the knee joint in the setting of acute inflammation revealed altered firing properties in the context of injury. Fiber populations from

inflamed knee joints demonstrated increased activity in the absence of any stimulation or joint movement (spontaneous activity). In addition, they demonstrated lower response thresholds to mechanical stimulation (hypersensitivity), and increased activity in response to mechanical stimulation from probing the joint with calibrated von Frey filaments and to joint movement (Coggeshall, Hong et al. 1983, Grigg, Schaible et al. 1986, Schaible, Schmidt et al. 1987). In addition, silent sensory fibers that normally do not demonstrate activity during non-noxious movement of the joint, became active following exposure to knee joint injection of kaolin/carrageenan, a model of acute experimental arthritis in the cat (Schaible and Schmidt 1985). Findings such as these have highlighted the potential of sensory neurons to undergo maladaptive change in their response to both natural and artificial stimuli.

Little was known about the protein expression patterns and identity/anatomy of the sensory nerves involved in transducing pain from the bone in naïve animals let alone disease treated animals (i.e. nociceptive, autonomic, large diameter, etc.). Several studies examining innervation of the bone using a combination of IHC and transgenic animals indicate that bone as well as the surrounding periosteum is well innervated by small-diameter peptidergic C-fibers, A-delta fibers, and sympathetic fibers (Mach, Rogers et al. 2002, Jimenez-Andrade, Mantyh et al. 2010, Guedon, Longo et al. 2016). Several reports suggest key differences in patterns of innervation of the bone and other deep tissue compared to skin. Initial work using staining methods (Mach, Rogers et al. 2002) was replicated utilizing a transgenic animal that selectively expressed eGFP under control of the mas-related G-coupled protein sub family D expressing (MrgD) promoter developed by Zylka et al. 2005, that serves as a marker for non-peptidergic nociceptors (Zylka, Rice et al. 2005). Analysis of tissue from these animals demonstrated a lack of eGFP+ fiber innervation to the bone and periosteum thus a lack of MrgD+ or nonpeptidergic nociceptors, but dense innervation within skin of the same animals (Mach, Rogers et al. 2002,

Jimenez-Andrade, Mantyh et al. 2010). Studies that directly compared innervation of skin and bone using these mice demonstrated that whereas skin is innervated by both peptidergic (CGRP+) and non-peptidergic populations of C-fibers, bone shows evidence of innervation by peptidergic and sympathetic, but not non-peptidergic C-fibers (Mach, Rogers et al. 2002, Jimenez-Andrade, Mantyh et al. 2010). Jimenez-Andrade et al. 2010 also demonstrated lack of purinergic receptor P2X3 (P2X3) IHC staining in the bone and periosteum, another marker of the stereotypical non-peptidergic nociceptor population (Jimenez-Andrade, Mantyh et al. 2010). Additional recent immunohistochemical evidence in the rat has also demonstrated TRPV1 expressing fibers in marrow, which can be sensitized by application of capsaicin (Morgan, Nencini et al. 2019). This has led to the proposal that bone and joints are not innervated by the non-peptidergic population of C-fibers in mice (Mantyh 2014). However, evidence regarding the presence of non-peptidergic C-fibers innervating the bone has been reported in rat studies using retrograde tracers injected into the intramedullary space of the bone (Ivanusic 2007, Kaan, Yip et al. 2010, Ivanusic 2017).

Such discrepant findings suggest the possibility that there may be a subpopulation of non-peptidergic fibers that innervate the bone that have not been directly assessed in previous studies. Alternative explanations include the possibility of differences in the methods used to examine innervation. The processes of decalcification of the bone may have altered binding sites for markers of non-peptidergic fibers such as isolectin B4 (IB4) or P2X3 diminishing potential visualization of fibers innervating the bone and leading to false negative findings (Jimenez-Andrade, Mantyh et al. 2010). However, IB4 binding has been reported in muscle that had been processed for decalcification in the same manner as bone that did not show these markers of non-peptidergic fibers (Jimenez-Andrade, Mantyh et al. 2010). In addition, MrgD expressing and IB4 binding fibers were not observed in periosteum whole mount tissue that did not undergo

decalcification whereas in side by side control tissue, both were expressed in the skin (Jimenez-Andrade, Mantyh et al. 2010). These observations indicate that the decalcification process does not explain the absence of these markers of non-peptidergic fibers within the bone. Alternatively, as bone is a site of perfusion, it is possible that injection of the retrograde tracers may have leaked to other sites resulting in false positive findings. It is also of importance to note the difficulty to process calcified tissue, especially following the establishment and degradation of tissue due to cancer. Let alone locate fibers of small to medium diameter neurons when processing slices of this tissue. Methods continue to improve to allow such analysis, including here at the University of New England's histology core.

Finally, it is possible that there are species differences in innervation or population (peptidergic vs non-peptidergic) separation and identity that causes these discrepant findings. Indeed, differences between rats and mice related to expression of these specific molecular markers of neuronal subtypes have been reported (Price and Flores 2007). In the mouse these populations have been demonstrated to be mostly non-overlapping in the DRG (Molliver and Snider 1997, Molliver, Wright et al. 1997, Cavanaugh, Lee et al. 2009, Scherrer, Imamachi et al. 2009, Thakur, Rahman et al. 2012, Usoskin, Furlan et al. 2015), whereas in the rat these populations show a ~45% overlap in expression in the DRG, and these expression profiles vary between DRG and trigeminal ganglia (Price and Flores 2007). In addition to these differences between rats and mice, distribution of these fiber populations have been reported to differ across different strains of mice (Laedermann, Pertin et al. 2014). Future studies examining potential differences in innervation of bone and joint across multiple species is warranted to better understand whether patterns of innervation of bone is conserved.

In addition to these populations of nociceptors, some recent studies have implicated low threshold mechanoreceptors (C-LTMRs) in mediating mechanical pain to normally non-

noxious stimuli in conditions of injury and chronic pain (Rutlin, Ho et al. 2014, Zimmerman, Bai et al. 2014, Abraira, Kuehn et al. 2017). The C-LTMRs have been most studied within the skin. Whether this population innervates bone or joint or mediates pain associated with trauma or pathology that generates chronic pain is unknown and difficult to assess due to the nature of joint and bone tissue accessibility. Improved understanding of subpopulations innervating the bone and surrounding tissues as well as how they may contribute to diverse aspects of bone and joint pain are needed to develop a more comprehensive understanding of mechanisms underlying the multiple components of bone and joint pain.

1.2.4. Site of Injury or Pathology:

Inflammation. Tissue damage leads to an innate immune response that results in release of molecules including chemokines, cytokines, and growth factors from local tissue (e.g. fibroblasts, chondrocytes), blood, and local and migrating inflammatory cells (Mantyh 2014, Krustev, Rioux et al. 2015, Jeon, David et al. 2018, Syx, Tran et al. 2018). These factors may promote disease progression and pathology in disease states such as arthritis or cancer-induced bone pain. Pro-inflammatory cytokines such as tumor necrosis factor-alpha (TNF-alpha), Interleukin 6 (IL-6) and IL1-beta have been implicated in bone resorption by increasing osteoclast activity (Braun and Schett 2012). In addition, these cytokines produce peripheral sensitization of nociceptive fibers, resulting in decreased thresholds for activation and amplified signaling (Cook, Christensen et al. 2018). Growth factors NGF, vascular endothelial growth factor (VEGF) and insulin-like growth factor (IGF) are also implicated in development of bone or joint pathology in disease states such as arthritis and cancer-induced bone pain. VEGF has been implicated in angiogenesis associated with arthritis and skeletal metastases (Felson 2005, Mantyh 2014).

NGF has been implicated in peripheral sensitization through mechanisms such as upregulation of key channels such as sodium channels and transducers that regulate neural activity and by phosphorylation of transducers such as TRPV1 within neurons leading to enhanced activity and increased neuronal excitability (Chang, Hsu et al. 2016, Denk, Bennett et al. 2017). In addition, NGF has been shown to mediate pathological sprouting of nociceptive and sympathetic fibers within the bone and joint across various rodent models of bone and joint pain including cancer-induced bone pain (Jimenez-Andrade, Bloom et al. 2010), arthritis (Jimenez-Andrade, Mantyh et al. 2012) and fracture (Jimenez-Andrade, Martin et al. 2007, Chartier, Thompson et al. 2014). Building upon these preclinical studies, therapies such as anti-TNF-alpha, anti-IL6 and anti-NGF antibodies are in clinical use or in clinical trials for pain associated with bone or joint pathology has not been investigated. However, the role of many of these inflammatory signaling molecules has not been assessed in models of ongoing pain assessment or, primarily due to a lack of models, BTP.

Neuropathic Pain. In addition to the development of inflammation, neuropathic changes have also been reported in animal models of bone and joint pain (Thakur, Rahman et al. 2012, Falk, Bannister et al. 2014, Falk and Dickenson 2014, Mantyh 2014, Thakur, Dickenson et al. 2014). Studies in rat and mouse models of cancer-induced bone pain and chemical-induced osteoarthritis joint pain have demonstrated expression of activated transcription factor 3 (ATF3), a neural marker of nerve damage, in cell bodies within the dorsal root ganglion innervating the bone or joint (Peters, Ghilardi et al. 2005, Sabino and Mantyh 2005, Csont, Bereczki et al. 2007, Thakur, Rahman et al. 2012). Pathological changes to sensory and sympathetic nerve fibers within the bone and joint have been demonstrated across models of cancer bone pain, arthritis pain, and fracture pain (Jimenez-Andrade, Martin et al. 2007, Jimenez-Andrade, Bloom et al. 2010, Jimenez-Andrade, Mantyh et al. 2012, Chartier, Thompson

et al. 2014). These studies describe development of neuromas and disorganized structures of fibers similar to those reported following traumatic nerve injury in patients and animal models of nerve-injury induced neuropathic pain. Finally, pharmacological studies in animal models of bone and joint pain have demonstrated that knee joint arthritis pain and cancer bone pain associated with markers of nerve damage are resistant to pain alleviating effects of anti-inflammatory drugs such as NSAIDs (e.g. ketorolac, diclofenac) (Okun, Liu et al. 2012, Thakur, Dickenson et al. 2014, Remeniuk, Sukhtankar et al. 2015).

In contrast, these pain states were found to be responsive to drugs typically used to treat neuropathic pain within the clinical setting, duloxetine, pregabalin and gabapentin (Thakur, Dickenson et al. 2014, Havelin, Imbert et al. 2016). Importantly, these studies demonstrate that anti-inflammatory drugs may be effective in some aspects of pain whereas they are ineffective on others, results echoed by clinical observations of the need to elevate patients with CIBP to analgesics using molecular targets that differ from inflammatory mediators. In a rat model of advanced osteoarthritis in which both evoked measures of joint pain and non-evoked ongoing pain are observed, the NSAID diclofenac effectively blocked weight asymmetry whereas it failed to block persistent ongoing joint pain (Okun, Liu et al. 2012) whereas duloxetine blocks both evoked and ongoing joint pain (Havelin, Imbert et al. 2016). Similarly, in a rat model of CIBP, diclofenac was demonstrated to effectively block tactile hypersensitivity, a measure of referred evoked pain, but not ongoing pain (Remeniuk, Sukhtankar et al. 2015). Specific to peripheral neurons, treatment with anti-NGF antibody relieved many of the measurable pain behaviors in mice with CIBP whereas anti-P2X3 antibodies only reversed referred tactile hypersensitivity (Guedon, Longo et al. 2016). Such observations indicate that there are mechanistic differences between different clinically important aspects of bone and joint pain. Such complexity highlights the need for more

comprehensive analysis of the multiple aspects of bone or joint pain when examining potential molecular mechanisms of pathological chronic pain and for effectiveness of potential therapeutic targets.

1.2.5. Sensitization

Many animal and clinical studies have demonstrated that sensitization of peripheral and central neurons develops in the context of chronic bone or joint pain (Falk and Dickenson 2014, Arendt-Nielsen, Egsgaard et al. 2015, Eitner, Hofmann et al. 2017). The international association for the study of pain (IASP) defines sensitization as “Increased responsiveness of nociceptive neurons to their normal input, and/or recruitment of a response to normally subthreshold inputs”. They note that sensitization may include a decrease in activation threshold, increase in suprathreshold responses, spontaneous discharges of neurons, and increases in receptive field of neurons. They further clarify that sensitization is a neurophysiological term and can only be applied when both input and output of the neural system being studied (e.g. peripheral input, spinal signaling) are known. It is emphasized that clinically, sensitization may only be inferred indirectly from observations such as exacerbated pain from a known painful response (hyperalgesia) or a painful response from a previously non-painful stimulus (allodynia). Temporal summation is also used within the clinical literature as a sign of sensitization (Arendt-Nielsen, Egsgaard et al. 2015). Sensitization can be measured in the periphery, termed peripheral sensitization defined by IASP as “Increased responsiveness and reduced threshold of nociceptive neurons in the periphery to the stimulation of their receptive fields”. Sensitization can also be measured at sites within the central nervous system such as the spinal cord, termed central sensitization defined by IASP as “Increased responsiveness of nociceptive neurons in the central nervous system to their normal or subthreshold afferent input.”

This has been described in patients with moderate to severe knee osteoarthritis (Arendt-Nielsen, Egsgaard et al. 2015). Further, in patients with knee osteoarthritis associated with spread of allodynia and temporal summation, functional magnetic resonance imaging demonstrated that whereas direct painful stimulation at the osteoarthritic site did not distinguish between sensitized and non-sensitized patients, stimulation at an area of spreading sensitization resulted in increased signals within brain regions associated with pain processing (Pujol, Martinez-Vilavella et al. 2017). Stimulation of an area associated with spreading sensitization also produced activation of brain regions not associated with pain processing, extending to the auditory, visual, and ventral sensorimotor cortices (Pujol, Martinez-Vilavella et al. 2017). Such studies will be critical in gaining a better understanding of changes associated with development of central sensitization that contribute to worsening of pain and to medication resistant pain states associated with bone and joint pain.

There are many well written overviews of mechanisms contributing to development of peripheral sensitization (Schaible 2018, Syx, Tran et al. 2018) and central sensitization (Woolf 2011, Falk, Bannister et al. 2014, Falk and Dickenson 2014, Schaible 2018). Much has been learned about the impact of many of the factors that are released by local tissues, such as adenosine triphosphate (ATP), adenosine diphosphate (ADP), endothelins, bradykinin, and growth factors (Jimenez-Andrade, Bloom et al. 2010, Mantyh 2014, Schaible 2018, Syx, Tran et al. 2018, Woller, Eddinger et al. 2018). These factors have been shown to act both directly on neurons to activate them and to alter the properties of the neurons. These actions including lowering of activation thresholds and increased in responses are key characteristics of peripheral sensitization (Jimenez-Andrade, Mantyh et al. 2010, Syx, Tran et al. 2018, Woller, Eddinger et al. 2018). Several factors including proinflammatory cytokines (e.g. IL-1 beta, TNF alpha, IL-6) have been shown to be catabolic and may enhance bone resorption promoting

underlying pathology (Lee, Ellman et al. 2013). Mechanisms underlying peripheral sensitization include translation and trafficking of transducer channels as well as phosphorylation of transducer channels such as TRPV1 resulting in altered activation thresholds and increased transfer of cations allowing for enhanced depolarization of the neurons and amplified signaling (Jimenez-Andrade, Mantyh et al. 2010, Syx, Tran et al. 2018, Woller, Eddinger et al. 2018). Similarly, increased translation and trafficking of sodium channels resulting in amplified action potentials and increased numbers and phosphorylation of calcium channels result in enhanced neurotransmitter release from afferent terminals within the spinal cord (Devor 2006, Bao 2015). In addition, pathophysiological changes in neurons such as pathological sprouting and formation of neuromas may contribute to ectopic discharge and amplified signaling from the bone or joint (Jimenez-Andrade, Mantyh et al. 2010).

Ongoing afferent input has been suggested to result in spinal sensitization (Devor 2009, Latremoliere and Woolf 2009, Woolf 2011). Various studies in animal models of cancer-induced bone pain and osteoarthritis have demonstrated development of central sensitization including lowered thresholds for activation, amplification of signal, and widening of the receptor field (Thakur, Rahman et al. 2012, Thakur, Dickenson et al. 2014), as well as activation of spinal neurons in response to normally non-noxious stimuli such as movement of the tumor bearing hind limb (Schwei, Honore et al. 1999) or arthritic joint (Havelin, Imbert et al. 2016). Various mechanisms have been implicated in mediating spinal sensitization, including activation of glia, upregulation and excitatory signaling by dynorphin, and diminished tonic inhibition by GABAergic interneurons (Coull, Beggs et al. 2005, De Koninck 2007, Lai, Luo et al. 2008, Gao and Ji 2010, Trang, Beggs et al. 2011, Beggs and Salter 2013, Clark, Old et al. 2013, Ji, Berta et al. 2013, Mapplebeck, Beggs et al. 2016). Several studies have demonstrated a role for spinal

microglia and elevated pro-inflammatory cytokines in mediating cancer-induced bone pain (Zhou, Liu et al. 2016) and in animal models of osteoarthritis (Tran, Miller et al. 2017).

In addition to release of pro-inflammatory cytokines, spinal microglia mediated release of the brain derived growth factor (BDNF) has been implicated in mediating spinal changes resulting in disinhibition and spinal sensitization (Coull, Beggs et al. 2005, Trang, Beggs et al. 2011, Beggs and Salter 2013). These changes have been described in animal models of nerve injury as well as opioid-induced hypersensitivity. Release of BDNF is proposed to increase chloride channels (KCCL) leading to disruption of the gradient balance of chloride ions (Trang, Beggs et al. 2011, Beggs and Salter 2013). This is proposed to result in GABA activation of normally inhibitory channels become excitatory, thereby facilitating sensitization and hyperexcitability (Coull, Beggs et al. 2005, De Koninck 2007, Prescott, Ma et al. 2014, Bonin, Wang et al. 2016). Whether such changes are implicated in chronic bone and joint pain has not been well studied. The role of these changes in mediating evoked hypersensitivities compared to persistent ongoing pain has not been systematically studied. Upregulation of dynorphin has also been implicated in spinal sensitization in preclinical models of nerve injury-induced pain through activation of non-opioid receptors such as the bradykinin receptor (Lai, Luo et al. 2008). Upregulation of dynorphin has been reported in a mouse model of cancer-induced bone pain (Schwei, Honore et al. 1999). However, further investigation regarding the role of spinal dynorphin in mediating chronic bone or joint pain has not been investigated.

1.2.6. Descending Pain Modulation

Another important aspect of pain processing is the ability for the brain to modulate pain signals through descending pain pathways that can amplify (descending pain facilitatory pathways) or diminish (descending pain inhibitory pathways) the pain signal (reviewed by

(Suzuki, Rahman et al. 2004, Ossipov, Dussor et al. 2010)). Key sites implicated in descending pain modulation include the anterior cingulate cortex, the periaqueductal grey, and the rostroventromedial medulla (RVM) (Suzuki, Rahman et al. 2004, Ossipov, Dussor et al. 2010). In the uninjured/non-pain state, pain can be modulated in response to physical or psychological stress. Much has been learned about how stress can activate these descending pain modulatory pathways to dampen pain or induce analgesia through endogenous opioid and cannabinoid signaling within the brain (Ossipov, Dussor et al. 2010). Following injury, a time-dependent increase in net descending pain facilitation occurs, wherein descending facilitatory pathways promote enhanced spinal cord activity to noxious and non-noxious stimuli (Ossipov, Dussor et al. 2010, Falk, Bannister et al. 2014) as well as behavioral responses showing enhanced responsiveness to noxious and non-noxious stimuli modeling hyperalgesia and allodynia, respectively (Burgess, Gardell et al. 2002, Qu, King et al. 2011, King, Qu et al. 2012, Havelin, Imbert et al. 2016, Bannister, Qu et al. 2017).

1.2.7. Conclusion

Much has been learned regarding biological mechanisms contributing to bone and joint pain. The continued improvement and development of animal models that more accurately represent the human condition will continue to advance the field and allow basic researchers to identify translational proteomic, cellular and systems to better treat pain. In addition, the relatively recent advent of specific genetic tools including transgenic animals with alterations to “pain-specific” genes (i.e. knock-ins and knock-outs), reporter genes, and development of virally deliverable tools to induce genetic alterations allow dissection and analysis of molecular targets and microcircuitry underlying specific and distinct aspects of chronic pain. Optogenetic and chemogenetic tools offer increased ability for spatial and temporal precision of the investigation

of key cell subtypes and circuits within the CNS. Fluorescent proteins that serve as a surrogate for neuronal firing/activity such as GCaMP6 and the continued incorporation of light sensitive ion channels and pumps that allow for selective activation or inhibition of cells are immensely powerful tools working their way to the forefront of the pain field. In addition, improvements in imaging techniques both at the site of pathology (Felson 2005) and brain imaging assessing brain activity and changes in processing in chronic pain patients will guide future studies on molecular and circuit changes that are associated with chronic pain.

Such analyses will open new potential targets as genomic and proteomic analyses reveal novel targets at the site of pathology or the neural circuitry driving chronic pain. In addition, brain imaging will allow for potential insights into development of comorbidities associated with chronic pain such as development of depression, anxiety and altered cognitive processing (Borsook, Hargreaves et al. 2011, Parks, Geha et al. 2011, Tetreault, Mansour et al. 2016, Bajic, Craig et al. 2017, Colon, Bittner et al. 2017, Peng, Steele et al. 2018). Beyond the development of exciting new tools there remain complexities that go beyond the scope of this review of work, such as integral contributions by the immune system and the endocrine system. Continued and growing analysis of genetic susceptibility to increased or decreased pain sensitivity, and epigenetic modifications that result from chronic pain will guide our understanding of the predisposition of different races/ethnicities/sexes to chronic pain and the potential effectiveness or insensitivity to specific pain treatments.

1.3. Preclinical Models of Cancer-Induced Bone Pain

Several variations of animal models exist to examine CIBP in preclinical studies. Much of the initial work done to examine the mechanisms underlying CIBP was performed in a murine model that utilizes an injection of a primary tumor line into the femur, and to date most

published work still uses this approach. The first published piece of working using this approach was performed by Clohisy et al. 1995, where injection of the 2472 sarcoma cells into the femur of osteoclast deficient mice resulted in the upregulation of macrophage colony-stimulating factor and a pathological increase in osteoclast activity and morphology that coincided with osteolysis (Clohisy, Ogilvie et al. 1995). It is important to note that unless using immunocompromised animals it is necessary to use syngeneic cell lines with the species and strain of animal being used. Work immediately following this expanded on this observation looking at the differences between the 2472 sarcoma cell line and G3.26 melanoma cell line (Clohisy, Ogilvie et al. 1996). Investigation here demonstrated that whereas the sarcoma cell line induced osteoclast pathology and bone destruction, the melanoma line grew but failed to alter osteoclast numbers or structure and no change in bone remodeling was reported (Clohisy, Ogilvie et al. 1996). Further support that this approach resulted in maladaptive bone remodeling resulted when a human breast cancer cell line MDA-MB-45s, induced an increase in the number and size of osteoclasts in a mouse model of cancer-induced bone loss, as well as induced osteoclasts to increase bone resorption (Clohisy, Palkert et al. 1996). In general, these bodies of work demonstrated bone remodeling that mimicked in the clinical observations, leading to this approach to be heavily utilized to study CIBP.

Following the initial establishment of this approach, work by Dr. Patrick Mantyh adapted this with the intent to examine mechanisms underlying CIBP. His work examined alterations to the peripheral and central nervous system and corresponding emergence of behaviors that are still used as measures of pain. This work and previous work by Clohisy and colleagues demonstrated pain measures were induced by tumor growth within the bone as they are only observed in the mice that received cells implanted, and upon improvement of the surgical implantation of cells, sealed directly into the femur (Schwei, Honore et al. 1999). Schwei et al.

1999 was the first paper published in the series of work by Dr. Mantyh and established this approach as a clinically relevant method to evaluate CIBP. An initial clinically relevant observation being that this approach resulted in tumor induced drastic bone remodeling and prolonged growth resulted in invasion of the tumor into the periosteum of the femur, observations that had not been documented in the previous work by Clohisy and colleagues (Schwei, Honore et al. 1999).

This was furthered by a direct comparison between pain models within Dr. Mantyh's lab in the subsequent publication of Honore et al 2000 suggesting that difficulty in treating CIBP might be due to its apparent "unique" neurochemical footprint, a combination of oxidative stress within the spinal cord, increased expression of dynorphin within the spinal cord, and increased glial cell hypertrophy (Honore, Rogers et al. 2000). In an effort to compare the efficacy of morphine in treating CIBP vs inflammatory pain this group also demonstrated that comparable to observations in the clinic, higher doses of morphine are required to temper pain measurements in this model of CIBP (Luger, Sabino et al. 2002). This work was soon echoed by Wacnik et al. 2003 who also demonstrated that in advanced CIBP, the required doses of morphine were nearly 2.5 times as high (measured by ED50) when compared to a model of carrageenan induced muscular pain to reverse movement-related hyperalgesia as measured by grip strength (Wacnik, Kehl et al. 2003). These works notably only observed acute effects of morphine at potentially behavior altering doses (30 mg/kg and ED50 23.9 mg/kg Luger et al. 2002 and Wacnik et al. 2003 respectively) and didn't compare efficacy of morphine in a chronic regimen to observe the effects of morphine tolerance development or whether an increase in dosing would be necessary to manage pain as the cancer progressed.

Work by King et al. 2007 demonstrated that mini-pump implantation to deliver varying doses of morphine not only failed to attenuate CIBP behaviors 3-5 days after implant, but

exacerbated measures of pain. Alarmingly this work also demonstrated that this regiment of morphine also induced an increase in tumor-induced bone destruction after as short a time as 3-5 days of chronic morphine exposure, and this effect was blocked by naloxone indicating these observations to be opioid receptor mediated (King, Vardanyan et al. 2007). These are two of the fundamental challenges within the clinic when treating CIBP in patients, as patients are on regiments of increasing opioids for long durations of time (Luger, Sabino et al. 2002). Interestingly Peters et al. 2005 demonstrated that chronic administration of gabapentin, also attenuated flinching as a measure of ongoing pain, as well as palpation induced increase in flinching, a proposed behavioral measure of pain exacerbated by movement of the cancer-afflicted limb (Peters, Ghilardi et al. 2005). These observations demonstrate that not only does CIBP have a unique neurochemical footprint, but an interesting response to various pharmacological agents, implicating the potential for multiple mechanisms driving this pain state.

A similar rat model exists to study CIBP, where the major difference (excluding cancer cell line utilized) is that primary tumor cells are sealed and restricted to the tibia rather than the femur. The first report of this approach was in 2002 by Medhurst and colleagues using the MRMT-1 rat mammary gland carcinoma cells. They reported tumor-induced bone destruction indicated by both radiographic analysis and microcomputed tomography (Medhurst, Walker et al. 2002). These observations are not only similar to results in the mouse model, but more importantly, similar to clinical observations of osteolytic bone loss in many breast cancer patients with skeletal metastasis (Mantyh 2002, Mantyh, Clohisy et al. 2002). A corresponding decrease in mechanical thresholds, a relative decrease in wheel running, altered weight bearing away from the cancer afflicted limb and increased glial fibrillary acidic protein (GFAP) staining ipsilateral to the cancer-afflicted limb in the dorsal horn was reported (Medhurst, Walker et al.

2002). This initial characterization established a model that allowed future analysis and use of rats that would allow additional techniques that could not be achieved in the mouse due to technical challenges, such as electrophysiological recordings in awake animals, and behavioral assays that may be more reliable in the rat.

Recent novel methods used to measure ongoing pain in models has allowed us to assess the role of pain in a non-evoked way (King, Vera-Portocarrero et al. 2009, Navratilova and Porreca 2014). Within the rat model of CIBP, Remeniuk et al. 2015 demonstrated that peripheral blockade of sensory fibers (by lidocaine) to the cancer-afflicted tibia in rats resulted in conditioned place preference (CPP) to the lidocaine paired chamber indicating pain relief along with an increase in dopamine release in the nucleus accumbens indicating that relief of CIBP as other pain states is rewarding (Remeniuk, Sukhtankar et al. 2015). These two observations not only demonstrate that generation and likely maintenance of ongoing pain from the cancer afflicted limb in rats requires sensory neuron activity, but holds measures that blockade of the pain signal has a rewarding behavioral effect and a physiological response in the reward centers of the brain. These two measures went further to demonstrate that while administration of a systemic NSAID reverses tactile hypersensitivity, it fails to induce CPP to pain relief or dopamine release in the nucleus accumbens (Remeniuk, Sukhtankar et al. 2015). However, systemic morphine successfully blocks peripheral nerve block induced CPP and dopamine release in the nucleus accumbens, suggesting that morphine successfully manages ongoing pain and tactile hypersensitivity, recapitulating clinical reports that NSAIDs fail to manage advanced CIBP whereas opioids have some effect (Bruera and Paice 2015, Kane, Hoskin et al. 2015).

1.4. Known Mechanisms Driving Cancer-Induced Bone Pain

The following is meant to expand on the previous section and discuss with slightly more detail some of the key findings in preclinical models of CIBP that led to the specific direction of the work included in this dissertation.

Evidence from the earliest bodies of work investigating these preclinical models of CIBP have uncovered many important factors involved in CIBP. As mentioned previously Schwei et. Al 1999, described evidence that implied the neurochemical changes observed in their mouse model to be “unique” from other models of pain, or perhaps more of a hybrid signature when compared to previous results from inflammatory and neuropathic pain models (Schwei, Honore et al. 1999). Non-noxious stimulation that consisted of a 2-minute hind limb movement, induced c-fos expression and neurokinin-1 receptor (NK-1) internalization in the superficial dorsal horn of the spinal cord ipsilateral to the implantation of the tumor, as well as deep lamina c-fos expression (Schwei, Honore et al. 1999). Beyond this these animals displayed increased GFAP staining ipsilateral to the tumor, and dynorphin and c-fos expression in deep lamina of the spinal cord dorsal horn. These findings were replicated in a follow up publication from Honore et al. 2000 that directly compared neurochemical changes between models of inflammation and neuropathic pain (Honore, Rogers et al. 2000).

Honore et al. 2000 and Luger et al. 2001 demonstrated that both the bone destruction and neurochemical changes induced by the tumor were blocked by OPG, an effective osteoclast “decoy” that inhibits osteoclast function as previously mentioned through the RANK-RANKL activation pathway (Honore, Rogers et al. 2000, Luger, Honore et al. 2001). These observations paired well with previous results from Clohisy and colleagues that demonstrated OPG effectively reduces the number of osteoclasts at the site of an osteolytic tumor, effectively blocking them from degrading bone. This effectively demonstrated that osteoclasts are required for bone

degradation, and bone degradation plays a key role in the generation of pain from the bone, connecting this preclinical model to the clinic (Clohisy and Ramnaraine 1998, Clohisy, Ramnaraine et al. 2000). This highlighted the role for osteoclasts direct involvement in degrading the bone and emphasized the role for bone destruction and osteoclasts in driving neurochemical changes and pain in this model. Investigation of different cell lines and their potential impact on CIBP behavior and osteoclast reprogramming by Sabino et al. 2003 (Sabino, Luger et al. 2003) demonstrated that in immunocompromised mice the injection of sarcoma, melanoma and colon cancer cell lines resulted in different patterns of pathology (Sabino, Luger et al. 2003).

Perhaps most remarkably with respect to bone remodeling, a similar observation was recorded to Clohisy and colleagues' earlier work with a melanoma cell line (G3.26 derived from C57BL6 mouse) in this model and approach (Clohisy, Ogilvie et al. 1996). The previously categorized sarcoma line (2472) replicated findings of the generation of unevoked flinching/guarding behaviors and an increase in pain behaviors during forced ambulation on a rotarod apparatus and palpation-evoked guarding. Whereas melanoma (B16-F10 derived from C57/bl6) and colon (NCI derived from Balb/c mice) cell lines failed to induce unevoked guarding behaviors and have differential effects on ambulation and palpation-evoked behaviors (Sabino, Luger et al. 2003). Beyond this, normally non-noxious palpation of the hind limb of animals injected with all cell lines demonstrated increased c-fos expression in the deep lamina of the spinal cord, but only sarcoma and melanoma cell lines, not colon, induced pathological c-fos expression in the superficial lamina of the spinal cord dorsal horn. Demonstrating a unique pattern of sensitization that correlated to palpation-induced guarding of the hind limb. Interestingly, GFAP expression was also demonstrated to be upregulated in animals injected with the sarcoma and colon cell lines (but not melanoma), reflecting cancer-induced alteration

of ambulatory pain scores (Sabino, Luger et al. 2003). Evidence such as this demonstrates that the effects of different primary tumors within the bone can have unique neurochemical as well as behavioral changes, further exemplifying the heterogeneity of CIBP (Sabino, Luger et al. 2003).

Little was known about the actual identity or anatomy of the sensory nerves involved in transducing pain from the femur in naïve animals let alone disease treated animals (i.e. nociceptive, autonomic, large diameter, etc.). Early work in the mouse utilizing immunohistochemical (IHC) staining demonstrated that innervation in naïve bone as well as the periosteum was primarily CGRP and tyrosine hydroxylase (TH) positive with additional staining suggesting the presence of A-delta fibers (Mach, Rogers et al. 2002). These observations were accompanied by a notable lack of IB4-binding fibers (Mach, Rogers et al. 2002). This work was replicated utilizing a transgenic animal that selectively expressed eGFP under control of the MrgD promoter originally developed to visualize non-peptidergic nociceptors without the need for staining and the caveats introduced by different methodological approaches (Zylka, Rice et al. 2005). Analysis of tissue from these animals demonstrated a lack of eGFP+ fiber innervation to the bone, thus a lack of MrgD+ or non-peptidergic nociceptors in the bone, but dense innervation within skin of the same animals (Jimenez-Andrade, Mantyh et al. 2010). However, dense innervation of CGRP+ fibers was observed within the bone and periosteum, again consistent with previous experiments identifying peptidergic nociceptors in the periosteum and bone (Jimenez-Andrade, Mantyh et al. 2010). This study also demonstrated lack of P2X3 IHC staining in the bone and periosteum in mice, another marker of the stereotypical non-peptidergic nociceptor population.

This lent further evidence to the ideology in mice the innervation of the bone and periosteum is primarily peptidergic, CGRP+ fibers, and that these native populations undergo

sprouting that may be contributing directly to ongoing and spontaneous pain originating from this site. Counter intuitively, additional investigation within this model demonstrated that while in the early stages of cancer cell growth within the bone pathological sprouting is observed, denervation occurs in the distal end of the femur at late stages of disease progression, perhaps highlighting a role for active damage to neurons within the bone and periosteum, and a role for neuronal damage to contribute to the pain generated from the cancer-afflicted hind limb (Peters, Ghilardi et al. 2005). Of note the peptidergic population of nociceptors also reliably express the TRPV1, and one body of work in the dog demonstrated ablation of TRPV1 fibers improved several outcomes in companion dogs affected by bone cancer and CIBP (Brown, Agnello et al. 2015).

Work that immediately followed this sought to observe fiber anatomy following the implantation of cancer cells into the femur. Jimenez et al 2010, demonstrated that not only was pathological sprouting observed following cancer cell implantation but that the fibers undergoing pathological sprouting were primarily CGRP+, TrkA+ and neurofilament protein 200 (NF-200+) (Jimenez-Andrade, Bloom et al. 2010). As mentioned previously, this pathological sprouting was blunted by administration of an NGF-sequestering antibody, and observed pain behaviors also decreased, however bone pathology remained unaffected by the NGF-antibody. Bloom et al. 2011 demonstrated similar sprouting in TrkA+ fibers in the periosteum, a location close proximity to the tumor cells, stromal cells and bone remodeling, this too was blocked by the NGF sequestering antibody (Bloom, Jimenez-Andrade et al. 2011). These findings were supported by additional results in experiments that utilized a TrkA receptor antagonist, further highlighting the role for NGF-induced changes in peripheral nerve structure and CIBP (Ghilardi, Freeman et al. 2011). It is not clear whether blockade of bone remodeling by OPG blocks pathological sprouting of fibers. Both of these key bodies of work demonstrated a role for

neuronal plasticity induced by the presence of NGF following bone remodeling and tumor growth.

In an attempt to compare effects of mitigating pain on the peptidergic and non-peptidergic populations work was performed in both the mouse and the rat. As previously mentioned work in the rat utilizing retrograde labeling from the tibia implicated the possibility that some fibers innervating the bone were in fact non-peptidergic (Ivanusic 2009). Work from Mantyh's group demonstrated the two fiber types likely have differential roles in CIBP by performing a side by side comparison using an NGF-sequestering antibody and an antibody targeting the P2X3 protein in the mouse (Guedon, Longo et al. 2016). As previously observed the NGF-antibody blocked/reversed pain behaviors both in the skin and measures of pain from the bone in the mouse model of CIBP, whereas the P2X3 antibody only blocked the tactile hypersensitivity that reliably develops in these models of CIBP (Guedon, Longo et al. 2016). Perhaps in line with the differing observations of fiber type innervation of the bone in the rat, Kaan et al. 2010 used a P2X2/P2X3 antagonist and demonstrated that while bone pathology was unaltered by drug treatment, mechanical allodynia and phosphorylated extracellular receptor kinase (pERK) expression in DRG were reversed (Kaan, Yip et al. 2010). Wu et al 2012 also demonstrated that antagonism of the P2X3 receptor transiently blocked cancer-induced tactile hypersensitivity (Wu, Xu et al. 2012).

While this work was informative to the peripheral identity of cell types innervating the femur, and the potential for altering each fiber types transduction of pain, observation of the cellular bodies of these neurons within the DRG of animals has added some specifics to the story of CIBP. Peters et al 2005 investigated the anatomical location of cells that may be undergoing damage following cancer cell implantation. While compared to sham treated animals, cancer cell implantation resulted in an upregulation of the neuronal damage marker ATF3 in L1, L2 and

L3 DRG, with a distinct lack of ATF3 expression in other DRG (Peters, Ghilardi et al. 2005). This work was run in comparison to femoral nerve transection, which displayed similar patterns in DRG of ATF3 expression, and sciatic nerve transection which displayed a shifted pattern of ATF3 expression towards the L3-L5 DRG (Peters, Ghilardi et al. 2005). Intuitively implicating the role of innervation from the femoral nerve, which contains fibers from cell bodies within L2 DRG. Additionally, marked galanin expression and immune cell activation/migration was observed in the L2 DRG of cancer treated animals when compared to sham (Peters, Ghilardi et al. 2005).

Sevcki et al 2004, demonstrated an interesting link between bone destruction and the development of ATF3 expression, demonstrating that bisphosphonate blockade of bone destruction results in a decrease in cell bodies within the DRG expressing ATF3 (Sevcik, Luger et al. 2004). Interestingly work by King et al. 2007 demonstrated an upregulation of ATF3 in L4 DRG compared to shams, demonstrating that establishment and growth of the cells within the femur reliably induce neuronal damage in sensory neurons and this coincides with c-fos expression in the L4 spinal cord segment by Sabino et al 2003 (Sabino, Luger et al. 2003, King, Vardanyan et al. 2007). Notably ATF3 expression was exacerbated by exposure to chronic mini-pump delivered morphine, an observation that coincided with enhanced bone destruction as previously mentioned (King, Vardanyan et al. 2007). Ivanusic et al. 2009 who performed a characterization of retrograde labeling to identify the DRG(s) in which the cell bodies innervating the tibia in the rat, reported that the tibia and periosteum contain terminals of cells primarily within the L2-L5 DRG. This report also contained information that the diameter of these cells ranged from small (likely C-fibers) to larger (A-delta) cell bodies, with more positive cells being small diameter neurons (Ivanusic 2009). In addition to this, tumor growth and perhaps CIBP as a result, increases the presence of CGRP RNA and protein in the DRG of mice (King, Vardanyan et al. 2007, Isono, Suzuki et al. 2011). An effect exacerbated in the presence of chronic morphine, and

diminished by the lack of activated prostaglandin E2 (PGE2) (King, Vardanyan et al. 2007, Isono, Suzuki et al. 2011).

This addition to the literature gave the anatomical location of sensory nerves innervating the femur in these mice and tibia of the rat, as well as likely the identity of the cells generating and maintaining pain signals, an important contribution to future work that would/will allow for targeted proteomic and genomic investigation of sensory neurons following cellular implant.

Evidence that tumor cells alter cellular signaling of osteoclasts and immune cells has also been demonstrated in both the mouse and rat model of CIBP. Work as early as Clohisy et al. 1995 has demonstrated the likelihood of tumor cells inducing cellular changes within close proximity to their growth. Remeniuk et al. 2018 demonstrated that in animals that received tumor implant, markedly increased levels of interleukin-6 were found in bone exudate and plasma, an observation closely following measures of clinical patients with metastatic breast cancer (Remeniuk, King et al. 2018). The authors of this paper found that acute administration of an IL-6 antagonist temporarily reversed tactile hypersensitivity, while having no effect on ongoing pain measured by CPP to pain relief. However, chronic administration of the IL-6 antagonist beginning at the time of tumor implantation resulted in blockade of the development of tactile hypersensitivity, ongoing pain as well as bone remodeling, a most promising result with clinical translation indeed. Isono et al. 2011 demonstrated that microsomal prostaglandin E synthase-1 (mPGES-1) knock out mice, that lack the ability to activate PGE2 showed diminished pain behaviors along with tumor growth potentially due to a lack of RANKL activation, implicating a role of cancer-induced activation of the gene in order to produce certain aspects of CIBP (Isono, Suzuki et al. 2011).

Electrophysiological recordings from spinal cord dorsal horn neurons in cancer cell injected rats has demonstrated that as pain behaviors develop and bone destruction occurs, central sensitization occurs, however it did so in a manner unique from previously observed neuropathy models (Urch, Donovan-Rodriguez et al. 2003). CIBP caused hyperexcitability in wide dynamic range cells in the spinal cord in response to a number of nociceptive stimuli, changes that remained even when a chronic morphine regiment was given to rats (Urch, Donovan-Rodriguez et al. 2003, Urch, Donovan-Rodriguez et al. 2005). Interestingly the hyperexcitability of dorsal horn neurons evoked by A-delta and C-fibers in the periphery in the rat was blocked by administration of the P2X3 antagonist, an interesting contradiction to the observed role in mice for the non-peptidergic fibers (Kaan, Yip et al. 2010). The reactivity and sensitization that is recorded from superficial dorsal horn neurons not only agrees with the known innervation patterns of the spinal cord from previously reported evidence, but coincides with retrograde labeling from the tibia. Both Kaan et al. 2010 and Ivanusic 2009 report the identity of cell bodies within DRG that innervate the tibia in the rat, and demonstrate co-labeling for stereotypical nociceptive markers, eg. SP, CGRP and notably IB4, in contrast to results noted in the mouse (Ivanusic 2009, Kaan, Yip et al. 2010) .

These examples and efficacy of approaches varies between measurable pain behaviors, i.e. certain approaches treat tactile hypersensitivity but fail to manage supposed measures of ongoing pain, and vice versa. Acute administration of a p38-MAPK inhibitor reversed cancer-induced increases in flinching and decreased cancer-induced hind limb guarding, but failed to ameliorate cancer-induced tactile hypersensitivity (Sukhtankar, Okun et al. 2011). Chronic administration of the kappa opioid receptor (KOR) agonist U50-488 has similar effects, where U50-488 reversed these measures although to a lesser extent (Edwards, Havelin et al. 2018).

While these additions to the body of literature surrounding CIBP have been informative, few have resulted in the development of novel improvements in the clinic. One potential limitation of the translation of these findings are the methods used to evaluate their efficacy. While behaviors such as shifted weight bearing, evoked tactile hypersensitivity, increased flinching/guarding and impaired limb use have been the mainstay for nearly 20 years of CIBP preclinical work, it is not necessarily clear that reversal of these behaviors is truly due relief of ongoing pain. A dramatic implication of work published by King et al. 2009, where the authors demonstrated compounds that alleviate tactile hypersensitivity in preclinical models do not necessarily always alleviate ongoing pain, similar to observations from the clinic (King, Vera-Portocarrero et al. 2009). While some work is likely more convincing than others, e.g. blockade of neuronal sprouting by NGF-antibodies that may have clinical efficacy, and blockade of osteoclast induced bone remodeling which does show clinical efficacy, other approaches may be more limited in their translatability. Recently the development and successful implementation of CPP to ongoing pain relief in models of CIBP has provided a novel and non-evoked measure of pain relief that may serve for screening of more effective therapeutics (Remeniuk, Sukhtankar et al. 2015, Remeniuk, King et al. 2018). This, in addition to the lack of a model of BTP that truly involves a non-painful stimulus are truly two hindrances to the field. In the case of BTP, this has been a detriment to the field in the development and screening of novel analgesics to treat BTP, as little is known about the underlying neurophysiology of BTP. In the following I share the results of our group in developing a novel model of BTP in a rat model of CIBP along with a unique role for the non-peptidergic IB4-binding fibers in being critical to BTP. Following this, due to limitations of the techniques used in our rat work, we sought to expand and clarify the role of unique populations of sensory fibers in ongoing pain and BTP in the mouse using an optogenetic approach that would allow us to transiently silence peripheral fibers rather than ablate them.

CHAPTER 2

MEDIATION OF MOVEMENT-INDUCED BREAKTHROUGH CANCER PAIN BY IB4-BINDING NOCICEPTORS IN RATS

The section below is work that is published as a primary research article in The Journal of Neuroscience (Havelin, Imbert et al. 2017). It has been slightly modified for this dissertation.

2.1. Abstract

Cancer-induced bone pain (CIBP) is characterized by moderate to severe ongoing pain that commonly requires the use of opiates. Even when ongoing pain is well controlled, patients can suffer breakthrough pain (BTP), episodic severe pain that “breaks through” the medication. We developed a novel model of cancer-induced BTP using female rats with mammary adenocarcinoma cells sealed within the tibia. We previously demonstrated that rats with bone cancer learn to prefer a context paired with saphenous nerve block to elicit pain relief (i.e., conditioned place preference, CPP), revealing the presence of ongoing pain. Treatment with systemic morphine abolished CPP to saphenous nerve block demonstrating control of ongoing pain. Here, we show that pairing BTP induced by experimenter-induced movement of the tumor-bearing hind limb with a context produces conditioned place aversion (CPA) in rats treated with morphine to control ongoing pain, consistent with clinical observation of BTP. Preventing movement-induced afferent input by saphenous nerve block prior to, but not after, hind limb movement blocked movement-induced BTP. Ablation of isolectin B4 (IB4) binding, but not TRPV1⁺, sensory afferents eliminated movement-induced BTP suggesting that input from IB4 binding fibers mediates BTP. Identification of potential molecular targets specific to this

population of fibers may allow for development of peripherally restricted analgesics that control BTP and improve quality of life in patients with skeletal metastases.

2.2. Introduction

Pain is the most feared consequence of cancer (Breivik, Cherny et al. 2009, Paice and Ferrell 2011). Metastatic bone pain is characterized by moderate-to-severe persistent ongoing pain associated with tumor growth, nerve destruction and bone remodeling. As many as 40-80% of these patients also experience breakthrough pain (BTP), transient episodes of severe to excruciating pain occurring in the presence of medication controlling background cancer pain (Portenoy and Hagen 1989, Portenoy and Hagen 1990, Mercadante 2015). BTP is frequently reported for 15-30 min following voluntary or involuntary movements, such as changing position or coughing, with as many as 4-6 episodes reported within a day dramatically reducing patients' quality of life (Haugen, Hjermstad et al. 2010, Mercadante 2015). Treatment of BTP typically requires rapid onset opioids that while often effective, are confounded by uncertainty of dosing requirements for safe and effective treatment of individual patients (Mercadante 2011, Mercadante 2015). Further complicating treatment, BTP takes place on a background of medication, primarily opioid, controlled ongoing pain. Increasing the opioid dose results in a high likelihood of adverse side effects, further diminishing these patients' quality of life (Mercadante 2015). The discovery of safe and effective medications to treat BTP is an urgent unmet medical need.

The observation that BTP occurs in the setting of opioid medication that sufficiently controls ongoing pain suggests that these pain states are mechanistically distinct (Bennett 2010). Analgesic actions of drugs such as morphine occur at mu opioid receptors (MOR) that are located within the periphery, spinal cord and brain. One possibility is that movement may

recruit additional fibers that are not blocked by peripheral MOR agonists at doses that block persistent background pain. In the setting of pain-induced central sensitization, such signals may elicit excruciating BTP (Mantyh 2013, Falk and Dickenson 2014, Mantyh 2014), that requires fast-acting opioids that likely exert their effects at supraspinal sites.

While recent RNAseq studies have described as many as 11 subpopulations of sensory fibers (Usoskin, Furlan et al. 2015), two broad classes of fibers that have been widely characterized are TRPV1 expressing fibers IB4 binding neurons (Molliver and Snider 1997, Snider and McMahon 1998, Basbaum, Bautista et al. 2009, Wang and Zylka 2009). Previous studies have demonstrated that long-lasting desensitization of TRPV1 expressing sensory fibers produces insensitivity to thermal stimulation and ongoing pain, without altering tactile hypersensitivity, in models of neuropathic and inflammation-induced pain (Yaksh, Farb et al. 1979, Ossipov, Bian et al. 1999, Okun, DeFelice et al. 2011). Others have demonstrated that ablation of MrgD expressing or IB4 binding fibers blocks tactile hypersensitivity without altering thermal responses (Joseph, Chen et al. 2008, Cavanaugh, Lee et al. 2009, Ye, Dang et al. 2012). Given the mechanical component of movement-evoked BTP, we tested the hypothesis that blocking nociceptive input from IB4 binding fibers will block movement-evoked BTP whereas blocking nociceptive input from TRPV1 expressing fibers will not block movement-evoked BTP.

Evaluation of BTP and cancer-induced ongoing pain has been limited by the lack of available preclinical models. We recently reported capturing ongoing cancer pain through a learning paradigm assessing motivation to seek a context associated with pain relief (Remeniuk, Sukhtankar et al. 2015). Here, we developed a novel measure of BTP by assessing the motivation to avoid a context associated (conditioned place avoidance, CPA) with pain following movement of the tumor-bearing hind limb. Critically, this model assessed CPA in rats with morphine-controlled ongoing bone cancer pain, simulating movement triggered BTP in patients.

2.3. Materials and methods

2.3.1. Animal Care

Female and male Fischer F344/NhSD (Harlan Laboratories Inc, Indianapolis, IN, USA) weighing 125-150g were chosen based on their histocompatibility with the MAT BIII tumor line. The rats were maintained on a 12-hour light/dark cycle with food and water available *ad libitum*. All experiments were performed in accordance with the policies and recommendations of the International Association for the Study of Pain, National Institutes of Health, and the Institutional Animal Care and Use Committee of the University of Arizona and University of New England.

2.3.2. Cell Line Maintenance

The Fischer rat mammary adenocarcinoma cell line 13762 MAT BIII (ATCC, CRL 1666, RRID:CVCL_3475, Manassas, VA) was maintained in McCoy's media with L-Glutamine (CellGro, Manassas, VA) with 10% fetal bovine serum (ATCC, Manassas, VA) and 1% penicillin/streptomycin at 37°C in a 5% CO₂ atmosphere. Prior to surgical implantation, cells were washed with phosphate-buffered saline and detached with 0.05% trypsin-EDTA (CellGro, Manassas, VA). The cells were spun at 2300 rpm for 3 minutes and re-suspended at a concentration of 2×10^5 cells/ μ L in McCoy's serum free media.

2.3.3. Surgical Procedures and Drug Treatment

Intratibial Surgery and Cancer Implantation. This surgical procedure was performed according to previously published methods (Remeniuk, Sukhtankar et al. 2015). Briefly, rats were anaesthetized under gas anesthesia (2% isoflurane O₂ mixture). The right hind limb of the

rat was shaved and disinfected with 70% ethanol and betadine. The animal was placed on its back and a 1 cm incision was made horizontally across the femoral-tibial region to expose the patellar tendon, and surrounding skin retracted to expose the proximal end of the tibia. A small hole was drilled between the lateral and medial condyles into the intramedullary canal followed by insertion of a 5 cm, 28-gauge guide cannula (Plastics One) attached to Tygon tubing (Cole-Palmer) to a 25 μ L syringe (Hamilton, Reno, NV), with location verified by x-ray imaging (Faxitron, Tucson, AZ). Injection of 5 μ L of MAT BIII cells, or cell free McCoy's serum free media (vehicle), was followed by sealing the drilled hole with bone cement (Stryker Orthopaedics, Simplex P Bone Cement, Mahwah, NJ). The area was flushed with sterile saline and the knee joint was reinforced with a vicryl 5-0 suture (Ethicon, Cornelia, GA) placed across the drilled area. Each rat received 1 mg/ml of gentamicin sulfate (Sparhawk Laboratories Inc, Lenexa, KS) via subcutaneous (s.c.) injection and was allowed to recover from anesthesia prior to return to the housing colony. Animals did not receive treatment with analgesics following tumor implantation as treatment with NSAIDs, specifically COX inhibitors, as well as morphine have been demonstrated to impact aspects of disease progression including tumor growth and tumor-induced bone remodeling (Sabino, Ghilardi et al. 2002, Sabino, Ghilardi et al. 2002, King, Vardanyan et al. 2007). For ethical considerations, all experiments were terminated within 14 days of tumor inoculation into the tibia. A total of 83 tumor-bearing rats and 50 sham rats were used across all studies.

Morphine Pellet Implantation. Effects of morphine on tumor-induced bone pain were assessed by insertion of morphine or placebo pellets 11 days post-intratibial surgery and behavioral testing 20-24 hours post-pellet implantation, 12 days post intratibial surgery. Morphine sulfate (75 mg) or placebo pellets, generously provided by the National Institute on Drug Abuse (NIDA) Drug Supply Program, were inserted (s.c.) under gas anesthesia (2%

isoflurane O₂ mixture) on the side contralateral to tibia surgery of the rat in front of the pelvic region. The region was shaved and disinfected with 70% ethanol and betadine. A 1 cm incision was made into the skin, and a pocket created with forceps in between the skin and muscle. A single pellet was inserted into the pocket region, and the incision closed using a surgical wound clip. Rats received 1 mg/mL (s.c.) of gentamicin sulfate (Sparhawk Laboratories Inc, Lenexa, KS) and were allowed to recover from anesthesia prior to return to the housing colony. For CPP and CPA experiments, pellets were implanted immediately following assessment of baseline (pre-conditioning) time spent in the conditioning chambers.

Intrathecal Catheterization and Spinal Drug Delivery. Rats underwent surgical implantation of an intrathecal catheter for drug administration at the level of the lumbar spinal cord a minimum of 7 days prior to intra-tibial surgeries to allow sufficient recovery time from the intrathecal surgeries. Intrathecal catheters were surgically implanted as previously described (Yaksh and Rudy 1976, Yaksh, Farb et al. 1979, King, Qu et al. 2011). Rats were anesthetized under gas anesthesia (2% isoflurane O₂ mixture) while secured in a stereotaxic frame (Stoelting, Wood Dale, IL). The atlanto-occipital membrane was exposed, punctured, and a section of polyethylene-10 tubing (PE-10) 6.5 cm in length was passed caudally from the cisterna magna to the lumbar enlargement for a single spinal administration of the appropriate drug or vehicle. To determine the effect of eliminating input from TRPV1 expressing fibers, rats received spinal administration of capsaicin (20 µg/10 µl 10% Tween, 10% Ethanol, 80% saline) followed by 10 µl saline flush or equivolume vehicle (10% Tween, 10% Ethanol, 80% saline) vehicle followed by 10 µl saline flush. To determine the effect of eliminating input from IB4-binding fibers, separate groups of rats received spinal administration of IB4-Saporin (IB4-SAP, Advanced Targeting Systems, 3.2 µg /20 µl saline) or the control, blank-SAP (Advanced Targeting Systems, 3.2 µg /20 µl saline) followed by a 10 µl flush of saline. Movement of an air bubble placed between drug

solution and saline was used to monitor progress of the injection. Immediately following injection, catheters were slowly removed from the spinal cord and the wound closed. Any animals displaying motor impairment or paralysis during recovery (<10% total rats) were immediately euthanized. Animals were routinely checked throughout the experiment to monitor health. Following behavioral testing, rats were euthanized and tissue collected for immunohistochemical verification of elimination of TRPV1 or IB4 immunofluorescence in the spinal dorsal horn of capsaicin or IB4-SAP treated rats, respectively.

Immunofluorescent Analysis of Effect of Spinal Capsaicin or IB4-SAP on TRPV1, SP, CGRP and IB4 Immunofluorescence in the Spinal Dorsal Horn. To verify that these treatments produced selective ablations of targeted nociceptor terminals, tissue was collected for immunofluorescent staining and semi-quantitative image analysis D21 post intrathecal administration of IB4-saporin, blank-SAP, capsaicin, or the vehicle for capsaicin. Rats were deeply anesthetized with Beuthanasia-D (Henry Schein Animal Health, Dublin, OH) and underwent intracardiac perfusion through the left ventricle with PBS containing heparin (100 U/mL) followed by 4% PFA containing PBS, pH 7.4. The L3-L4 spinal cord segments were immediately dissected out and post-fixed in 10% formalin overnight. The spinal cord was then moved into a 30% sucrose solution at 4°C for 12 to 24 hours for cryoprotection. Spinal cords were embedded in OCT (VWR, Radnor, PA) and frozen on dry ice for sectioning. Sections were cut on a cryostat (Leica, Wetzlar, Germany) at 30 microns, collected onto positively charged slides (Azer Scientific, Morgantown, PA), and allowed to dry before storage at -80°C. Sections were rinsed 3 times with PBS containing 0.05% Tween (PBST) to remove OCT, then non-specific binding proteins were blocked by 30 min incubation with 5% normal donkey serum (EMD Millipore, Billerica, MA) and 1% bovine serum albumin (Amresco, Solon, OH) in PBST. This blocking solution was also the antibody diluent. Primary antibodies and Alexa 488-conjugated IB4 were incubated overnight at

4°C as follows: IB4-AF488 1:500 (Molecular Probes Cat# I21411 also I21411 RRID:AB_2314662); goat anti-TRPV1 1:100 (AF3066, R&D Systems, Minneapolis, MN); rabbit anti-Substance P 1:500 (ImmunoStar Cat# 20064 RRID:AB_572266, Hudson, WI); rabbit anti-CGRP 1:2000 (ImmunoStar Cat# 24112 RRID:AB_572217). The TRPV1 antibody was validated in rat DRG tissue by competition experiments with the TRPV1 antigen peptide that completely abolished binding of the TRPV1 antibody as well as verifying that the antibody detected a protein of the appropriate molecular weight in western blots (Isensee, Wenzel et al. 2014). Both the CGRP and SP antibodies are widely used and cited in the literature, with 504 citations for the SP antibody and 110 citations for the CGRP antibody verifying that these antibodies are widely used in peer-reviewed journals (<https://www.citeab.com/>), proposed as the most reliable way to identify a suitable antibody (Helsby, Leader et al. 2014). Sections were rinsed 3 times with PBST and incubated in the dark for 1 hour at RT with appropriate cross-adsorbed secondary antibodies: Donkey anti-goat Alexa Fluor 568 1:1000 (A-11057, Life Technologies, Carlsbad, CA); donkey anti-rabbit Alexa Fluor 568 1:1000 (ab175692, Abcam, Cambridge, MA); donkey anti-goat Alexa Fluor 488 1:1000 (ab150133, Abcam). Sections were rinsed with PBS 3 times and mounted with DAPI-containing Fluoroshield (ab104139, Abcam). Primary and/or secondary antibody omission controls under identical staining conditions resulted in no fluorescent signal.

Images were acquired using a Leica TCS SP5 confocal laser scanning microscope using a 20x/0.7 NA plan apo objective lens. Excitation light was generated at 488 nm by an argon gas laser or 561 nm by a diode pumped solid state laser through a double dichroic beam splitter, and emission was detected sequentially via photomultiplier tubes to avoid cross-talk between fluorophores. Z-stack images were collected with a 0.71 μm step size, and maximum projections generated for subsequent analysis. All z-stack images within each staining condition were acquired in a single session using the same laser intensity settings. Images were analyzed using

Fiji image analysis software (Schindelin, Arganda-Carreras et al. 2012). Confocal z-stack images captured using the Leica confocal software were opened using the Bioformats plug-in. Images were rotated on the X/Y axis so that the dorsal portion of the spinal dorsal horn is located at the top of the image and a Z projection image was created using maximum intensity for 2D visualization of the stack. The split channels function was used to create red (TRPV1, SP or CGRP) or green (IB4) fluorescent images. Regions of interest (ROI) were selected from a file and arranged to calculate ratios of the mean grey value of pixels within the ROI for 1) an area of lamina 1 and the same area in the deep dorsal horn (L1/L1con) and 2) an area of lamina 2 and the same area in the deep dorsal horn (L2/L2con) (See Fig 4). This allowed for an internal reference to normalize intensity ratings for comparison across sections. The number of sections analyzed for TRPV1 analyses are reported in table 1. These numbers include sections from TRPV1/IB4, SP/IB4 and CGRP/IB4 co-stains as there were no significant differences in intensity ratings for IB4-fluorescence across these three immunofluorescent conditions. Average intensity ratios across sections were used to calculate means and SEM across samples from individual animals. Ratios were calculated across spinal dorsal horn images from 3 control rats, 4 capsaicin treated rats for SP and CGRP, 3 for TRPV1 and 2 IB4-SAP treated rats.

Table 2.1. Numbers of Sections Analyzed for Staining Intensity

	Sample 1	Sample 2	Sample 3	Sample 4
TRPV1				
Control	8	14	15	
IB4-SAP	6	9		
Capsaicin	11	12	17	
SP				
Control	13	15	15	
IB4-SAP	9	9		
Capsaicin	9	12	17	18
CGRP				
Control	12	13	16	
IB4-SAP	10	13		
Capsaicin	7	13	17	18
IB4				
Control	35	41		
IB4-SAP	15	31		
Capsaicin	27	36	40	41

2.3.4. Behavioral Measures

Behavioral Measure of tactile hypersensitivity. Rats were placed into elevated chambers with a wire mesh floor and allowed to acclimate for 30 min. Paw withdrawal thresholds were determined in response to probing with calibrated von Frey filaments with spaced increments ranging from 0.5 to 15 g. Each filament was applied to the middle of the plantar surface of the paw using the "up and down" method and analyzed using a Dixon nonparametric test (Chaplan, Bach et al. 1994).

Behavioral measure of impaired limb use. Limb use was assessed as previously described (Luger, Honore et al. 2001). The animal was placed in an empty pan and observed while walking.

Usage of the treated limb was rated on the following scale: 0=complete lack of use, 1=partial non-use, 2=limping and guarding, 3=limping and 4=normal walking.

Behavioral measure of BTP using CPA. Analysis of movement-induced BTP was performed using CPA to a chamber associated with movement triggered BTP. Within the clinical setting, voluntary or involuntary movement has been reported to trigger episodes of BTP lasting approximately 30 min following the movement (Haugen, Hjermsstad et al. 2010, Mercadante 2015). Therefore, we hypothesized that placing the rat into the chamber following a 2-min period of movement of the tumor-bearing hind limb would produce a transient period of BTP and that association of the BTP with the novel context produces motivation to avoid the chamber on test day resulting in CPA. CPA was assessed in a three-chamber apparatus with chambers distinguishable by visual, tactile and odor cues. One pairing chamber within the apparatus had striped walls, a smooth floor, and pink-lemonade chap stick (Lipsmackers) applied to the ceiling. The other pairing chamber within the apparatus had uniformly gray walls, a rough floor, and vanilla chap stick (Lipsmackers) applied to the ceiling. The neutral chamber had white walls, a smooth floor, no chap stick, and a LED light (Sylvanna, LED/DOTS/BLACK/1X12/BL) on the ceiling to diminish time spent in the middle chamber and encourage exploration of the pairing chambers. The boxes were cleaned (Sparkleen, Fisherbrand) between each baseline, conditioning, and testing session. Each rat underwent baseline, conditioning and testing in the same CPP apparatus.

Both tumor-bearing and sham control rats underwent a one-day pre-conditioning period (D11 post-surgery) where they were placed in the three-chamber apparatus with open access to all chambers for 15 min. Behavior was video recorded and time spent in each chamber determined by video tracking software (Anymaze, Stoelting, Wood Dale, IL). Any rats spending less than 180 seconds in a single chamber were removed from the study (<25% total animals

tested). On conditioning day (D12), rats were paired with an enclosed chamber (striped or grey) for 30 min with no treatment to minimize potential-accidental movement of the tumor-bearing hind limb. Four hours later, rats underwent 2 minutes of movement to the cancer-bearing limb and were placed in the opposite chamber. This treatment was previously demonstrated to induce spinal FOS and NK-1 receptor internalization in tumor bearing mice but not sham treated mice (Schwei, Honore et al. 1999). Hind limb movements were completed in a separate room from the conditioning chambers to prevent other rats from being unnecessarily exposed to signs of distress from the rats during the hind limb movement. Both sham and tumor-bearing rats vocalized during the treatment. On the test day (D13), rats were once again placed in the three-chamber apparatus with open access to all chambers. Behavior was video recorded and time spent in each of the pairing chambers was determined by Anymaze video tracking software. Difference scores were calculated as the preconditioning baseline (BL) scores subtracted from test scores (test - BL). A negative score indicates aversion, and a positive score indicates preference.

Morphine's effects on BTP. To determine whether movement-induced CPA breaks through ongoing morphine treatment that controls ongoing pain (Remeniuk, Sukhtankar et al. 2015), the ability of morphine infusion across 20-24 hours to block movement-induced CPA was determined. On day 11 following injection of cancer cells into the tibia, rats underwent baseline analysis of time spent in each of the conditioning chambers as described above followed by implantation of extended release morphine or placebo pellets. Pellets were surgically implanted (s.c.) on the lower back 1 inch above the pelvic bone under isoflurane anesthesia immediately after pre-conditioning baselines were performed. The following day (conditioning day), movement of the tumor-bearing hind limb was performed 20-24 hours into morphine infusion.

Measure of sensory input on movement-induced BTP. To determine whether blocking sensory input blocks movement-induced BTP, rats underwent the 3-day CPA conditioning protocol as described above. In the morning of conditioning day, rats received saphenous saline (350 μ l) and no hind paw movement of the tumor bearing hind limb, and were then confined to the appropriate conditioning chamber. Afternoon conditioning occurred 4 hours later. To determine if saphenous lidocaine blocks movement-induced BTP, rats received saphenous lidocaine (4% w/v, 350 μ l) 10 min prior to the 2 min movement of the tumor bearing hind limb and confinement within the opposite conditioning chamber. To determine whether blocking sensory input after hind limb movement blocks movement-induced BTP, afternoon conditioning consisted of hind limb movement for 2 min followed 10 min later by saphenous lidocaine and confinement to the opposite conditioning chamber. All saphenous injections were performed as previously described (Remeniuk, Sukhtankar et al. 2015). Rats were anaesthetized with a 2% isoflurane O₂ mixture. To produce an effective peripheral nerve block, lidocaine was administered over the saphenous nerve in a single s.c. injection (4% wt/vol, 350 μ L). Equivolume saline was given as a vehicle control.

2.3.5. Radiograph Analysis of Disease Progression

Bones were rated according to a 4-point scale. 0: represented a normal, non-tumor bearing bone with no bone remodeling; 1: represented slight signs of bone remodeling; 2: represented diffuse bone loss or pitting without full cortical bone loss; and 3: represented clear pitting and full cortical bone loss.

2.3.6. Statistical Analysis

All statistical analysis was performed and all graphs were made using GraphPad Prism 6.0. Group differences in tactile sensory thresholds were analyzed across time by a two-way analysis of variance (ANOVA). Post-hoc analysis of time-dependent changes following treatment was performed using the Bonferroni's multiple comparisons test wherein each time-point was compared to pre-treatment values within each group. A probability level of 0.05 was used to establish significance. For CPA, the effects of treatment (cancer vs control) and conditioning chamber were analyzed by a 2-way analysis of variance (ANOVA). Sidack's multiple comparison tests were used for post hoc analysis of pre-conditioning (BL) vs post-conditioning values within each treatment group. Group differences were analyzed by ANOVA using the difference scores that were calculated as post-conditioning (test) – preconditioning (BL) time spent in the drug-paired chamber. A negative value indicates CPA whereas a positive value indicates CPP. Post-hoc analysis was performed using Dunnett's multiple comparison's test. Where appropriate, analysis was performed to determine whether the difference score was significantly different from zero using a one-sample t-test. Group differences in intensity ratios for immunofluorescence were determined using one-way ANOVAs followed by Dunnett's multiple comparison's test. F values and degrees of freedom for all ANOVAs are presented in Table 2.2 and 2.3.

Table 2.2. Statistical Analysis Results for ANOVA

Factor	F _(DF1, DF2)	P Value
2-way ANOVA of Tumor-induced tactile hypersensitivity (Figure 2.1A)		
Interaction	F _(8, 76) =2.733	P=0.0015
Time	F _(4, 76) =11.23	P<0.0001
Sex	F _(2, 19) =5.46	P<0.0134
2-way ANOVA of Tumor-induced hindlimb impairment (Figure 2.1B)		
Interaction	F _(8, 76) =7.238	P<0.0001
Time	F _(4, 76) =30.23	P<0.0001
Sex	F _(2, 19) =28.21	P<0.0001
2-way ANOVA of BTP in morphine pellet treated rats (Figure 2.2B)		
Interaction	F _(1, 23) =0.3347	P=0.5685
Tumor	F _(1, 23) =31.59	P<0.0001
Drug	F _(1, 23) =0.0409	P=0.8415
2-way ANOVA of Lidocaine pretreatment on BTP (Figure 2.3A)		
Interaction	F _(1, 24) =20.26	P<0.0001
Tumor	F _(1, 24) = 2.99	P=0.0966
Lidocaine	F _(1, 24) = 26.01	P<0.0001
2-way ANOVA of Lidocaine post-treatment on BTP (Figure 2.3B)		
Interaction	F _(1, 18) = 0.1254	P=0.7273
Tumor	F _(1, 18) = 19.42	P=0.0003
Lidocaine	F _(1, 18) = 0.05562	P=0.8162

Table 2.2. Statistical Analysis Results for ANOVA (continued)

Factor	F _(DF1, DF2)	P Value
1-way ANOVA of IB4 intensity ratio (Figure 2.4M)		
Treatment	F _(2,5) =6.93	P<0.036
1-way ANOVA of TRPV1 intensity ratio (Figure 4N)		
Treatment	F _(2,6) =20.97	P<0.002
1-way ANOVA of SP intensity ratio (Figure 2.4O)		
Treatment	F _(2,6) =8.82	P<0.016
1-way ANOVA of CGRP intensity ratio (Figure 2.4P)		
Treatment	F _(2,6) =5.85	P<0.039
2 way ANOVA of Ablation effects on tactile hypersensitivity (Figure 2.5A)		
Interaction	F _(2, 47) =2.518	P<0.0914
IB4 vs TRPV1 ablation	F _(2, 47) =29.68	P<0.0001
Tumor	F _(1, 47) =0.2817	P<0.5981
2 way ANOVA of Ablation effects on BTP (Figure 2.5B)		
Interaction	F _(2, 54) =1.12	P=0.3338
Tumor	F _(2, 54) =5.199	P=0.0086
IB4 vs TRPV1 ablation	F _(1, 54) =1.065	P=0.30368
2 way ANOVA of Ablation effects on bone remodeling (Figure 2.6B)		
Interaction	F _(1, 21) =0.6508	P=0.4289
Drug	F _(1, 21) =0.3508	P=0.2715
IB4 vs TRPV1 ablation	F _(1, 21) =0.0005	P=0.9818

2.4. Results

2.4.1. Tumor-induced Bone Loss, Tactile Hypersensitivity, and Impaired Limb Use

Intratibial injection of rat breast cancer cells produced bone remodeling with bone loss apparent by D12 post-surgery in both male and female rats (Fig. 2.1A). Corresponding tactile hypersensitivity and impaired limb use was observed in both male and female rats (Fig. 1B, C, respectively). No overt differences in pain behaviors were observed between male and female rats. All subsequent experiments were performed in female Fischer 344/NhSD rats.

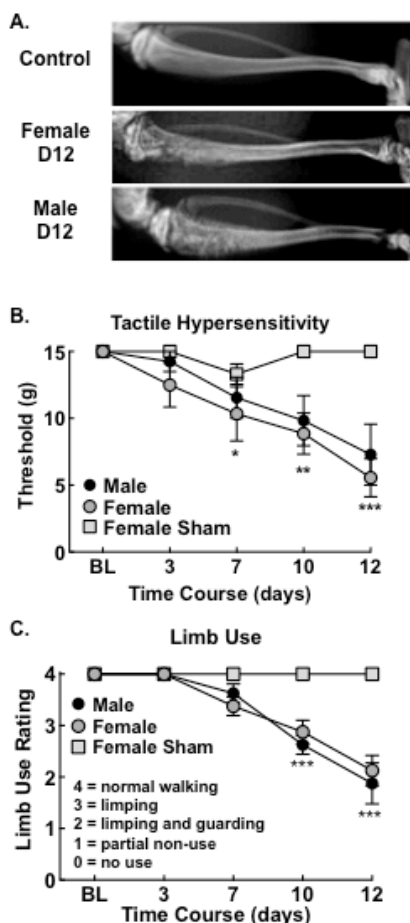


Figure 2.1: Tumor-induced Bone Remodeling, Referred Pain and Impaired Limb Use. A. Representative radiographs demonstrate significant bone loss in male and female rats with fractures developing within D12 post-injection. B. Time-dependent development of tactile hypersensitivity and C. impaired limb use, *p<0.05, **p<0.01, ***p<0.001 vs pre-surgery BL. Graphs are mean \pm SEM, n=8.

2.4.2. Movement-induced Pain Induces CPA That Breaks Through Morphine Infusion

To determine whether movement of the tumor-bearing hind limb induces a transient increase in pain intensity consistent with reports of BTP, rats underwent a single-trial conditioning protocol as outlined by the flow-chart (Fig. 2.2A). Movement of the tumor bearing hind limb significantly reduced time spent in the movement-paired chamber indicating CPA selectively in the tumor-bearing rats (Fig. 2.2A, $**p < 0.01$ vs sham). Sham treated control rats did not show any difference in time spent in the conditioning chambers following movement (Fig. 2.2A; $p > 0.05$ vs 0).

To determine whether movement induced BTP was observed in morphine treated rats, rats underwent a single-trial conditioning protocol as outlined by the flow-chart (Fig. 2.2B). Continuous administration of morphine across 24 hours failed to block movement-induced CPA (Fig. 2.2B), indicating that movement-induced pain breaks through morphine previously demonstrated to block tumor-induced ongoing pain (Remeniuk, Sukhtankar et al. 2015). Both placebo and morphine treated tumor-bearing rats spent significantly decreased amounts of time in the movement-paired chamber compared to sham rats (Fig. 2.2B, $*p < 0.05$ vs sham-placebo, $***p < 0.001$ vs sham-morphine). The degree of CPA did not differ between the placebo and morphine treated tumor bearing rats ($p > 0.05$, Bonferroni t-test). Sham controls did not demonstrate a decrease in time spent in the movement-paired chamber irrespective of placebo or morphine treatment (Fig. 2.2B, $p > 0.05$ vs 0).

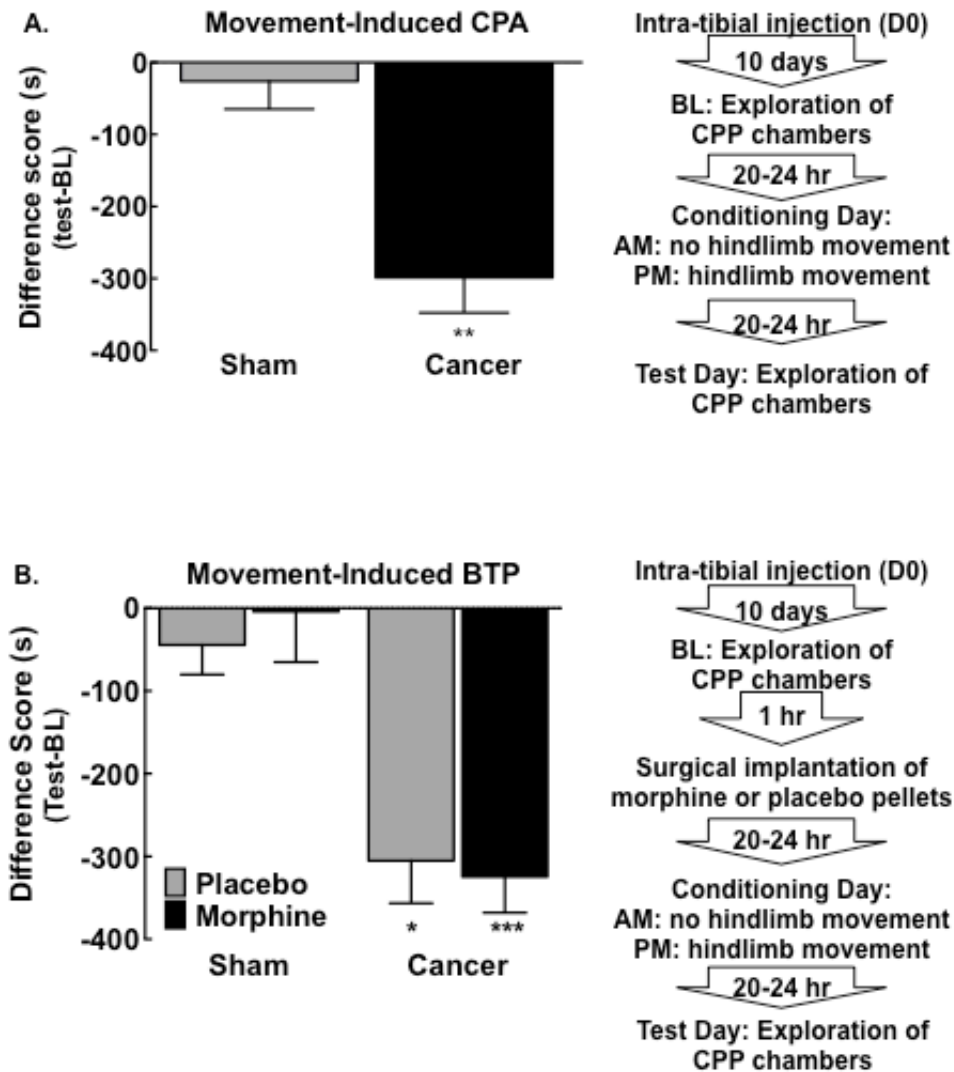


Figure 2.2. Hindpaw Movement Induces Breakthrough Pain in the Presence of Morphine. **A.** Group comparison of difference scores demonstrate that tumor-bearing rats spend decreased time in the chamber paired with movement compared to sham treated rats in the absence of morphine, ** $p < 0.01$ vs. sham, $n = 7$ sham; 12 cancer. **B.** Group comparison of difference scores verify that movement induced equivalent CPA in placebo and morphine treated rats, with both treatment groups demonstrating significant decreases in time spent in the movement paired chamber compared to sham-operated rats, * $p < 0.05$ vs sham placebo; *** $p < 0.01$ vs sham morphine, $n = 5/7$ in placebo/morphine treated sham rats, 6/9 in placebo/morphine treated cancer rats. All graphs show mean \pm SEM.

2.4.3. Blockade of Sensory Afferent Input from Tibia Prevents, But Does Not Reverse Movement-induced BTP

To determine whether saphenous lidocaine induced peripheral nerve block prevented movement-induced BTP, rats underwent a single-trial conditioning protocol as outlined by the flow-chart (Fig. 2.3A). Pretreatment with saline did not alter movement-induced CPA in tumor-bearing rats (Fig. 2.3A, $*p < 0.05$ vs sham saline). In contrast, pretreatment with lidocaine 10 min prior to movement of the cancer-bearing hind limb produced CPP (Fig. 2.3A, $***p < 0.001$ vs sham lidocaine), likely indicating alleviation of tumor-induced ongoing pain. Sham control rats did not alter time spent in the movement-paired chamber following saline or lidocaine treatment 10 min prior to hind limb movement (Fig. 2.3A, $p > 0.05$ vs 0).

To determine whether saphenous lidocaine induced peripheral nerve block following movement blocked BTP, rats underwent a single-trial conditioning protocol as outlined by the flow-chart (Fig. 2.3B). Blockade of afferent input from the tibia by lidocaine administration to the saphenous nerve 10 min following hind limb movement did not reverse movement-induced CPA (Fig. 2.3B). Cancer treated rats show equivalent decreases in time spent in the movement treated chamber following saline or lidocaine administration 10 min following movement (Fig. 3B, $**p < 0.01$ vs sham-saline; $*p < 0.05$ vs sham-lidocaine). Sham rats did not demonstrate CPA to the movement-paired chamber irrespective of saline or lidocaine treatment 10 min post-movement (Fig. 3B, $p > 0.05$ vs 0).

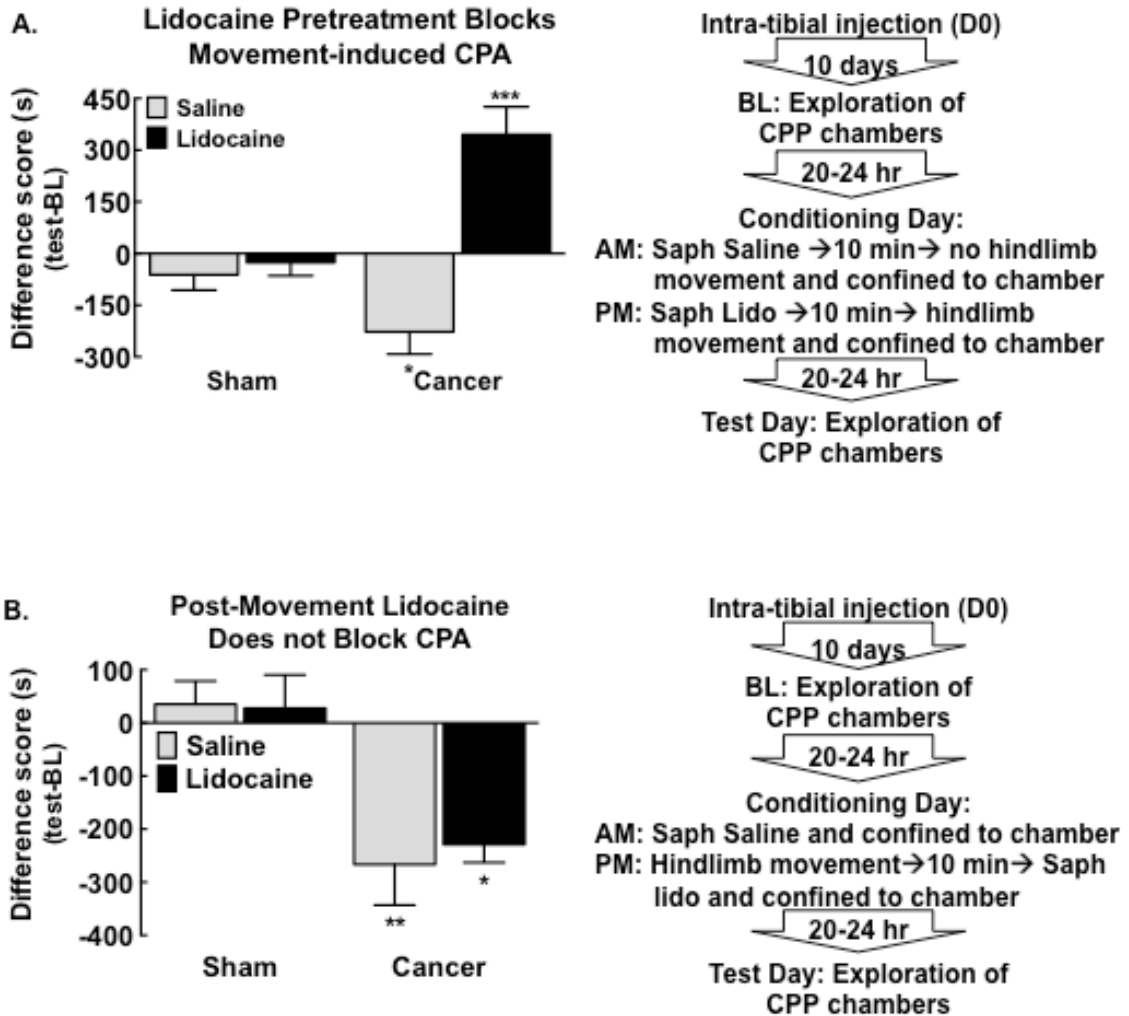


Figure 2.3. Movement-induced Breakthrough Pain is Prevented, but not Reversed, by Saphenous Lidocaine. **A.** Group comparison of difference scores demonstrate that movement of the tumor bearing hindlimb 10 min following saphenous saline induced CPA in tumor-bearing rats, * $p < 0.05$ vs. sham saline. Pretreatment with lidocaine 10 min prior to movement resulted in a significant increase in time spent in the movement-paired chamber, *** $p < 0.001$ vs. sham saline. Neither saline nor lidocaine treatment 10 min prior to movement altered time spent in the movement-paired chamber in sham rats, $n = 7$ /group. **B.** Group comparison of difference scores show that cancer-treated rats demonstrated equivalent decreases in time spent in the movement-paired chamber when treated with saline or lidocaine 10 min following movement, ** $p < 0.01$ vs sham saline, * $p < 0.05$ vs sham lidocaine. Neither saline nor lidocaine treatment 10 min following movement altered time spent in the movement-paired chamber in sham rats. Graphs show mean \pm SEM, $n = 5$ /group sham rats; 7/group tumor bearing rats.

2.4.4. Spinal Capsaicin Eliminates TRPV1, SP, CGRP Immunofluorescence and IB4-SAP Diminishes IB4 Immunofluorescence in the Spinal Cord Dorsal Horn

Immunofluorescent imaging was focused on lamina corresponding to lamina I – IV/V as indicated in the map (Fig. 2.4A). High resolution images of lamina I-II demonstrate that DAPI immunofluorescence (blue) does not overlap with IB4 (green Fig. 2.4B-D)) or TRPV1 (red, Fig. 2.4B); SP (red, Fig. 2.4C) or CGRP, Fig. 2.4D). A representative image demonstrating the regions of interest used to calculate intensity ratios for immunofluorescence in lamina I (TRPV1, SP, or CGRP; L1) and lamina 2 (IB4; L2) and the corresponding control regions (L1con, L2con) in the deep dorsal horn (Fig. 2.4E). Representative images demonstrating co-immunofluorescent stains for TRPV1 (red)/IB4 (green) (Fig. 2.4F); SP/IB4 (Fig. 4G); and CGRP/IB4 (Fig. 2.4H) in the spinal dorsal horn from control treated rats demonstrate similar immunofluorescent patterns to previous reports (Yaksh, Farb et al. 1979, Vulchanova, Olson et al. 2001, Cavanaugh, Lee et al. 2009). Immunofluorescence for TRPV1, SP and CGRP appear in the lamina I region and IB4 immunofluorescence is observed in lamina II region of the spinal cord dorsal horn. Representative images of co-immunofluorescent stains for TRPV1 and IB4 in the spinal dorsal horn of an IB4-SAP treated rat (Fig. 4I) demonstrate that IB4-SAP diminished IB4 immunofluorescence as reported in previous publications (Vulchanova et al., 2001). Representative images from spinal dorsal horns of capsaicin treated rats demonstrate elimination of terminals expressing TRPV1 (Fig. 2.4J), SP (Fig. 2.4K) and CGRP (Fig. 2.4L) without significant alteration of IB4 immunofluorescence.

Intensity ratios of immunofluorescence confirmed that IB4-SAP significantly diminished IB4 immunofluorescence compared to control samples (Fig. 4M, * $p < 0.05$ vs control). IB4-SAP did not alter immunofluorescence for TRPV1 immunofluorescence (Fig. 2.4M). TRPV1 intensity ratios confirm that capsaicin eliminated TRPV1 immunofluorescence, with values dropping to

96.21 ±12.22 % of the internal control ROI (Fig. 2.4N, **p<0.01 vs control). Capsaicin did not alter the immunofluorescence of IB4 (Fig. 2.4N, p>0.05 vs control). SP intensity ratios demonstrate that capsaicin eliminates SP values (Fig. 2.4O, **p<0.01 vs control), with mean intensity ratio dropping to 124.71 ± 11.19 % of the control ROI, a value not different from 100% (p>0.05 vs null hypothesis). Capsaicin did not alter IB4 immunofluorescence compared to control treated samples (Fig. 2.4O, p>0.05 vs control). CGRP intensity ratios demonstrate that capsaicin significantly diminishes CGRP values compared to control treated samples (Fig. 2.4P, *p<0.05 vs control), although the values remain significantly elevated compared to 100% control ROI (p<0.05 vs null hypothesis). IB4-SAP did not alter immunofluorescence of CGRP compared to control treated samples (Fig. 2.4P).

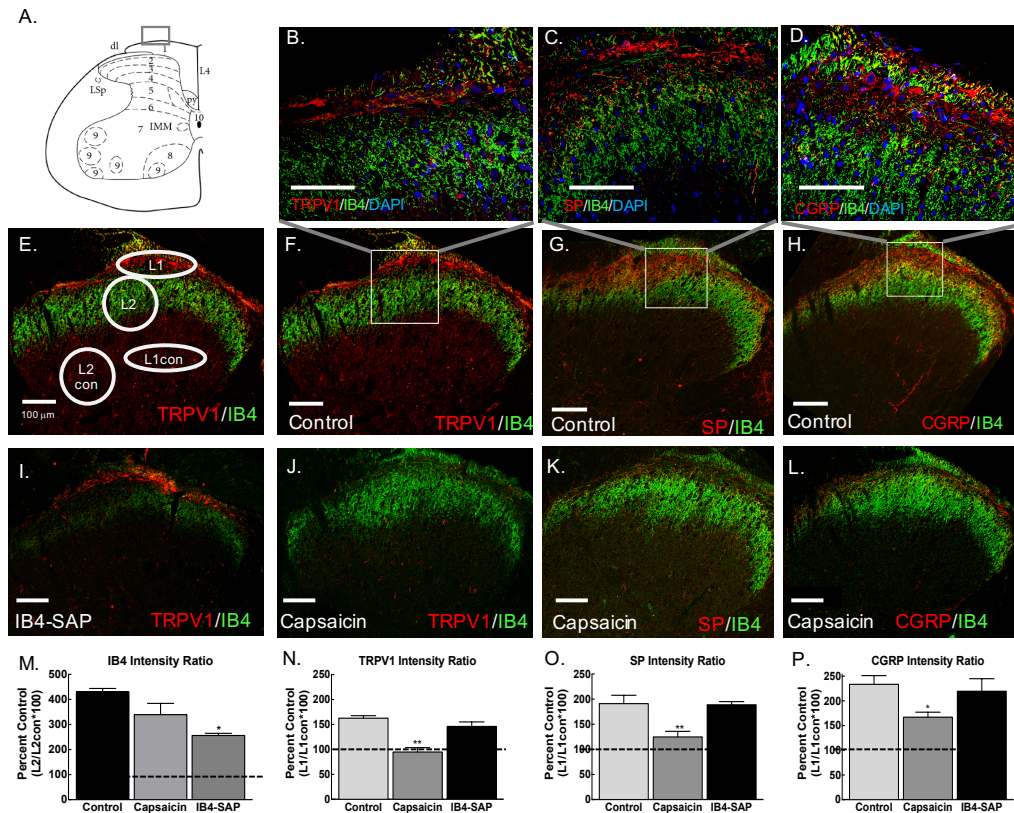


Figure 2.4. Capsaicin Eliminates TRPV1, SP and CGRP Immunofluorescent Staining and IB4-SAP Diminishes IB4 Immunofluorescence in the Spinal Dorsal Horn.

Figure 2.4. (continued). Capsaicin Eliminates TRPV1, SP and CGRP Immunofluorescent Staining and IB4-SAP Diminishes IB4 Immunofluorescence in the Spinal Dorsal Horn. **A.** Spinal map from *The Rat Brain in Stereotaxic Coordinates*, Fourth Edition, Paxinos and Watson ([Paxinos and Watson, 1998](#)). **B.** Representative 40x image inset from panel F of DAPI (blue), IB4 (green) conjugate fluorescence and TRPV1 (red) immunofluorescence, indicating a lack of overlap between IB4, TRPV1 and DAPI signal in a control animal. Images were collected using a single optical section. **C.** Representative 40x image inset from panel G. of DAPI (blue), IB4 (green) conjugate fluorescence and SP (red) immunofluorescence, indicating a lack of overlap between IB4 SP and DAPI signal in a control animal. **D.** Representative 40x image inset from panel H. of DAPI (blue), IB4 (green) conjugate fluorescence and CGRP (red) immunofluorescence, indicating a lack of overlap between IB4, CGRP and DAPI signal in a control animal. **E.** Representative image demonstrating regions of interest (ROI) used for calculation of intensity ratios. For TRPV1, SP, and CGRP, intensity values from an oval ROI targeting a section of lamina 1 (L1) was divided by intensity values from an oval ROI in the deeper lamina L1 control (L1con). For IB4 immunofluorescence, a circle targeting a section of lamina 2 (L2) was divided by L2 control (L2con). This provides a ratio of the target area of interest divided by an internal control. **F.** Representative 20x image demonstrating TRPV1 (red) and IB4 (green) immunofluorescence in a section from a control rat. **G.** Representative 20x image demonstrating immunofluorescence for SP (red) and IB4 (green) in a spinal cord section from a control treated rat. **H.** Representative 20x image demonstrating immunofluorescence for CGRP (red) and IB4 (green) in a spinal cord section from a control treated rat. **I.** Representative image demonstrating immunofluorescence of TRPV1 (red) and reduction of IB4 (green) immunofluorescence. **J.** Representative image demonstrating lack of TRPV1 (red) immunofluorescence following treatment with capsaicin with IB4 (green) immunofluorescence remaining. **K.** Representative image demonstrating lack of SP (red) immunofluorescence following treatment with capsaicin with IB4 (green) immunofluorescence remaining. **L.** Representative image demonstrating absence of CGRP (red) immunofluorescence in capsaicin treated rats with IB4 (green) immunofluorescence remaining. **M.** Intensity ratios demonstrate that there is a significant reduction in IB4-binding fibers within the spinal cord of IB4-SAP treated rats compared to controls. No significant difference was observed in capsaicin treated rats compared to controls. All dashed lines represent ratio value (100) at which there is equivalent mean grey values for L1/L1con or L2/L2con. All graphs represent mean +/- SEM, *p<0.05 vs control; **p<0.01 vs control. **N.** Intensity ratios demonstrate that there is a significant reduction in TRPV1 immunofluorescence in capsaicin treated rats compared to controls. No difference in TRPV1 intensity ratios were observed in IB4-SAP treated rats. **O.** Intensity ratios demonstrate a significant reduction in SP immunofluorescence compared to control, no difference in SP immunofluorescence is observed in IB4-SAP treated rats compared to controls. **P.** Intensity ratios demonstrate a significant reduction in CGRP immunofluorescence in capsaicin treated rats compared to controls with no significant change in CGRP immunofluorescence in the IB4-SAP treated rats. Scale bar indicates 100 μ m.

2.4.5. Functional Blockade of IB4-binding, not TRPV1-expressing Fibers Blocks BTP

The effects of capsaicin-induced elimination of TRPV1+ fibers or IB4-SAP ablation of IB4 binding fibers on tumor-induced tactile hypersensitivity were measured as outlined by the flow-chart (Fig. 2.5A). Cancer-induced tactile hypersensitivity was blocked by spinal administration of IB4-SAP, but not spinal capsaicin (Fig. 2.5A). Cancer-treated rats that had received spinal administration of vehicle or SAP developed tactile hypersensitivity by D12 post-cancer implantation (Fig. 2.5A, ***p<0.001 vs BL). Tumor-bearing rats treated with spinal capsaicin

demonstrated similar tactile hypersensitivity compared to the vehicle control (Fig. 2.5A, *** $p < 0.001$). In contrast, rats treated with spinal IB4-SAP demonstrated tactile withdrawal thresholds that were significantly higher than the vehicle treated rats (Fig. 2.5A, # $p < 0.05$ vs vehicle), and not significantly different from pre-tumor baselines (Fig. 2.5A, $p > 0.05$ vs BL)

The effects of capsaicin-induced elimination of TRPV1+ fibers or IB4-SAP ablation of IB4 binding fibers on movement-evoked BTP was determined using a single-trial conditioning protocol following spinal injection of capsaicin, IB4-SAP or the appropriate vehicle as outlined by the flow-chart (Fig. 2.5B). Movement failed to induce CPA in sham-treated rats irrespective of spinal treatment with capsaicin or IB4-SAP (Fig. 2.5B, $p > 0.05$ vs 0). Cancer-treated rats that received spinal administration of the appropriate intrathecal vehicle demonstrated movement-induced CPA as demonstrated by a significantly lower difference score compared to the sham-treated rats (Fig. 2.5B, * $p < 0.05$ vs sham). Tumor-bearing rats that received spinal capsaicin demonstrated movement-induced CPA represented by a significantly lower difference score compared to sham-treated rats (Fig. 2.5B, ** $p < 0.01$ vs sham). Notably, the difference scores of the spinal vehicle and spinal capsaicin treated tumor-bearing rats did not differ ($p > 0.05$, Bonferroni t-test). Cancer-bearing rats that received spinal IB4-SAP failed to show movement-induced CPA, demonstrated by difference scores that did not differ from sham control rats (Fig. 2.5B, $p > 0.05$).

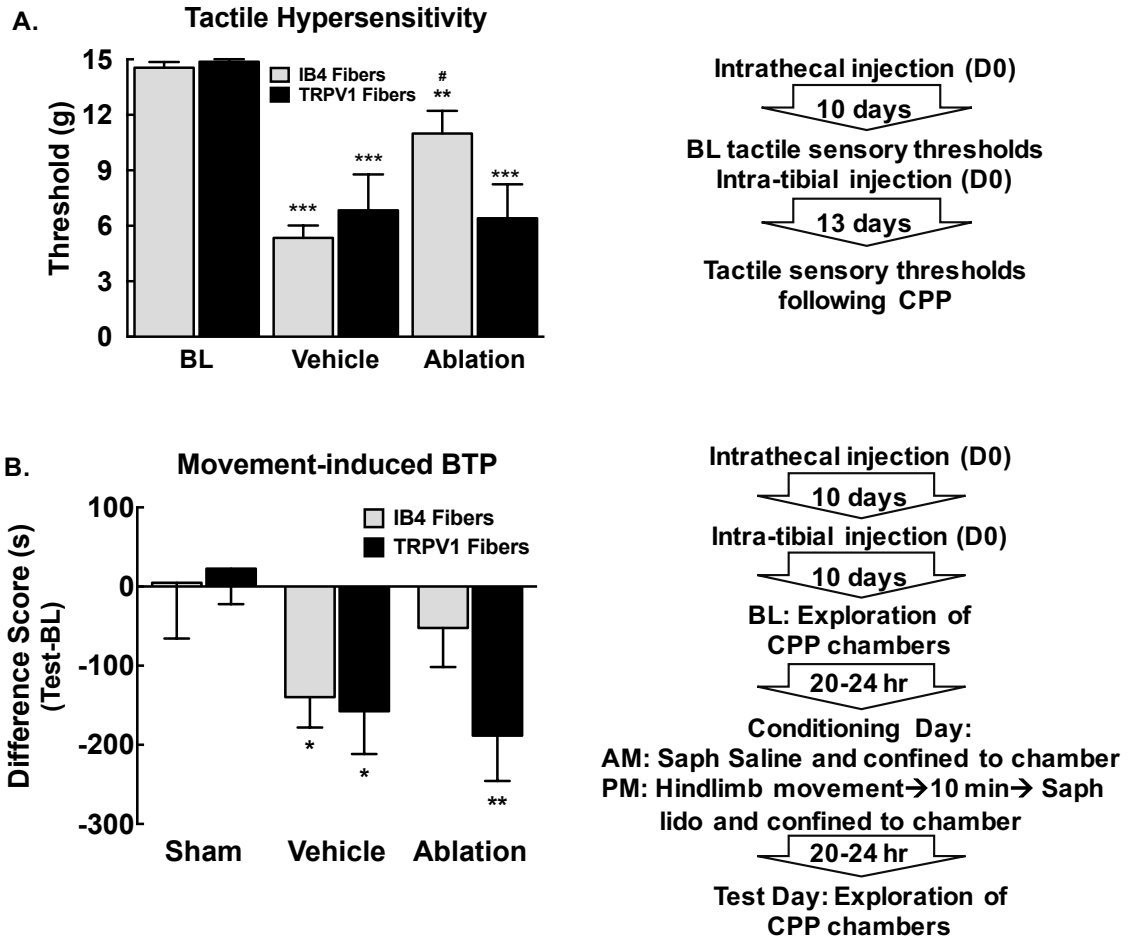


Figure 2.5. Tactile Hypersensitivity and Movement-induced Breakthrough Pain is Dependent on IB4 Positive Fibers. **A.** Spinal administration of IB4-SAP attenuated tumor-induced tactile hypersensitivity. Vehicle treated tumor-bearing rats demonstrated tactile hypersensitivity with paw withdrawal thresholds significantly lower than pre-cancer implantation baselines, *** $p < 0.01$ vs. BL. Ablation of IB4-binding fibers by spinal administration of IB4-SAP attenuated tumor-induced tactile hypersensitivity with paw withdrawal thresholds significantly higher compared to SAP control rats, # $p < 0.05$ vs. SAP. Spinal ablation of TRPV1 expressing terminals in the spinal dorsal horn by spinal administration of capsaicin failed to eliminate tumor-induced tactile hypersensitivity with paw withdrawal thresholds significantly lower than pre-cancer baselines, *** $p < 0.01$ vs. BL. **B.** Group comparison of difference scores demonstrates that movement induced CPA in vehicle treated rats compared to sham controls, * $p < 0.05$ vs sham. Ablation of IB4-binding fibers blocked movement-induced CPA. In contrast, ablation of TRPV1 expressing terminals in the spinal dorsal horn failed to block movement-induced CPA ** $p < 0.01$ vs. shams. Graphs show mean \pm SEM, n (sham) = 10 capsaicin, 10 IB4-SAP; n (cancer) = 9 SAP, 8 capsaicin vehicle, 11 IB4-SAP, 10 capsaicin.

2.4.6. Ablation of IB4 or TRPV1-expressing Fibers Did Not Alter Tumor-induced Bone Remodeling.

Radiograph images show representative bone remodeling illustrating the rating scale that was used to determine tumor-induced bone remodeling D13 post-surgery (Fig. 2.6A). Rats treated with spinal capsaicin or with IB4-SAP did not demonstrate altered bone remodeling compared to their respective vehicle controls (Fig. 2.6B).

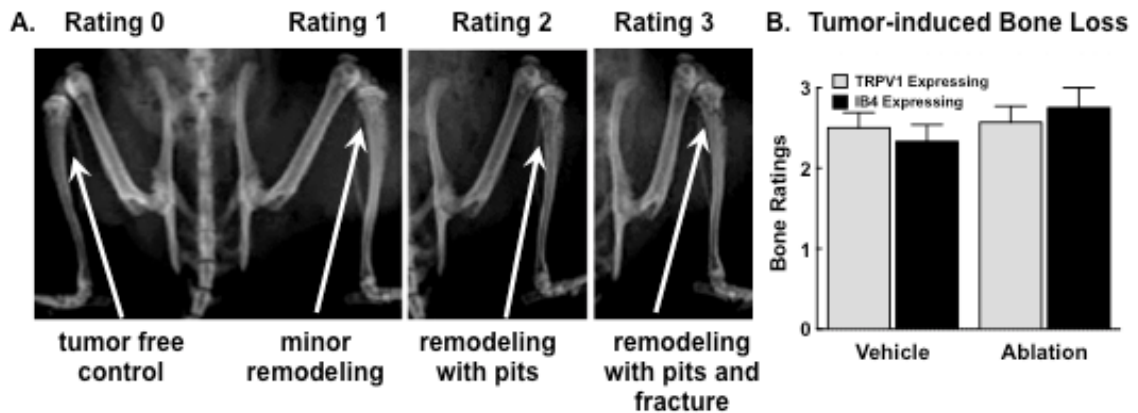


Figure 2.6. Tumor-induced Bone Loss is Observed in all Tumor-bearing Rats Irrespective of Treatment. A. Representative images of bone radiographs demonstrating ratings using a 4-point scale – 0: indicating normal bone; 1: indicating mild bone loss; 2: indicating diffuse bone loss with no pitting or fracture; and 3: indicating bone loss with pitting and/or fracture indicated by total cortical thickness. **B.** All treatment groups demonstrated equivalent levels of bone loss irrespective of spinal treatment. Graph represents mean \pm SEM.

2.5. Discussion

We have developed and characterized a novel measure of movement-evoked BTP in the setting of morphine-controlled ongoing pain in a rat model of cancer-induced bone pain. This measure uses the motivational aspects of pain averseness to capture a movement-triggered transient increase in the apparent intensity of cancer-induced bone pain. When this event is paired with a distinctive context, rats show avoidance of the chamber in a subsequent trial producing conditioned place aversion (CPA). This approach is consistent with clinical observations in which patients with bone metastases report transient increases in pain intensity

that can be triggered by voluntary (e.g. switching positions) or involuntary (e.g. cough) movement. Notably, this is relatively common in patients with skeletal metastases and can diminish daily activity of these patients due to their desire to avoid triggering BTP, greatly diminishing these patients' quality of life (Mercadante 2015).

2.5.1. Reverse Translation of BT Pain

Hind limb movement prior to placement into the pairing chamber produced CPA selectively in tumor bearing rats indicating that the movement-triggered increase in pain is aversive and provides learning that motivates animals to avoid that chamber. Movement-induced CPA is observed in rats undergoing morphine treatment previously demonstrated to control tumor-induced ongoing pain (Remeniuk, Sukhtankar et al. 2015). Notably, the defining feature of BTP is that it occurs in patients on opioid medication that is controlling the persistent background pain (Portenoy and Hagen 1989, Portenoy and Hagen 1990, Mercadante 2015). Moderate-to-severe cancer pain is often treated with extended release opioids that engage the mu-opioid receptor (MOR) (Paice and Ferrell 2011, Mercadante 2015). Therefore, our observations show reverse translation from the clinic to the rat model of cancer-induced bone pain. Opioids predominately act to modulate affective dimensions of pain by actions at opioid receptors within the brain (Fields 2004, Navratilova, Atcherley et al. 2015). Additionally, MOR agonists may act at receptors localized on primary afferent nociceptors and in the spinal cord (Fields 2004, Ossipov, Dussor et al. 2010). The clinical observations and our data indicate that movement likely engages additional nociceptive drive that is insensitive to MOR agonists at doses that control ongoing pain.

2.5.2. Potential Role of Peripheral and Central Sensitization

Nociceptors are likely to be sensitized as a consequence of tumor or immune-derived factors within the intramedullary space (Mantyh 2013, Falk and Dickenson 2014, Mantyh 2014). In addition, the ongoing pain from the tumor bearing bone can produce spinal sensitization (Urch, Donovan-Rodriguez et al. 2003, Yanagisawa, Furue et al. 2010, Falk, Bannister et al. 2014, Mantyh 2014). We propose that both peripheral and central sensitization amplifies nociceptive input from movement-evoked stimulation of the tumor-bearing limb resulting in a transient increase in pain intensity that occurs in the setting of opioids controlling the persistent background ongoing pain. Preclinical studies demonstrated that spinal cord neurons show enhanced responses to evoked stimuli and wide dynamic range neurons display an increase in receptive field, hallmarks of spinal sensitization (Urch, Donovan-Rodriguez et al. 2003, Falk, Bannister et al. 2014). These changes are observed in the setting of morphine and have been proposed to underlie opioid resistant allodynia and BTP (Urch, Donovan-Rodriguez et al. 2005). Such signaling likely increases the intensity of pain experienced, thereby also increasing the affective/motivational component of the tumor-induced pain (Fields 1999). The transient increase in pain and related unpleasantness surpasses the ability of the onboard dose of morphine to control the pain resulting in the requirement for additional rapid onset opioids as seen in the clinical setting, i.e., BTP.

2.5.3. Mechanistic Difference Between Initiation and Maintenance of BTP

Sensory input from the tumor-bearing bone is required for initiation of BTP. Saphenous nerve block administered 10 min prior to movement of the tumor-bearing hind limb prevented movement-induced BTP and induced CPP. This observation indicates that the peripheral nerve block not only prevented the movement-triggered BT pain, but also blocked tumor-induced

ongoing pain. Therefore, the rats experience pain relief in the lidocaine/movement paired chamber. Thus, pain relief is the motivating factor that results in the increased time spent in the chamber paired with nerve block and movement. This replicated our previous findings that peripheral nerve block produces relief from tumor-induced ongoing bone pain (Remeniuk, Sukhtankar et al. 2015). In contrast, blockade of sensory input following hind limb movement failed to block CPA. These observations suggest that once established, blocking sensory input from the tumor-bearing bone is no longer sufficient to reverse movement-induced BTP. We speculate that one possible explanation is the engagement of reverberating circuits that maintain activity within the spinal cord, or between the spinal cord and central nuclei, independently from peripheral input. Such altered processing could account for prolonged withdrawal responses to noxious pinprick as reported following chronic constriction injury of the sciatic nerve (Bennett and Xie 1988). A reverberating circuit between spinal cord dorsal horn and the dorsal reticular nucleus within the caudal medulla has been proposed to promote enhanced response capacity of spinal neurons to noxious stimulation and implicated in acute pain responses to noxious heat and formalin (Lima and Almeida 2002). Such reverberating circuitry may be critical in maintaining BTP and deserves further study.

2.5.4. Separate Roles of TRPV1+ and IB4-binding Fibers in BT Pain

The observation that saphenous nerve block prevents movement-induced CPA suggests that initiation of BTP is dependent on sensory input from the tumor-bearing bone. Our data indicate that IB4 binding fibers mediate movement-induced breakthrough cancer pain and referred tactile hypersensitivity, whereas TRPV1+ fibers do not. These observations are consistent with studies demonstrating that functional blockade of TRPV1+ fibers fails to alter responses to noxious mechanical stimulation and tactile hypersensitivity (Ossipov, Bian et al.

1999, Cavanaugh, Lee et al. 2009, Scherrer, Imamachi et al. 2009, Okun, DeFelice et al. 2011). Our findings are also consistent with studies demonstrating that ablation of IB4 binding fibers blocks tactile hypersensitivity in preclinical models of inflammation, neuropathic pain and cancer-induced orofacial pain (Stucky and Lewin 1999, Vulchanova, Olson et al. 2001, Joseph, Chen et al. 2008, Cavanaugh, Lee et al. 2009, Ye, Dang et al. 2012). Given these data, we propose that movement recruits TRPV1 negative nociceptive fibers resulting in an increased pain signal that initiates an episode of BTP that is not adequately prevented by peripheral or central actions of opioids used to control background persistent ongoing pain.

Following capsaicin, we saw reduced CGRP and complete elimination of SP immunofluorescence and TRPV1+ fiber terminals in the spinal dorsal horn, observations consistent with previous studies (Yaksh, Farb et al. 1979, Cavanaugh, Lee et al. 2009). IB4-Saporin eliminated IB4 immunofluorescence indicating elimination of input from IB4 binding sensory afferent fibers. The absence of sensory input by these nerve terminals within the L3 segment of the lumbar spinal cord likely eliminates much of the sensory input from the saphenous nerve, previously demonstrated to be the primary innervation for the rat tibia (Ivanusic 2009, Kaan, Yip et al. 2010). Previous studies have suggested a lack of IB4 binding fibers in mouse models of cancer-induced bone pain (Jimenez-Andrade, Mantyh et al. 2010, Castaneda-Corral, Jimenez-Andrade et al. 2011). In contrast, retrograde labeling techniques indicate that IB4 binding fibers do innervate the intramedullary space and the periosteum of the rat tibia (Ivanusic 2009, Kaan, Yip et al. 2010). It is unclear whether the discrepancies between these reports are due to methodological differences or species differences. Irrespective of whether IB4 binding fibers innervate the bone, it is likely that sensory input from tissue surrounding the bone may also contribute to the initiation of movement-evoked BTP.

Spinal capsaicin was demonstrated to reduce SP content within sensory fibers within seven days (Yaksh, Farb et al. 1979). Such observations indicate that the capsaicin-induced blockade of sensory input by TRPV1+ fibers in our studies occurred prior to tumor cell injection and subsequent growth of tumor cells within the tibia, thereby eliminating ongoing input from TRPV1+ nociceptive fibers throughout the experiment. Our data demonstrate that elimination of signaling by TRPV1+ fibers is not sufficient to block movement-induced CPA or referred pain as measured by tactile hypersensitivity in the ipsilateral hind paw. This is consistent with other observations that long-term desensitization of TRPV1 expressing fibers by systemic administration of the ultra-potent capsaicin analogue resiniferotoxin (RTX) blocks thermal and ongoing pain, but fails to block development of tactile hypersensitivity in other chronic pain models (Ossipov, Bian et al. 1999, King, Qu et al. 2011, Okun, DeFelice et al. 2011). Our observations of hind paw tactile hypersensitivity, a measure of referred pain, and initiation of BTP by a normally non-noxious stimulus suggest that the tumor bearing rats developed central sensitization in the absence of input from TRPV1 expressing fibers. Previous studies have demonstrated that development of central sensitization is dependent on input from nociceptive afferents, presumably C-fibers (Gracely, Lynch et al. 1992, Sang, Gracely et al. 1996). It is likely that sustained input from non-TRPV1 nociceptive fibers is sufficient to develop central sensitization that mediates hypersensitivity to non-noxious mechanical stimulation.

Further research is warranted to examine subpopulations of sensory fibers in relation to bone pain. As noted above, single cell RNA sequencing studies have demonstrated that there are many potential subcategories of sensory fibers, with as many as 11 types of sensory neurons in the mouse DRG (Usoskin, Furlan et al. 2015). Moreover, some studies have indicated overlap of CGRP in IB4 binding neurons in species and site-specific patterns (Aoki, Ohtori et al. 2005, Hwang, Oh et al. 2005, Price and Flores 2007). Future studies using techniques such as single cell

capture and RNAseq of DRG cells that have been retrogradely labeled from the bone, periosteum and perhaps the surrounding tissue are necessary to clarify potential subpopulations of IB4 binding neurons that may mediate BT pain. Additionally, studies examining corresponding protein expression and the relative functional contribution of observed subpopulations of fibers innervating the bone are necessary.

Our data indicate distinctive mechanisms underlying tumor-induced ongoing and BTP. As with all preclinical studies, future studies are required to show reproducibility of these findings across different strains and species. This highlights the need to determine whether therapeutic strategies currently under development block both ongoing and BTP. Notably, advances in non-opioid therapies for ongoing pain are urgently needed to diminish reliance on opioids irrespective of whether they effectively block BTP. Alternatively, novel compounds targeting IB4 binding nociceptors may improve pain management for cancer pain patients and other patient populations suffering from BTP that is inadequately treated by currently available medications.

2.6. Acknowledgments

Contributing Authors: Joshua Havelin,¹ Ian Imbert,¹ Devki Sukhtankar,² Bethany Remeniuk,² Ian Pelletier,¹ Jonathan Gentry,¹ Alec Okun,³ Timothy Tiutan,³ Frank Porreca,^{2,3} and Tamara E. King¹

¹Department of Biomedical Sciences, College of Osteopathic Medicine, Center for Excellence in the Neurosciences, University of New England, Biddeford, Maine 04005, and ²Department of Cancer Biology, Arizona Cancer Center, and ³Department of Pharmacology, College of Medicine, University of Arizona, Tucson, Arizona 85724

Author contributions: F.P. and T.E.K. designed research; J.H., I.I., D.S., B.R., I.P., J.G., A.O., T.T., and T.E.K. performed research; J.H., I.I., D.S., B.R., F.P., and T.E.K. analyzed data; F.P. and T.E.K. wrote the paper.

CHAPTER 3

UTILIZING OPTOGENETICS TO INVESTIGATE THE ROLE OF PERIPHERAL NEURONS INVOLVED IN CANCER-INDUCED BONE PAIN IN THE MOUSE

3.1. Introduction

3.1.1. Background of Fiber Types in Cancer-induced Bone Pain

Previous work by Patrick Mantyh and colleagues demonstrated a critical role for peptidergic nociceptors (i.e. CGRP, SP, TRPV1 expressing) in the role of CIBP. As mentioned previously, both through the use of IHC and a transgenic reporter mouse, work by this group had demonstrated the presence of CGRP+ fibers in naïve bone, and pathological sprouting of these fibers following cancer cell implantation and growth (Mach, Rogers et al. 2002, Jimenez-Andrade, Mantyh et al. 2010). Work by this group also demonstrated that sequestration of NGF by a primary antibody results in diminishment of pathological sprouting of these fibers and evoked pain behaviors (Jimenez-Andrade, Bloom et al. 2010). These findings coincide well with observations in the mouse demonstrating a lack of non-peptidergic nociceptors (IB4-binding, P2X3 and/or MrgD expressing) in the innervation of the bone and periosteum, leading much of the CIBP field to believe they play little role in communicating pain in preclinical models of CIBP in the mouse (Jimenez-Andrade, Mantyh et al. 2010). Pharmacological work using a primary antibody to NGF and an antibody that targets the cation channel P2X3 to investigate a comparative role for peptidergic vs non-peptidergic nociceptors was also investigated (Guedon, Longo et al. 2016).

The role for each antibody, being to either sequester NGF as previously described in Pat Mantyh's work, or presumably block the ion passage pore in the P2X3 channel, allowing for a side by side comparison in behavioral changes that these two agents may have. This was the

first attempt to assess the role of these fibers side by side in a behavioral paradigm in CIBP. This publication demonstrated a role for blocking the P2X3 channel in alleviating tactile hypersensitivity that develops after tumor growth consistent with the belief that non-peptidergic nociceptors convey mechanical nociceptive input (Cavanaugh, Lee et al. 2009). While sequestration of NGF ameliorated tactile hypersensitivity and measures of “skeletal pain” quantified by weight bearing away from the cancer afflicted limb, rearing, and nocifensive behaviors typical of CIBP in preclinical models (Guedon, Longo et al. 2016). This latter observation is likely due to the blunting of pathological sprouting of TrkA+ (and CGRP+) fibers within the bone and the role this plays in CIBP, as work has demonstrated this treatment does not blunt tumor growth or bone destruction.

While interesting, the most provocative piece of data shared in this body of work was the ability for the NGF antibody to reverse off-set weight bearing, and the failure of the P2X3 antibody to do so. One interpretation of this as the authors concluded, is that blockade of P2X3 fails to alleviate pain from the bone, however, while convincingly reliable, it is still debated whether weight bearing is effective in assessing ongoing/evoked pain from a pathological joint or bone. Additionally, this work did not directly assess the 2 populations of fibers themselves e.g. peptidergic vs non-peptidergic. Rather, this work investigated the function of the P2X3 channel specifically, which is primarily expressed on non-peptidergic fibers, and added to the body of work supporting the efficacy of NGF sequestration in reducing CIBP. This leaves the question of whether or not the non-peptidergic fibers themselves play a role in measures of CIBP, as blockade of one receptor population on a neuron does not necessarily silence the entire neuron’s function. Our work (Havelin et al. 2017) in the rat implicates a role for fibers that bind IB4 (i.e. non-peptidergic) in evoked BTP.

However, there is the possibility that these observations are a result of a species difference. Differences in the populations of fibers has previously been described between species and anatomical location (DRG versus TG) by Price et al 2009, and differing innervation patterns reported by Ivanusic 2009, and Kaan et al. 2010 in the rat vs Pat Mantyh's work in the mouse (Price and Flores 2007, Ivanusic 2009, Kaan, Yip et al. 2010). Classically peptidergic fibers have been implicated in driving thermal nociception and spontaneous pain while non-peptidergic fibers have been implicated in mechanical pain in both mouse (Cavanaugh, Lee et al. 2009, Scherrer, Imamachi et al. 2009) and rat studies (Ossipov, Bian et al. 1999, Vulchanova, Olson et al. 2001, King, Qu et al. 2011, Havelin, Imbert et al. 2017). Therefore, we wanted to examine whether the differential role of peptidergic and non-peptidergic fibers in the rat translates to the mouse. The potential for analgesic targets that may exist on the non-peptidergic population of fibers that inhibit the fiber rather than a single channel (i.e. the P2X3 channel) would be a worthwhile discovery. Further, lack of evaluation of peptidergic fibers in alleviating ongoing or breakthrough pain in models of cancer-induced bone pain sparked our interest in investigating the potentially differing roles these fiber populations may play in treating cancer-induced bone pain.

3.1.2. Justification of Targeting Subpopulations of Sensory Neurons

Nav1.8 Expressing Fiber Population. Nav1.8 is a voltage gated sodium channel that allows the conductance of sodium in a tetrodotoxin-resistant manner and is expressed on peripheral neurons (Shields, Ahn et al. 2012). Nav1.8 has been used as a selective marker for nociceptive neurons for at least 10-15 years, and has been implicated to be critical to nociception in a number of publications (Akopian, Souslova et al. 1999, Nassar, Stirling et al. 2004). Interesting clinical correlates have been demonstrated, in which gain of function

mutations in human Nav1.8 correlate with some patients that experience “painful neuropathy” (Han, Huang et al. 2016). The generation of the Nav1.8-cre mouse by John Woods group has allowed for the extensive use of the cre-lox system to target these nociceptive neurons for nearly 2 decades (Nassar, Stirling et al. 2004). While the original publication determined a critical role of the Nav1.7 channel in nociception normally expressed on Nav1.8 expressing fibers, subsequent work has highlighted the role of the fibers that express Nav1.8. While its utilization as a marker by crossing the cre mouse with a reporter line (cre-dependent reporter) for purely nociceptive neurons has its limitations as demonstrated by Shields et al. 2012, functional evaluation and involvement of Nav1.8 fibers in nociception implies their direct involvement in transducing nociceptive stimuli (Daou, Tuttle et al. 2013, Uhelski, Bruce et al. 2017). Interestingly, while in models of neuropathic injury some reports demonstrate a down regulation of Nav1.8 channels (Laedermann, Pertin et al. 2014) there are alternative reports that suggest in models of CIBP Nav1.8 expression actually increases (Liu, Yang et al. 2014). Beyond this, due to the well-characterized role of Nav1.8 fibers in transducing nociceptive input in preclinical models of pain (Bonin, Wang et al. 2016, Daou, Beaudry et al. 2016, Uhelski, Bruce et al. 2017), we hypothesized that transiently optogenetically silencing this population of fibers would block ongoing pain in our model of CIBP.

MrgD Expressing Fiber Population. Our interest in MrgD expressing fibers lies not necessarily in the function of the receptor, but the function of the cells that express MrgD. Although the effects of activating or inhibiting MrgD are not ignored in the grand scheme of our work. The GPCR MrgD was first reported by Dong et al. 2001 (Dong, Han et al. 2001) along with a number of other GPCRs in the Mrg family. Unique expression patterns of the protein were reported in sensory neurons within the DRG and TG in neonatal and adult mice, with special attention being given to a seeming overlap of MrgD expression in nociceptors (Dong, Han et al.

2001). Critical to its use as a cre-line, the authors demonstrated that between development and adulthood in the mice, expression patterns of MrgD became more restricted (Dong, Han et al. 2001). Analysis of expression between preclinical species was performed by Zylka et al 2003, who reported many of the same findings, including MrgD expression overlap with the IB4-binding population of sensory neurons in the mouse, as well as overlap of expression with the GDNF-receptor c-RET (Zylka, Dong et al. 2003). Interestingly while in the mouse the Mrg family of GPCRs can be subdivided into the MrgA, MrgB, MrgC and MrgD families, the rat and gerbil have a much less diverse repertoire of this family of GPCRs (Zylka, Dong et al. 2003). While humans do have an MrgD ortholog, potentially allowing rapid translational pharmacological work from preclinical models, humans have a set of “MrgX” genes that do not have “clear” orthologs to rodents but closely resemble the MrgA subfamily of Mrg GPCRs, highlighting the potential for translational work between species (Zhang, Taylor et al. 2005).

The generation of a transgenic fluorescent reporter mouse by Zylka et al. 2005, expanded on the previous work utilizing RNA specific in-situ hybridization. Namely that expression of MrgD appeared to be restricted to non-peptidergic sensory neurons, with distinct lack of co-expression with markers for peptidergic sensory neurons such as CGRP and TRPV1, an observation that may not directly translate to primates let alone humans (Zhang, Taylor et al. 2005, Zylka, Rice et al. 2005). Work by this group demonstrated that MrgD innervation is unique to a specific layer within the skin, the stratum granulosum, as well as the stratum gelatinosa of the spinal cord (lamina II) within the spinal cord (Zylka, Rice et al. 2005). The authors of this paper demonstrated that protein expression of MrgD coincided well with the RNA transcription previously reported (Dong, Han et al. 2001). Wang and Zylka 2009, demonstrated that synaptic terminals from MrgD afferent fibers were capable of generating excitatory postsynaptic currents in a number of types of lamina II spinal cord neurons in a monosynaptic fashion (Wang and Zylka

2009). In line with this work, Braz et al. 2005 investigated where this population of neurons project into higher orders of the CNS. Finding that projections from DRG cells selectively labeled by Nav1.8 induced expression of wheat germ agglutinin, project to interneurons in lamina II of the spinal cord dorsal horn. Beyond this, projections from these interneurons continue on to lamina V, and the amygdala, hypothalamus and other regions of the CNS, reportedly unique from the projections from the peptidergic class of peripheral nociceptors (Braz, Nassar et al. 2005).

While much is still unknown about implications of activating the MrgD receptor itself (other than inducing itch), some work has uncovered ligands capable of activating this population of neurons in-vitro and ex-vivo (Liu, Sikand et al. 2012). Beta-alanine a small amino acid, appears to be the endogenous ligand able to activate the MrgD receptor, as reports suggest it has nearly a 10 fold lower EC50 to GABA, its closest competitor (Shinohara, Harada et al. 2004). This work additionally indicated that activation of MrgD may result in the intracellular activation of Gq and Gi classes of G-proteins, on small diameter and nociceptive cells, leading authors to believe the possibility that activation of MrgD plays a role in regulating nociceptive signals in the periphery, differential to that of GABA (Shinohara, Harada et al. 2004). More diffuse investigation of MrgD expressing neurons has revealed that they have many of the electrophysiological hallmarks of nociceptors as well. Dussor et al. 2008 revealed that these neurons respond to extracellular ATP and can generate “long-duration action potentials” that are TTX-resistant, and that these cells possessed calcium currents that were inhibited the MOR agonist DAMGO, an effect blocked by naloxone. These findings led the authors to the conclusion that MrgD expressing fibers likely respond to keratinocyte release of ATP (Dussor, Zylka et al. 2008). Due to structural and anatomical descriptions of these fibers compared to peptidergic (CGRP expressing), they may play a unique role in transducing nociceptive stimuli from the skin

(Dussor, Zylka et al. 2008). An interesting body of work from Rau et al. also demonstrated that knocking out MrgD in mice resulted in decreased sensitivity to heat, mechanical sensitivity, cold, and demonstrated in-vitro that activation of MrgD via beta-alanine results in the hyper excitability of the neuron (Rau, McIlwrath et al. 2009).

While investigation of the cellular mechanisms of the MrgD receptor and MrgD expressing fibers has garnered interesting findings and implications to the pain field, little work has been published as to the role of the intact fiber in behavioral models. This may be a result of the challenges of effectively targeting these cells in a whole living animal, or a repercussion of the approaches used to target these cells in-vivo. MrgD, has a proposed >90% overlap in identity with IB4-binding neurons which was classically used to characterize non-peptidergic fibers (Cavanaugh, Lee et al. 2009). This population of neurons, much like the IB4-binding neurons, has been shown to be critical in the transduction of mechanical nociception, while not directly being involved in the transduction of thermal nociceptive input from the periphery (Cavanaugh, Lee et al. 2009). This may imply a unique function for these neurons (Cavanaugh, Lee et al. 2009). Another convincing piece of work targeting these cells in whole animals was a side by side comparison performed by Beaudry et al. 2017, where authors demonstrated that optogenetic activation of TRPV1 expressing neurons resulted in noxious behavior and an aversive state, but activation of MrgD afferents was not aversive to the animals (Beaudry, Daou et al. 2017).

Preclinical evidence in the mouse suggests that MOR and DOR may be differentially expressed on nociceptive fiber subtypes and play differing roles in alleviating modalities of pain in the mouse (Scherrer, Imamachi et al. 2009). Given the observations by Scherrer's group, we tested the hypothesis that the administration of the peptidergic MOR agonist DAMGO would alleviate ongoing pain in a model of CIBP in the mouse, whereas the peptidergic DOR agonist

Deltorphin II would fail to do so. The basis for this hypothesis relies on previous implications of the role of peptidergic, presumably MOR expressing nociceptive fibers, in the periphery transducing pain from the cancer-afflicted limb (Jimenez-Andrade, Mantyh et al. 2010) and clinical observations that MOR agonists can block persistent cancer-induced bone pain (Paice and Ferrell 2011, Mercadante and Bruera 2016).

It was our belief that due to MOR agonists inability to treat breakthrough pain, and the potential for differential expression of MOR and DOR on nociceptive fibers we would see a distinct difference in MOR and DOR agonists to ameliorate ongoing versus breakthrough pain (Havelin, Imbert et al. 2017). Here we report our utilization of both classic and novel approaches to investigate and demonstrate the differential effects on pain behaviors these fiber populations have in cancer-induced bone pain. Due to the lack of published work able to directly assess the role of non-peptidergic fibers, and our success in implicating a role for non-peptidergic fibers in a model of BTP in the rat, we chose to use a pharmacological and optogenetic approach to selectively and transiently silence targeted populations of nociceptive fibers. This approach would allow us to address some of the short-comings of our work in the rat, centered mainly around limitations associated with ablating neurons and the responsive neural adaptations that may arise after.

Working with our collaborators at the Canadian Neurophotonics Center in Quebec, we were able to selectively silence the fibers in the Nav1.8-cre and inducible Mrgpd^{CreERT2} (MrgD-cre) line of mice, by selectively expressing the light sensitive ArchT pump in these fibers. Initial work utilized a selectively cre-activated Flex viral vector to activate and induce expression of the ArchT cassette, while subsequent work utilized the ArchT transgenic mouse from Jackson labs. By delivering light to the lumbar section of the spinal cord using methods published by Bonin et

al. 2016, we have successfully modified nociceptive behavioral responses both in a model of CIBP and AITC-induced nociception.

We attempted to adapt our measure of hind limb movement-induced breakthrough pain that we previously characterized in the rat (Havelin, Imbert et al. 2017) to the mouse. However, this proved more difficult than simply repeating the approach utilized in the rat and instead characterized novel behavioral measures in response to hind limb movement.

3.1.3. Brief Overview of Utility of Optogenetics in the Study of Pain

The relatively recent integration of light sensitive ion channels and pumps into the field of neuroscience research has undoubtedly been one of the largest advances in decades. The ability to selectively activate or inhibit a neuron with spatial and temporal precision will play an immense role in furthering our understanding of how the nervous system functions both under “normal” circumstances and pathological ones. Additionally, the inability to resolve spatial and temporal challenges with tools that have been widely used has limited the progress of the pain field in locating anatomical and molecular changes in circuitry due to pathological pain. Perhaps one day this technology can also be used to treat pathologies in the clinic. To better understand where these tools came from and likely where they will go in the near future, it may help to give some background into their function and history. Several excellent reviews already exist encompassing the promising adventure and tale of optogenetics and its utilization in pain research (Copits, Pullen et al. 2016, Xie, Wang et al. 2018). Rather, I will have a brief explanation highlighting some key features that contribute to our utilization of this tool in studying CIBP.

The first critical piece of optogenetics was the discovery of microbial opsins, proteins isolated from various single celled organisms that respond with varying efficiencies to different wavelengths of light (Copits, Pullen et al. 2016). As a result of their native function, ion transport

across a membrane in response to light, they have lent themselves to a very suitable use in neuroscience research. Depending on the opsin, activation can result in a net increase in positive charge within a neuron, causing it to depolarize and become activated. Two opsins used for this are channel rhodopsin and the improved version channel rhodopsin 2 (Daou, Tuttle et al. 2013, Daou, Beaudry et al. 2016, Browne, Latremoliere et al. 2017). These 2 opsins respond to blue light and once activated allow cations to flow into the cell causing a wave of depolarization. With application of the correct parameters, it has been reported that this can be used to generate single action potentials, which when translated to an in-vivo prep, are capable of generating nocifensive behavioral responses in animal that express ChR2 under the TRPV1 promoter (Browne, Latremoliere et al. 2017).

While one major use of opsins results in the depolarization of neurons, activation of another major classes of opsins results in a net negative charge in the neuron, resulting in inhibition of the neuron. Two hyperpolarizing opsins exist and are widely used, the first being halorhodospin which is activated by yellow light and allows for chloride ions to flow through the cellular membrane. The other major opsins being archaerhodopsin (Arch) and archt-rhodospins (ArchT) which are activated by orange to green light and actively pump protons to the exterior of the cellular membrane. Both of these opsins net function result in the hyperpolarization of the interior of neurons, resulting in inhibition of the neuron (Xie, Wang et al. 2018). While at surface level both of the mechanisms of these opsins would seem to work to the same extent, our work was directed towards the use of the ArchT opsin. This was due to the observation that activation of halorhodospin can result in a net change in the chloride gradient within a cell, which in turn allowed for the unintentional depolarization of a cell following exposure to GABA (Raimondo, Kay et al. 2012). This observation was not made in work with the Arch pump (Raimondo, Kay et al. 2012). While Arch has been implemented and used successfully to inhibit

neuronal activity (Copits, Pullen et al. 2016, Daou, Beaudry et al. 2016, Xie, Wang et al. 2018), our work utilized the optimized ArchT proton cassette described by Han et al. 2011. Han and colleagues describe the ArchT pump isolated from *Halorubrum* strain TP009 in their work comparing to Arch isolated from *Halorubrum sodomense*, as readily trafficked in mammalian cells and a more light sensitive tool capable of inhibiting neurons. Work by our collaborators demonstrated a unique approach for delivery of the ArchT cassette and sight of neuronal inhibition that aided in the direction of our work, and laid feasibility for our approach in the mouse (Bonin, Wang et al. 2016).

The next challenge of using optogenetic intervention in an in-vivo setting is the hurdle of delivery of the opsin of choice as well as light to activate it. Several delivery methods of an opsin cassette are widely used currently for in-vivo, each with their own advantages and challenges. The first utilized here in this work and widely by others is through the delivery of a viral vector. Injection of a viral vector carrying the opsin cassette of interest can either be injected locally to allow for specific anatomical distribution of the virus or systemically to allow for widespread expression of the vector. The use of either approach depends on the ultimate goal of the research to be performed. If investigators wish to target a unique location in the CNS (spinal cord or brain), viral vector can be specifically delivered to that area and expression of the light sensitive opsin will be restricted to cell bodies and projections of those bodies. This approach can also be used to selectively deliver an opsin to a location in the peripheral nervous system, i.e. a specific portion of the hind paw, which allows for selective expression only in cells with terminal endings at that location. Alternatively, systemic injection of viral vector allows for widespread and diffuse expression of the virus, which as in our case, may be more optimal when targeting a diffuse region of neurons, i.e. the lumbar region of the spinal cord. The inclusion of Cre-sensitive components in viral cassette construction (loxP sites for flip-excision or stop-

cassette removal) allows for activation of viral vectors within Cre expressing cell populations of an investigators choice. The alternative to viral delivery of an opsin is the use transgenic animals that either selectively express an opsin under a specific promoter, or a transgenic animal that expresses an opsin in a Cre sensitive manner. Depending on the construct of the cassette, viral delivery of an opsin can also be used to target projections of a specific anatomical location, i.e. cassettes that jump a single synapse can allow for selective activation of opsins in the projections of a brain region (Gradinaru, Zhang et al. 2010). While use of transgenic animals imbue a less complicated technical approach, investigators must rely on breeding their own animals and ensuring genetic reliability of said colony.

Challenges of using a viral method to deliver an opsin include variables that can alter concentration of viral vector delivery, this may result in differential delivery and expression of opsins in tissue which may give rise to unavoidable variability in experiments. This is true of either localized or systemic injections. Depending on the timing of delivery of the viral vector it is possible to inadvertently induce long term changes to the immune system that may complicate or confound results in the future. Additionally, systemic injection of viral vectors may result in stark differences in opsin protein expression between individual animals, a complicated variable to account for. These however can also be strengths of the approach of viral vector delivery. Viral delivery of an opsin can allow for transfection and expression of an opsin beyond the normal levels of a transgenic animal, allowing for activation of opsins beyond what may be possible using a transgenic animal. This of course may result in its own confounds to the work at hand. Viral delivery, localized or systemic, can allow for timed delivery of cre sensitive opsin cassettes that bypass expansion of genetic activation during development, i.e. TRPV1, which would be unavoidable in a non-inducible mouse cre line (Daou, Beaudry et al. 2016).

Unavoidable activation of cre during a transgenic animal's development may result in opsin expression in undesired populations of cells in adult animals.

The last hurdle to consider when using optogenetics in an in-vivo approach is the delivery of light to the opsin at sufficient magnitude to activate the opsin. This depends heavily on the tissue of interest, e.g. a specific brain region, specific location in the spinal cord, specific location within the peripheral nervous system. The easiest form of light delivery is simply exposure of tissue through lighting within the test area, or directly applying light to the tissue with a laser (Daou, Tuttle et al. 2013). This form of light delivery lends itself to investigations targeting fibers in the skin or perhaps the eye, essentially tissue with exposed fibers to ambient light. Delivery of light to regions of the brain require skilled implantation of cannulas or fibers that illuminate the region of interest without confounding "normal" behavior of the animals. A similar approach has now been developed to target regions of the spinal cord, with the goal of both targeting afferent terminals prior to entering the spinal cord and regions of the deeper spinal cord (Bonin, Wang et al. 2016). Illuminating light cuffs to deliver light to the sciatic nerve have also been used (Towne, Pertin et al. 2009, Xie, Wang et al. 2018). The use of many of these approaches has progressed and will continue to progress as options for wireless light delivery continue to improve. One of the major challenges originally facing wireless delivery of light to tissues was delivering light of sufficient power to activate opsins in desired tissues, a hurdle that appears to be progressively nearer to being jumped (Copits, Pullen et al. 2016).

Many studies have used optogenetics to investigate mechanisms driving nociception and pain, whether targeting the central nervous system or the peripheral nervous system (Copits, Pullen et al. 2016, Xie, Wang et al. 2018). Of interest to the work completed here, where our goal is to use optogenetics to investigate the Nav1.8 and MrgD expressing populations of sensory fibers, I will report findings from a few papers that performed relevant work. Not only

to justify our approach to targeting these populations of peripheral neurons but the feasibility of our optogenetic paradigm. Optogenetic investigation of sensory neurons expressing ChR2 under the Nav1.8 promoter (cre-lox system) has demonstrated that many of the C-fibers that express Nav1.8 respond to nociceptive modalities such as mechanical and thermal stimuli and these fibers can be successfully activated by blue light (Uhelski, Bruce et al. 2017). Daou et al. 2013 has demonstrated by using blue light in mice that activation of Nav1.8 fibers results in both behavioral and immunohistochemical hallmarks of nociceptor activation. Namely by acutely inducing nocifensive behaviors following blue light stimulation of the hind paw, condition placed aversion to activation of Nav1.8 fibers blocked by morphine, and c-fos staining in superficial lamina of the spinal cord dorsal horn (Daou, Tuttle et al. 2013). Authors of this paper also demonstrated that prolonged activation of Nav1.8 fibers using blue light resulted in central sensitization of animals. Daou et al. 2016 demonstrated that through Arch-induced inhibition of Nav1.8 fibers, nociceptive stimuli and inflammation induced tactile hypersensitivity could also be blocked (Daou, Beaudry et al. 2016). Bonin et al. 2016 demonstrated light delivery of an epidural fiber meant to target afferent terminals in the spinal cord dorsal horn could also allow for optogenetic activation or inhibition of Nav1.8 fibers, and their associated behavioral responses. Due to the overlap between this epidural optogenetic surgery and our own in the rat (Havelin et al. 2017), and the ability to overcome potential adaptive/compensatory responses with that can occur in ablative approaches, we chose to use this surgical approach to investigate the role of these fibers in CIBP.

3.2. Materials and Methods

3.2.1. LLC Cell Line Maintenance

The C57BL/6 mouse cell line, Lewis Lung Carcinoma (LLC) cells were purchased from American Type Culture Collection (ATCC, CRL 1642, Manassas, VA) and were maintained in DMEM media with L-glutamine (CellGro, Manassas, VA) with 10% fetal bovine serum (ATCC, Manassas, VA) and 1% penicillin/streptomycin at 37°C in a 5% CO₂ atmosphere. Prior to surgical implantation, cells were washed with phosphate-buffered saline and lifted from cell culture plates with 0.05% trypsin-EDTA (CellGro, Manassas, VA). Cells were spun at 0.7 RCF for no more than 5 minutes and re-suspended at a concentration of 1 x 10⁸ cells/ μL in the same DMEM media used to culture the cells using a BioRad TC10 Automated Cell Counter (BioRad, Hercules, CA).

3.2.2. Animal Care and Treatment

Female and male C57BL/6 mice (Charles River, Willington, MA) aged 8-12 weeks, were chosen based on their histocompatibility with the LLC cell line. Mice were maintained on a 12-hour light/dark cycle with food and water available *ad libitum*. All experiments were performed in accordance with the policies and recommendations of the International Association for the Study of Pain, National Institutes of Health, and the Institutional Animal Care and Use Committee of the University of New England.

3.2.3. Transgenic Mouse Lines and Crosses

Transgenic reporter mice were purchased and maintained as homozygous lines in the animal facilities at the University of New England. Mice were paired in harem breeding with one male and two females. Both Nav1.8 and MrgD cre lines of mice were also maintained on a

homozygous background. Mice heterozygous for both genes were generated by crossing the male homozygous cre mice with homozygous floxed-stop transgenic female mice. For example, male Nav1.8 cre would be crossed with female tdtomato reporter mice. Mice were paired no earlier than 6 weeks of age and allowed to continue to breed until they were roughly 8 months of age or until they stopped producing litters. Pups were weaned at postnatal day 21 and females and males were housed separately. Mice that underwent optic fiber implantation were not used for experiments until they were roughly 12 weeks old to allow ease of surgical placement of optical fibers as described later.

Nav1.8-cre. The Nav1.8-cre mouse line was generously transferred to us by Dr. Ian Meng from the University of New England, the original origins of this mouse reported to be from John Woods group (Nassar, Stirling et al. 2004).

MrgD-Cre-ERT2. The MrgD^{creERT2} mouse line was generously transferred to us by Wengqin Luo from the University of Pennsylvania. Characterization of this specific mouse line is reported by (Olson, Abdus-Saboor et al. 2017). This mouse is also now commercially available through Jackson Labs, Bar Harbor, ME, at the time of this dissertation stock number 01286.

Floxed stop tdtomato Ai14. Experiments utilizing the fluorescent tdtomato reporter uses the Ai14 mouse purchased from Jackson Labs, Bar Harbor, ME, at the time of this dissertation stock number 007914. The Ai14 mouse utilizes a floxed-STOP cassette that requires cre activation for the functional expression of the red fluorescent protein variant “tdtomato”.

Floxed stop ArchT JAX Ai40D. Experiments utilizing the ArchT-eGFP transgenic mouse use the Ai40D mouse from Jackson Labs, Bar Harbor, ME, stock number 021188. The Ai40 mouse utilizes a floxed-STOP cassette that requires cre-activation to express the light sensitive ArchT-eGFP fusion protein. ArchT is a functionally enhanced version of the orange-yellow light

sensitive Arch protein which silences neurons by actively pumping protons into the extracellular space following exposure to orange light (Han, Chow et al. 2011). ArchT was chosen as it is reported to be more light sensitive than its predecessor, demonstrates adequate expression on axons, a critical component to our targeted area for light delivery, and has a much faster time of recovery from light-induced inactivity compared to other neuron inactivating light sensitive channels such as halorhodopsin (Han, Chow et al. 2011). Functionally, pumping protons into the extracellular space results in hyperpolarization of the transmembrane electrochemical potential, which has demonstrated efficacy in silencing neurons.

3.2.4. Genotyping of Mouse Lines

Genotyping of samples was completed by the COBRE Behavioral core at the University of New England. Tissue is collected from each mouse at approximately Day 21 of age simultaneous with weaning, using surgical scissors to remove a 2mm snip of tail. Tail snips were placed in a 1.5mL conical bottom tube and lysed by adding 50mM NaOH to the tube. Each sample was heated to 95°C for 35 minutes, followed by the addition of 50mM HCL and 1M Tris HCL buffer. Each sample was then spun down and stored at 4°C until processing. Animal genotypes were confirmed using three separate protocol methods once sample preparations were completed. Nav1.8 cre and ArchT mutant reactions were prepared using Promega GoTaq Flexi PCR buffer, while ArchT wild type and MrgD-cre reactions were prepared with Econotaq Plus 2x Buffer. 1 µL of DNA sample was added per reaction, into master mix of the appropriate buffer. The conditions for each protocol varied by annealing temperature and the number of cycles run to produce the desired product.

Nav1.8 cre/cre and Nav1.8 Wild Type must be processed as 2 separate reactions, due to final product band sizes being approximately the same (~538 bp). Primers and conditions for

performing Nav1.8 Cre and wild type are as follows, Nav1.8 cre common forward – GGAATGGGATGGAGCTTCTTA, Nav1.8 cre mutant reverse – CCAATGTTGCTGGATAGTTTTACTGC, Nav1.8 cre wild type reverse – TTACCCGGTGTGTGCTGTAGAAAAG. MrgD cre were performed as a single reaction, with final product sizes being 550 bp for the mutant allele and 200 bp for the wild type allele. Primers are as follows: MrgD cre mutant forward – GGATCCGCCGCATAACC, MrgD cre wild type forward – ATACTTTTTGCCGACTTGAAGTTG, MrgD cre common reverse – TTGGGCTGCTAAGAGTGG. ArchT mutant conditions: ArchT mutant and ArchT wild type must be processed as 2 separate reactions, due to final product band sizes for both being approximately the same (~300 bp). Mutant reactions performed with Promega GoTaq Flexi buffer using the following primers: ArchT mutant forward – ATTGCAGCCATTGTCTGAG, ArchT common reverse – CCGAAAATCTGTGGGAAGTC. ArchT wild type conditions: ArchT wild type processed with EconoTaq 2x Buffer and performed under the following conditions and primers: ArchT wild type forward – AAGGGAGCTGCAGTGGAGTA, ArchT common reverse – CCGAAAATCTGTGGGAAGTC. All DNA products were loaded on a 1.5% agarose gel for electrophoresis. Voltage was typically set for 130V, for a duration of 30 minutes to separate bands. Gels were then imaged under UV light for analysis.

3.2.5 Surgical Procedures and Manipulations

Viral Information and Transduction Protocol. Virus used for viral transfection of ArchT was purchased from the Canadian Neurophotonics Center, QC, Canada. Viral cassette information supplied by the Canadian Neurophotonics Center reported the vector used is AAV2/8-CAG-Flex-ArchT-eGFP. The AAV2/8 serotype is a combination of AAV2 and AAV8 serotypes. The CAG promoter is comprised of the cytomegalovirus enhancer element, the first exon and intron of the chicken beta-actin gene as a promoter, and the rabbit beta-globin splice

acceptor gene which has previously been shown to induce high expression when used in AAV vector delivery in vivo (Nitta, Kawamoto et al. 2005). “Flex” is an acronym for “flip-excision”, a function of the endonuclease protein Cre. When loxp sites are oriented appropriately, vectors are excised, inverted and re-inserted into the genome. In this case this vector is provided in the anti-sense direction, upon exposure to Cre, the vector is excised and flipped to a sense direction resulting in successful expression of the ArchT-eGFP pump and fluorescent reporter. Virus was prepared and purchased from Canadian Neurophotonics Center, QC, CA. Titer varied minutely between lots received. Virus was prepared in the absence of helper virus, purified from culture medium on iodixanol gradient and resuspended in PBS 320 millimolar sodium chloride and 5% sorbitol and 0.001% pluronic acid.

Mice received injections of 20 microliters of undiluted virus suspension at postnatal day 5. To reduce stress and potential for cannibalization of pups, the mother was removed and lightly anesthetized with isoflurane ~1-2% prior to handling pups. After removing the mother, gloves were rubbed in the bedding of the cage of pups in an attempt to reduce scent from the investigator and add scent from the home cage to the gloves of the investigator. Pups were then individually picked up and injected with 20 microliters of virus suspension from a modified Hamilton syringe that allowed minimal waste of virus. A blunted 30-gauge needle was attached to the luer tip of a 100 microliter syringe, this needle tip was then attached to PE10 tubing, which was then attached to the end another 30 gauge needle tip that was gripped with a pair of inter-locking hemostats. After injection pups were then returned to their home cage and covered with bedding prior to the return of the mother. Pups were observed for ~2 hours prior to being returned to the animal facility.

Cancer Implantation in Mice. Surgical implantation of the LLC cell line was consistent with those previously described (Schwei, Honore et al. 1999, Isono, Suzuki et al. 2011). Briefly,

mice that were 2-3 months old were anesthetized with isoflurane 2-3%. Animals had their right hind limb area shaved and wiped with 70% ethanol followed by iodine. A small incision was made laterally above the femur to expose underlying tissue. Going along the iliotibial band using a pair of curved forceps, muscle was separated with blunt dissection to allow the pair of forceps to hook over the femur and roll/displace the quadriceps over the femur exposing the distal end of the femur, taking care to avoid ripping or damaging tissue. A small hole was then drilled between the 2 condyles using a dental drill with a 0.6-millimeter bit. A small cannula was then inserted into the bone marrow and attached to a 50 microliter Hamilton syringe and 2 microliters of cell suspension (1×10^8 cells/mL) was injected delivering 2×10^5 cells or cell free media. After injection was complete the cannula was removed and the hole was then sealed with bone wax and bone cement. The muscles displaced previously in the procedure were returned to their original position and the incision in the skin closed with suture. Mice were then returned to their home cages and monitored for 1-2 hours prior to being returned to the animal facility. Mice were monitored for weight loss and any animals that lost greater than 20% of their original body weight at any given time were removed from the study (no animals removed due to weight loss prior to end of experiments).

Epidural Fiber Optic Manufacturing, Utilization of Laser diode system, and Quality Assurance. Optic fibers were used and purchased as described in Bonin et al 2016, from Doric lenses (QC, Canada). Fibers were custom made with a diffusive tip, product information, MMF_POF_240/250-0.6_8 cm DFL. Fibers were fixed in place within a ceramic ferrule with blue epoxy (Fiber Instrument Sales, Inc.) and allowed to dry overnight. Fibers were then cut with a ruby dualscribe S90R (THORLABS, Newton, NJ) to measure 4.8cm in length, to allow placement directly above the lumbar enlargement. After roughly cutting with the dualscribe implants, were held within a polishing disc D50-FC (THORLABS, Newton, NJ) and progressively polished in a

figure 8 motion to ensure even polishing of the end of the fiber optic. Polishing paper increments used were as follows: M15 silicon carbide 15 micrometers (Fiber Instrument Sales, Inc., Oriskany, NY), diamond lapping 6 micrometer (THORLABS, Newton, NJ), 3M aluminum oxide 3 micrometers (Fiber Instrument Sales, Inc., Oriskany, NY). Implants were then sealed in dental cement molded to rubber caps to imitate the shape of a mouse skull and allowed to dry overnight. Fibers were then tested for transmittance to ensure adequate transmission of light to the end of the fiber and ensure the manufacturing process did not compromise the integrity of the fiber. Testing of representative group of fibers is displayed in Figure 3.1, fibers with <30% transmittance at the measured power output of the laser were not used.

After mice received surgical implantation of the fiber, animals were attached in line with the following fiber optics for transmittance of light from the laser source to the diffusive fiber optic. Light sources used in experiments were generated from a fiber-coupled laser diode module – 450 and 520 nm, LDFLS_450/080_520/060 (Doric Lenses, QC, Canada). Laser diodes were connected to a patch cord MFP_100/125/LWMJ-0.22_0cm_FC-FCA, core 100 micrometers, NA0.22, jacket 2400 micrometers (Doric Lenses, QC, Canada). This cord was attached to a fiber optic rotary joint, FRJ_1x1_FC-FC and fiberoptic rotary joint holder, holder FRJ_small rotary (Doric Lenses, QC, Canada). The rotary was then connected to an optical fiber patchcord, MFP_200/240/900-0.22_1.5m_FC-ZF2.5, core 200um, NA 0.22, jacket 900 micrometers (Doric Lenses, QC, Canada). This was then attached to a bronze split jacket used to connect the laser source and patch cords to the fiber optic implant attached to the mice. Depending on the behavioral test, lasers were either manually activated by hand, setting the laser diode system to “constant wave”, or controlled by signals from ANYMAZE software (Stoelting, Wood Dale, IL) with TTL signals.

Epidural Fiber Implant Surgery. Implanting the fiber optic cable to target the lumbar enlargement of the spinal cord was performed as previously described (Bonin, Wang et al. 2016). Animals were anesthetized with 2-3% isoflurane with oxygen flow of 1 liter/minute. The neck and top of the head of the mouse was shaved using small hair clippers and then treated with 70% ethanol wipe and iodine. A small incision, ~3cm, was made cutting rostral to caudal from roughly the middle of the skull (immediately rostral to lambdoid suture) down to the middle of the neck. The skull was then rubbed with a cotton tip applicator that had been soaked in 3% hydrogen peroxide to remove residual tissue on the skull. This aided in ensuring a dry skull surface for later in the surgery. A set of microscissors were used to cut underlying neck muscle along the midline of the animal taking care to not shear tissue lateral to the midline. After an incision of roughly 2 cm was made a cotton tip applicator was inserted into the incision and vigorously rubbed and spun to bluntly force tissue away from the skull and to increase workable space within the incision. Following this, tissue spreaders were inserted into the incision and used to open the incision to a workable area. Using fine tipped forceps, a small hole was made in the layer of tissue lying over the duramater just rostral to the C1 vertebra, taking care to avoid puncturing the dura which was made obvious by the release of cerebrospinal fluid (CSF) if the dura mater was punctured.

Occasionally this did happen and animals were recorded and noted as such. After blunt dissecting a small useable hole, the end of the fiber optic implant with the diffusive tip was held with ceramic tip forceps, 7 MZ Ceramic Tip Tweezer (Electron Microscopy Series, Hatfield, PA) and carefully placed into the hole. After the fiber optic implant was successfully inserted using the ceramic tip forceps, the implant was carefully and slowly threaded down the length of the vertebral column and spinal cord to the lumbar enlargement. Noting two points of resistance, initially as the implant passes the arch in the cervical region of the mouse's vertebral column

and again nearing the lumbar enlargement. These hurdles were overcome by manipulating the mouse and gently applying force to the fiber to encourage it to terminate where necessary. Using Loctite brand superglue (blue cap) the dental cement cap was fixed to the skull of the mouse. The incision was then closed using suture and the animals were placed into cages and individually housed. Animals were monitored for paralysis or complications from the surgery for 2-3 hours and then returned to the animal facility. Animals that were paralyzed were euthanized. Prior to testing animals were attached to a laser diode light source to determine if the implants were successfully (hit) or incorrectly placed (miss). Roughly <20% of animals received incorrectly implanted fibers or required euthanasia due to complications of the surgery, representative images can be found in Figure 3.1.

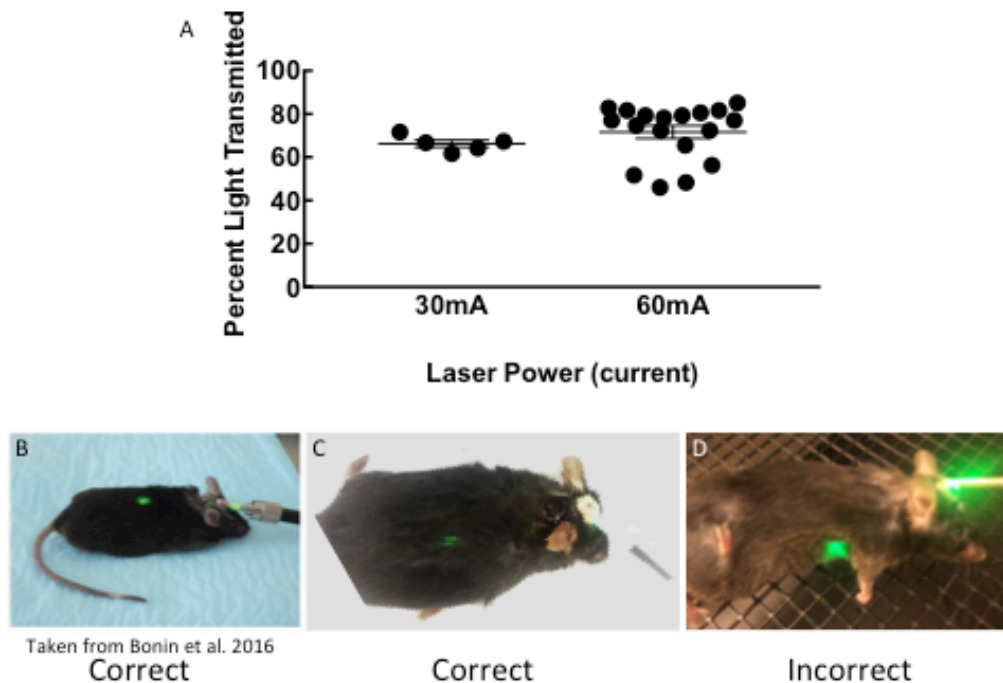


Figure 3.1. Verification of Fiber Optic Output and Implant Placement. Various considerations and hurdles considered when using the fiber optic implant to deliver light to the lumbar section of the spinal cord. **A)** Representative data from fiber optic testing. Light output was measured at 2 powers to verify consistent light output percentage (30mA and 60mA), after verification of this, fibers were only measured at a power output of 60mA. **B)** Representative image taken from Bonin et al 2016. of a successful surgical implant, the diffusive tip is placed directly over the lumbar enlargement of the spinal cord. **C)** Representative image from a correctly implanted fiber in our lab. **D)** Representative image of an incorrectly placed fiber optic, mice typically with incorrectly placed fibers exhibited no signs of distress.

Animals were allowed 5-7 days to recover prior to verification of implant as well as experimental procedures. At least one day prior to behavioral testing animals were attached to the laser and allowed 30 minutes to acclimate to being attached to the fiber. This was performed prior to verification of proper placement of the implants. Proper placement was determined by verifiable light transmitted through the back of the animal in the lumbar region of the spinal cord, see Figure 3.1 for correct vs incorrect implant of fiber. Animals with

incorrectly implanted fibers were used as offsite controls as the animals did not appear to find the misplaced fiber aversive, painful or stressful.

Estimates made by Bonin et al. 2016 place light penetration to a rough maximum of 100-200 micrometers through spinal cord myelin, indicating that light penetration is limited and likely not possible to deep lamina of the spinal cord. Cells beyond the reach of this light are also protected which allows for specific illumination of cells shallow into the spinal cord dorsal horn.

3.2.6. Behavioral Assays and Observations

Quantification of flinching, guarding, limb use behaviors. Quantification of altered behavior due to the development of CIBP was assessed as previously described (Honore, Rogers et al. 2000). Mice were allowed to acclimate to a small pan empty of bedding for at least 15 minutes prior to observation of behavior. Mice were then observed for 2 minutes and the total number of flinching bouts and time spent guarding was assessed. Some mice were also observed via video camera set to record from underneath them in clear box, and total time spent guarding the cancer-afflicted hind limb was measured. Limb use behavior was assessed over a 2-minute time frame and rated by the following scale. 4, normal limb use, 3, limping with less use of the cancer afflicted limb, 2, limping and guarding of the impaired limb, 1, partial non-use of the hind limb, and 0, complete lack of use (dragging) of the hind limb.

Von-frey assessment of tactile hypersensitivity. Development of tactile hypersensitivity following implantation of LLC cells in to the femur of mice was assessed using the up-down method as previously described (Chaplan, Bach et al. 1994, Honore, Rogers et al. 2000). Mice were allowed to acclimate to small elevated chambers with mesh flooring for 30-60 minutes prior to testing. Testing was conducted using the calibrated von frey filaments: 2.44, 2.83, 3.22, 3.61, 4.08, 4.31, 4.56, and beginning with filament 3.61. A maximal threshold obtained from lack

of a response from the 4.56 filament was recorded as 4 grams, and a minimal response with a positive response from the 2.44 filament was recorded as 0.04 grams.

Quantification of rearing behaviors. Similar to previously described (Guedon, Longo et al. 2016), mice were placed into a clear bottom plastic bin and recorded for either 5 or 30 minutes as described in each experimental paradigm. Total number of times mice placed their full weight on their hind limbs was totaled, this simultaneously occurred when animals removed all weight from their forepaws.

Mustard oil (AITC) induced nocifensive behaviors in animals with virally delivered ArchT. Previous reports have demonstrated the efficacy of AITC to induce robust, but short lived nocifensive behaviors mediated by activation of the TRPA1 channel (Eid, Crown et al. 2008, Okun, Liu et al. 2012). Due to the overlap of TRPA1 RNA expression with Nav1.8 and MrgD RNA expression (Figure 3.2), we chose to use this robust behavior to assess whether our optogenetic approach could activate ArchT in Nav1.8 or MrgD fibers and block nocifensive behaviors, prior to use in our CIBP model. Wildtype animals that did not have fiber implants were restrained and received either an injection of 20 microliters of 30% DMSO, or 1% AITC dissolved in 30% DMSO into the plantar surface of their hind paw. Mice with fiber optic implants were first handled and restrained (scruffed) and attached to the brass collar to connect the laser source to the fiber implant attached to the mouse's head. Mice were then allowed a 15 to 30 minute habituation period in their home cages before proceeding with testing. Most animals immediately returned to normal mouse behavior within their home cages, i.e. grooming, sifting through bedding and locomotion behavior. Immediately prior to injection of AITC, lasers were activated at 200mA on continuous wave for constant delivery of light to the animal during injection and the 5 min observation period. These mice then received either an injection of 20uL of 30% DMSO, or 1% AITC dissolved in 30% DMSO into the plantar surface of their hind paw. Following injections of

either vehicle or AITC animals were immediately placed into a plastic chamber with a camera set up beneath to record time spent licking and flinching bouts for 5 minutes.

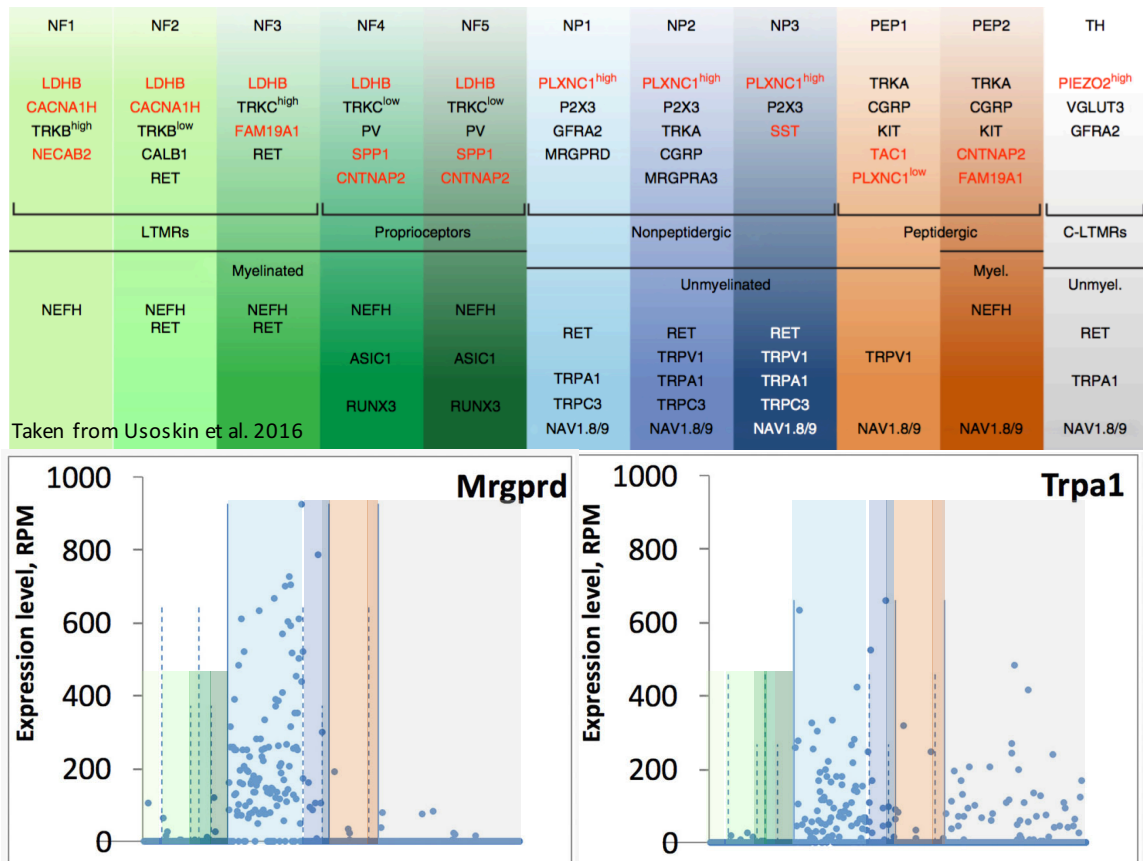


Figure 3.2. Potential Overlap in the Mrgprd (MrgD) and Trpa1 (TRPA1) Expressing Cells in the DRG. Single Cell RNAseq demonstrating subpopulations of sensory fibers. Colored table taken from Usoskin et al. 2015. Data mined from Linnarsson Lab website, (<http://linnarssonlab.org/drg/>). Figure adapted with color scheme by Joshua Havelin for ease of visualization.

Locomotor assay chamber assessment of behaviors. Work previously published by Majuta et al. assessed the effects CIBP on distance travelled in animals with cancer cells implanted into their femurs. Animals with cancer were shown to have reduced movement simultaneous with disease progression (Majuta, Guedon et al. 2017). Behaviors were analyzed as previously reported (Lowery, Raymond et al. 2011). Animals were placed into a 10 by 10 inch plastic chamber (Coulbourn Instruments, Allentown, PA) and data was acquired and reported using TruScan software (Coulbourn Instruments, Allentown, PA). Animal movements were

tracked by a set of infrared beams at the floor level, as well as a set of infrared beams 2 inches above to detect rearing behaviors. Total distance traveled, time spent in the center of the chamber, at the edges of the chamber and number of center entries was recorded. Breaking the vertical infrared beams allowed for quantification of time spent rearing and number of rears. Distance traveled is reported in centimeters. Data was collected and summed across 1-minute bins. Representative time course data is displayed as sum values across 5-minute bins throughout the 30-minute experiment, and area under the curve was calculated using the trapezoidal Riemann sum between bins.

Conditioned place preference to pain relief or aversion to hindpaw movement. A number of previous publications have demonstrated the efficacy of conditioning animals to pain relief (King, Vera-Portocarrero et al. 2009, Remeniuk, Sukhtankar et al. 2015, Havelin, Imbert et al. 2017).

Using a conditioned place preference (CPP) paradigm animals undergo a 3-day testing procedure. The basic single trial CPP protocol occurs within a three-chambered box as previously described (Havelin, Imbert et al. 2017). The three chambers are distinct from each other in texture of flooring, visual cues (shades of construction paper, and black and white stripes), and scent (pink lemonade vs vanilla chap stick), a representative image can be found in Figure 3.3. On day 1 of testing animals are allowed to freely explore the box for 15 minutes while their movements and time spent in each chamber are tracked and quantified by ANYMAZE software (Stoelting, Wood Dale, IL). Time spent in each of the unique pairing chambers is counter balanced to ensure no unintentional bias is introduced into the experiment. The following day animals are placed into the AM chamber with exposure to a control stimulus for 30-minutes. In the case of evaluating a drug this chamber would be paired with vehicle (i.e. saline), or hooked up to the lasers without having the laser turned on, or undergo handling with

explicit attention to cause no movement of the hind paw. Animals are then removed and returned to their home cages for 4 hours. Following the intermission period, animals are placed into the PM chamber with the experimental stimulus for 30-minutes. In the case of evaluating a drug, this chamber would be paired with drug (i.e. the MOR agonist DAMGO), or hooked up to the lasers with the laser turned on, or a 2-minute period of movement of the hind paw. Animals are then removed and returned to the animal facility. The following day animals are again allowed to freely explore the CPP chambers for 15 minutes and their time in each chamber is quantified by ANYMAZE software. Results are reported as time spent in each chamber pre-conditioning and post-conditioning, an increase time spent in either chamber pre vs post considered CPP to that chamber, whereas a decrease is CPA. In addition, “different scores” are calculated by subtracting time spent in the afternoon chamber pre-conditioning from post-conditioning, a positive number indicates CPP to the pairing where as a negative value indicates CPA, this measurement is used to compare whether treatment effects differed between groups.

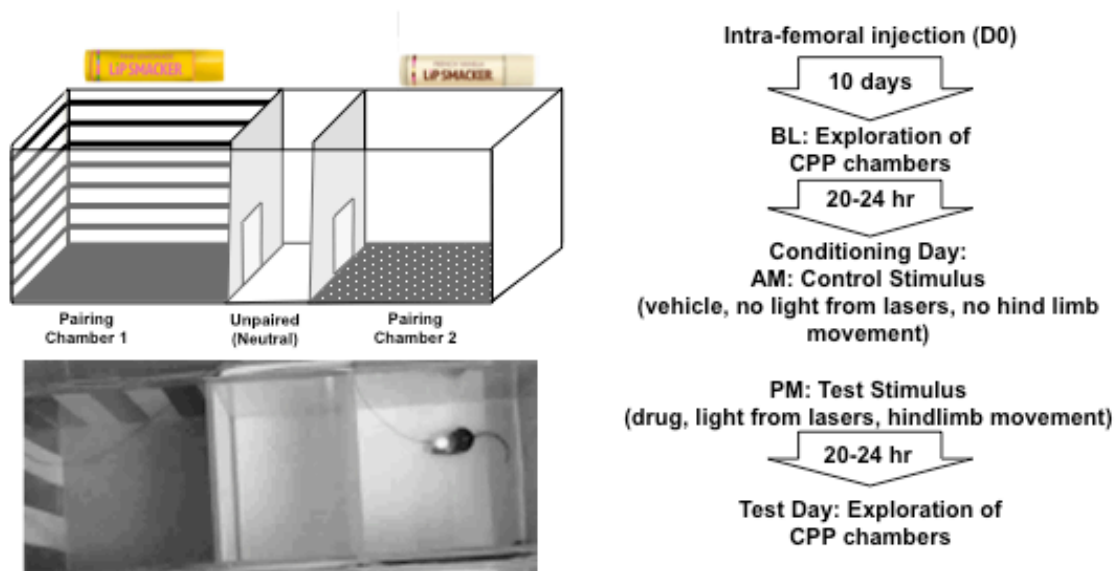


Figure 3.3. Representative Images of Condition Place Preference (CPP) Boxes and CPP Paradigm. In the top left a cartoon diagram of the the CPP boxes. Each box has 3 separate chambers, the two outer pairing chambers and an inner unpaired/neutral chamber. Each of the pairing chambers is distinct from the other by visual (stripes vs solid colors), texture (smooth floors vs rough), and odor cues (pink lemonade vs vanilla). Bottom left is an image captured when an animal is exposed to light from the laser source and constrained to a pairing chamber. On the right is a text description of typical CPP protocol.

Pharmacological intervention for CPP. Mice were briefly anesthetized with isoflurane ~2% and their tails were warmed in 42 C° water. Mice were then quickly injected i.v. with either normal saline for AM conditioning or during PM conditioning DAMGO or Deltorphin II to deliver a dose of 3 mg/kg. Solutions were injected at 10mL/kg, eg. a 20-gram (0.02kg) mouse would receive 0.2 mL of injection. Mice were then allowed to wake from light anesthesia before being placed into their respective pairing chambers.

Laser activation paradigm for CPP. Mice were handled and restrained (scruffed) and attached to the brass collar to connect the laser source to the fiber implant attached to the mouse's head. Mice were then allowed a 15 to 30 minute habituation period in their home cages before proceeding with conditioning. Most animals immediately returned to normal mouse behavior within their home cages, i.e. grooming, sifting through bedding and locomotion behavior. Animals were then placed into their respective conditioning chambers and ANYMAZE

software was activated. In the AM conditioning phase the lasers remained off and animals did not receive any light to their spinal cord dorsal horn. During the PM conditioning phase ANYMAZE software was set to deliver a continuous 200 mA pulse of green light (520nm wavelength) to the mouse for 2 minutes, then the laser would turn off for 1 minute, and then the laser would turn on at 200 mA output. This cycle continues for the entirety of the 30-minute conditioning phase. After each session the animals were then removed and restrained and detached from the brass collar and laser source and returned to their home cages.

Total distance travelled as assessed by ANYMAZE software. Animals were placed into a clear bottom plastic bin and recorded for varying amounts of time while being tracked by calibrated ANYMAZE software. Total distance traveled is reported in meters with this analysis.

Radiographic analysis of cancer-induced bone remodeling for inclusion/exclusion of animals in behavioral studies. X-ray radiographs were taken at the completion of all behavioral studies (except when the x-ray machine was not functioning). A qualitative scoring system was used to score the level of bone remodeling induced by tumor growth similar to previously described (Edwards, Havelin et al. 2018). Digital radiographs were taken using a MINXRAYHF100/30 X-ray source (MinXray, Inc Northbrook, IL), at an exposure setting of 40kV, 1.5 mAs and 0.05 seconds captured on a Wireless Digital Flat Panel Detector (Model Mars1417V-TSI, iRay Technology Co. Shanghai, China) and analyzed with Opal Software (20/20 Imaging, Konica Minolta Healthcare Wayne, NJ) at the completion of all behavioral testing. Bone loss was rated by a blinded experimenter according to a 3-point scale. 0 = being a “normal” bone, consistent with the contralateral leg, 1 = osteolytic or osteoblastic bone remodeling compared to the contralateral bone, and a 2 = unicortical or bicortical bone fracture. Representative images can be found in Figure 3.4. Animals with radiograph measurements of

“0” that had undergone cancer cell implantation were removed from the study due to lack of apparent cancer-induced bone remodeling.

3.2.7. Tissue Collection and Immunohistochemical Staining for Verification of MrgD-cre-ER2 mouse line

Verification of MrgD-Cre line of mice and induction protocol was determined by IHC in DRG and spinal cord tissue using the following protocols. Mice were deeply anesthetized with Beuthanasia-D (Henry Schein Animal Health) and underwent intracardiac perfusion through the left ventricle with 50mL of ice cold PBS followed by 50mL of ice cold 4% PFA containing PBS, pH 7.4. The L2–L4 spinal cord segments were immediately dissected out and post fixed in 4% PFA overnight. L2-L4 DRG were also immediately dissected and post fixed in 4% PFA overnight. Tissue was then moved into a 30% sucrose solution at 4°C for 12–24 h for cryoprotection. Spinal cords and DRG were embedded in optimal cutting temperature (OCT) medium (VWR) and frozen in a 70% ethanol bath at -80°C. Spinal cord sections were cut on a cryostat (Leica) at 30 um, whereas DRG sections were cut at 12 um, collected onto positively charged slides (Azer Scientific), and allowed to dry before storage at -20°C.

Staining protocols used to visualize CGRP and IB4 were performed by the UNE Histology Core. Sections were rinsed 3 times for 10 minutes with PBS containing 0.1% triton (PBSTx) to remove OCT, then non-specific binding proteins were blocked by 30 min incubation with 5% normal donkey serum (EMD Millipore, Billerica, MA) in 0.1% PBS-Tx for 15-60 minutes. This blocking solution was also the antibody diluent. Primary antibodies and Alexa 647-conjugated IB4 were incubated overnight at 4°C as follows: IB4-AF647 1:750 (1.3ug/mL, Invitrogen I32450); rabbit anti-CGRP 1:2000 (ImmunoStar Cat# 24112 RRID:AB_572217). Sections were rinsed 3 times with PBS-Tx and incubated in the dark for 1 hour at room temperature with appropriate

cross-adsorbed secondary antibodies: Donkey anti-rabbit Alexa Fluor 647 1:1000 (2 ug/mL, ab150063, Abcam, Cambridge, MA). Sections were rinsed with PBS-Tx 3 times and mounted with DAPI-containing Fluoroshield (ab104139, Abcam). Representative images were taken using a wide field epifluorescence Leica DM2500 microscope, using either 5x or 10x objective, using suitable filters for DAPI, GFP, tdtomato, and Alexa Fluor 647. Tissue was imaged using Leica Application software with a Leica DFC365 FX 16-bit CCD camera, gain and exposure settings varied between channels and tissue samples.

3.2.8. Statistical Analysis and Graphing

Data was transformed from raw data gathered either via ANYMAZE, Truscan, or by hand to grouped data using Microsoft Excel. Data was then graphed and statistically analyzed using Graphpad Prism software. Results from quantification of flinching, guarding, limb use behaviors were analyzed with a 2-way ANOVA and a Tukey post hoc to compare between groups at each time point. Results from Von-frey assessment of tactile hypersensitivity were analyzed with a 2-way ANOVA and a Tukey post hoc to compare between groups at each time point. Results from quantification of rearing behaviors were analyzed with a 2-way ANOVA and a Sidak post hoc to compare between groups at each time point, and a Tukey post-hoc to compare within group differences. Data from mustard oil (AITC) induced nocifensive behaviors in animals with virally delivered ArchT were not statistically analyzed due to the small n size of the groups. Results from LMA chamber analysis of cancer-induced change in behaviors were analyzed with a 2-way ANOVA and a Tukey post hoc to compare between groups. Pre-conditioning versus post-conditioning time spent in chamber in experiments testing conditioned place preference to pain relief or aversion to hind paw movement were analyzed using a within subject 2-way ANOVA with Sidak's post hoc test comparing pre vs post conditioning values within each group.

Difference scores between groups were analyzed with either an unpaired student T-test, or a 1-way ANOVA with Uncorrected Fisher's Least Squared Difference post hoc. Groups were considered statistically significantly different when p values less than 0.05. Outliers were calculated using Graphpad Prism Grubb's Outlier test, exclusion criteria set at alpha < 0.05.

Table 3.1. Statistical Analysis of Results

Factor	F _(DF1, DF2)	P Value
2-way ANOVA of Tumor-induced Flinching (Figure 3.4, Top)		
Interaction	F _(6, 222) =13.01	P<0.0001
Time	F _(1, 222) =44.81	P<0.0001
Treatment	F _(2, 42) =23.27	P<0.0001
2-way ANOVA of Tumor-induced Limb Use Detriment (Figure 3.4 Middle)		
Interaction	F _(6, 222) =16.47	P<0.0001
Time	F _(1, 222) =61.66	P<0.0001
Treatment	F _(2, 42) =55.56	P<0.0001
2-way ANOVA of Tumor-induced Tactile Hypersensitivity (Figure 3.4 Bottom)		
Interaction	F _(6, 222) =10.38	P<0.0001
Treatment	F _(1, 222) =52.88	P<0.0001
Time	F _(2, 42) =50.25	P<0.0001
2-way ANOVA of Guarding Behaviors (Figure 3.5 Top)		
Interaction	F _(2, 28) =8.265	P=0.0004
Time	F _(1, 28) = 8.265	P=0.0004
Treatment	F _(2, 28) = 18.03	P=0.0017
2-way ANOVA of Rearing Behaviors Within Groups (Figure 3.5 Bottom)		
Interaction	F _(2, 28) = 4.784	P=0.0077
Time	F _(1, 28) = 18.29	P<0.0001
Lidocaine	F _(2, 28) = 4.49	P=0.0601
2-way ANOVA of Rearing Behaviors Between Groups (Figure 3.5 Bottom)		
Interaction	F _(2, 28) =8.265	P=0.0004
Time	F _(1, 28) =8.265	P=0.0004
Treatment	F _(2, 28) =18.03	P=0.0017
2-way ANOVA of DAMGO Induced Pain Relief (Figure 3.6A)		
Interaction	F _(2, 28) =2.675	P=0.1176
Pre vs Post	F _(1, 28) =12.32	P=0.0022
Treatment Group	F _(1, 28) =0.1098	P=0.7438
One Tailed Unpaired T-Test of DAMGO Induced Pain Relief (Figure 3.6B)		
Difference	t ₍₂₈₎ =1.636	P=0.0588
Variances	F _(22, 9) =1.741	P=0.4143
2-way ANOVA Nav1.8 and MrgD Inhibition CPP (Figure 3.12A)		
Interaction	F _(2, 24) =8.758	P=0.0104
Time	F _(2, 24) =15.29	P=0.0016
Treatment Group	F _(2, 24) =3.015	P=0.1044
1-way ANOVA of Comparison Between Groups (Figure 3.12B)		
Treatment	F _(2, 24) =2.863	P=0.0767

Table 3.1. Statistical Analysis of Results (continued)

Factor	F _(DF1, DF2)	P Value
2-way ANOVA of Hind Limb Movement Induced Distance Decrease (Figure 3.14A₁)		
Interaction	F _(1, 18) =0.3956	P=0.5369
Surgery	F _(1, 18) =53.26	P<0.0001
Treatment	F _(1, 18) =10.82	P=0.0039
2-way ANOVA of Hind Limb Movement Induced Rearing Decrease (Figure 3.14B₁)		
Interaction	F _(1, 18) =0.01582	P=0.9013
Surgery	F _(1, 18) =44.81	P<0.0001
Treatment	F _(1, 18) =1.472	P=0.2407
2-way ANOVA of Hind Limb Movement Induced Decrease in Margin Distance (Figure 3.15A)		
Interaction	F _(1, 18) =3.133	P=0.0937
Surgery	F _(1, 18) =8.715	P=0.0085
Treatment	F _(1, 18) =2.585	P=0.1253
2-way ANOVA of Cancer-Induced Increase in Margin Time (Figure 3.15A₁)		
Interaction	F _(1, 17) =0.000366	P=0.9850
Surgery	F _(1, 17) =15.78	P=0.0010
Treatment	F _(1, 17) =7.128	P=0.0162
2-way ANOVA of Cancer-Induced Decrease in Center Distance (Figure 3.15B)		
Interaction	F _(1, 18) =0.0008383	P=0.9772
Surgery	F _(1, 18) =24.41	P<0.0001
Treatment	F _(1, 18) =4.125	P=0.0565
2-way ANOVA of Cancer-Induced Decrease in Center Time (Figure 3.15B₁)		
Interaction	F _(1, 17) =0.000366	P=0.9850
Surgery	F _(1, 17) =15.78	P=0.0010
Treatment	F _(1, 17) =7.128	P=0.0162
2-way ANOVA of Hind Limb Movement Induced Decrease in Center Entries (Figure 3.15B₂)		
Interaction	F _(1, 18) =1.463	P=0.2421
Surgery	F _(1, 18) =27.47	P<0.0001
Treatment	F _(1, 18) =11.37	P=0.0034
Linear Regression Analysis of Power Output to Different Scores (Figure 3.12C)		
	R ² Value	P Value
Nav1.8 Cancer	0.1132	0.9922
Nav1.8 Sham	0.2527	0.1879
MrgD Cancer	0.08018	0.6750

3.3. Results

3.3.1. Classical Cancer-Induced Measures of Pain.

Consistent with previous reports, both male and female mice that underwent LLC cell injection into the femur underwent dramatic bone remodeling and loss (Figure 3.4) that was accompanied by the development of tactile hypersensitivity, decreased limb use and presented with increased flinching bouts (Figure 3.5). Female and male cancer bearing animals showed elevated flinching at Day 12 post cancer cell implantation into the femur compared to female sham animals ($p < 0.0001$, n size = 12 female cancer, 11 female sham, 21 male cancer). Female and male cancer treated animals displayed decreased levels of limb use at Day 12 post cancer cell implantation compared to female sham animals ($p < 0.0001$, n size = 12 female cancer, 11 female sham, 21 male cancer). Female and male cancer animals demonstrated decreased tactile withdrawal thresholds compared to female shams at Days 7 and 12 post cancer cell implantation ($p < 0.0001$, n size = 12 female cancer, 11 female sham, 21 male cancer). In a separate set of experiments animals were observed for changes in time spent guarding of the cancer-afflicted hind limb and rearing activity displayed in Figure 3.6.

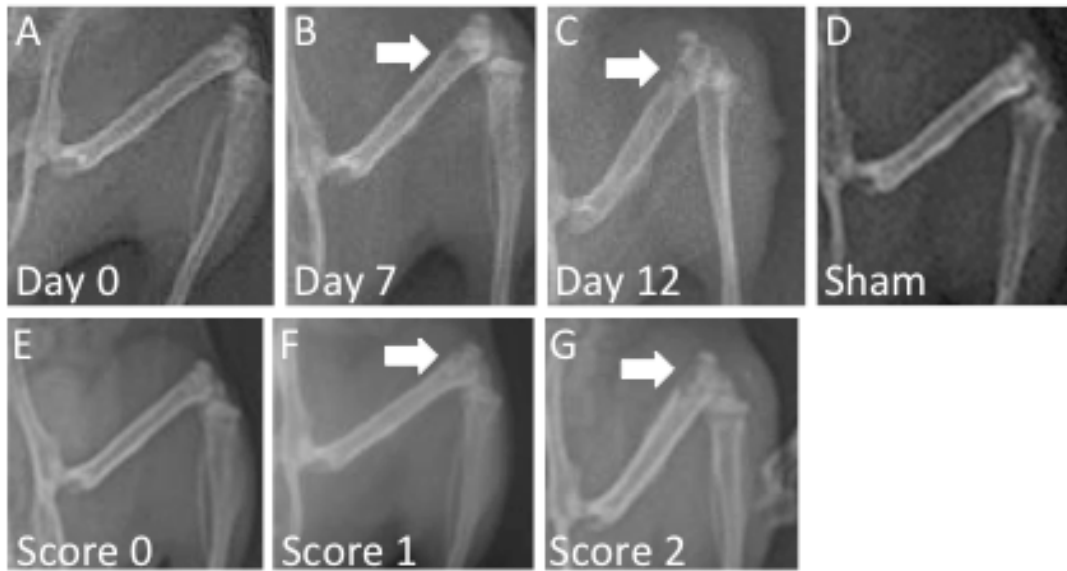


Figure 3.4. Radiographic Images Demonstrating Tumor Induced Bone Loss. **A-C)** Representative images demonstrating progressive cancer-induced bone loss within the same animal. **D)** Representative image of sham animal 12 days after surgery. **E-G)** Panels E-G show representative image of bone scores 0, 1 and 2 (BS). **C, G)** Representative image of unicortical fracture, which represents a bone score of "2" with major pathological bone loss. White arrows indicate bone pathologies.

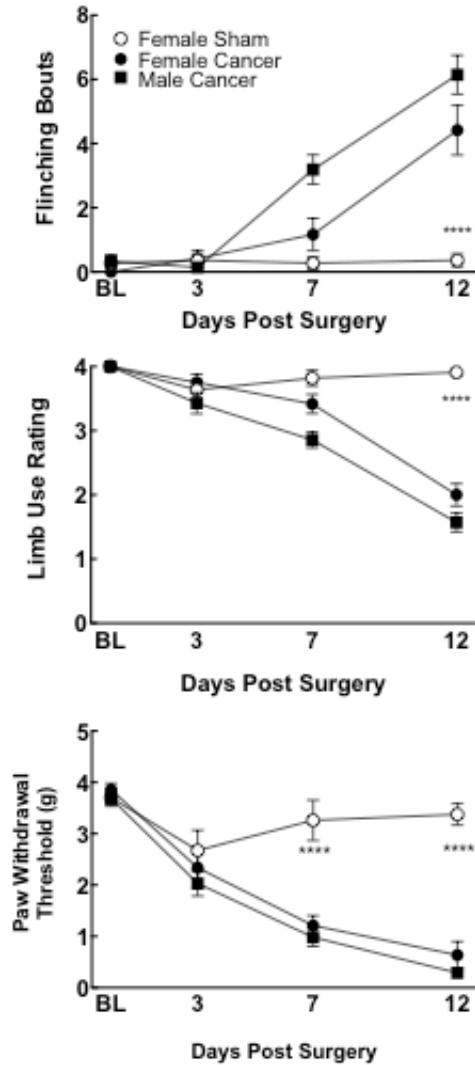


Figure 3.5. Classical Measures of Cancer-induced Bone Pain. Evaluation of classical measures of CIBP in our hands replicate previous findings both within our group and others. **Top)** Increased total number of flinches over 2-minute observation period in animals that received cancer cell injection into the femur. **Middle)** A decrease in limb-use in animals that received cancer cell injection into the femur as disease progresses. **Bottom)** As disease progresses animals that received cancer cell implant develop mechanical tactile sensitivity. **** Represents statistical difference from Female Cancer group and Male Cancer group, $p < 0.0001$.

A separate cohort, female mice were observed for guarding and rearing behaviors.

Consistent with previous reports at Days 11 and 12 post cancer cell implantation female animals

that received cancer cell implantation into the femur spent more time guarding the cancer afflicted hind limb compared to female sham controls ($p < 0.05$ and $p < 0.001$, n size = 6 female cancer, 6 female sham). Female cancer animals showed a decreased in rearing compared to female shams at Days 11 and 12 post cancer cell implant ($p < 0.05$ and $p < 0.0001$), and cancer treated animals showed a decrease compared to their own baseline values 11 and 12 days post cancer cell implant ($p < 0.001$, $p < 0.0001$), sham treated animals showed a significant decrease from their baseline values at day 12, likely due to repetitive exposure to observation chambers ($p < 0.05$, n size = 8 female cancer, 8 female sham). Combined these results indicate that in our hands this surgical intervention produces CIBP results similar to other groups (Guedon, Longo et al. 2016).

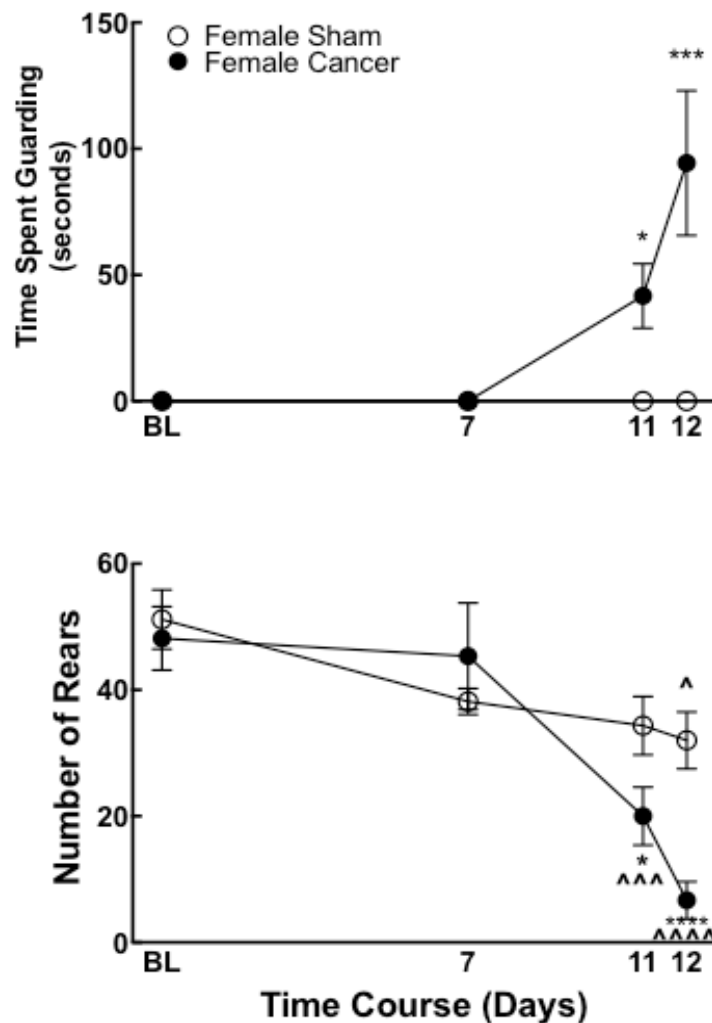


Figure 3.6. Additional Measures of Cancer-induced Behavioral Changes in Female Mice over 5 minute Observation Period. **Top)** In mice as disease progresses, time spent guarding the cancer-afflicted hind limb increases. **Bottom)** As disease progresses the total number of rearing episodes decreases in animals that received cancer injection into the femur. *, ***, **** represent significant differences from Female Sham group with $p < 0.05$, 0.001 , 0.0001 respectively. ^, ^^, ^^ represent significant difference from BL values with $p < 0.05$, 0.01 , and 0.001 respectively.

3.3.2. DAMGO Induced Pain Relief, and Failure of Deltorphin II to Relieve Ongoing Pain.

Administration of the peptidergic MOR agonist DAMGO at a dose of 3 mg/kg in cancer bearing but not sham treated animals resulted in an increase in time spent in the drug paired chamber post-conditioning, indicating a relief of ongoing pain in the cancer bearing animals (Figure 3.7A ** $p < 0.01$, n size = 10 sham, 12 cancer animals). A nearly significant difference

between groups when comparing “different scores” was detected indicating a difference between groups in response to being treated with 3 mg/kg DAMGO (Figure 3.7B, one tailed unpaired t-test, $p = 0.058$, n size = 10 sham, 12 cancer animals). Neither sham nor cancer treated animals demonstrated an increase in time spent in the 3 mg/kg Deltorphin II paired chamber post-conditioning, indicating at this dose Deltorphin II fails to alleviate ongoing pain, and no difference was detected between groups when comparing “different scores” in Figures 3.7C and 3.7D (no significance, $n = 12$ sham, 12 cancer animals).

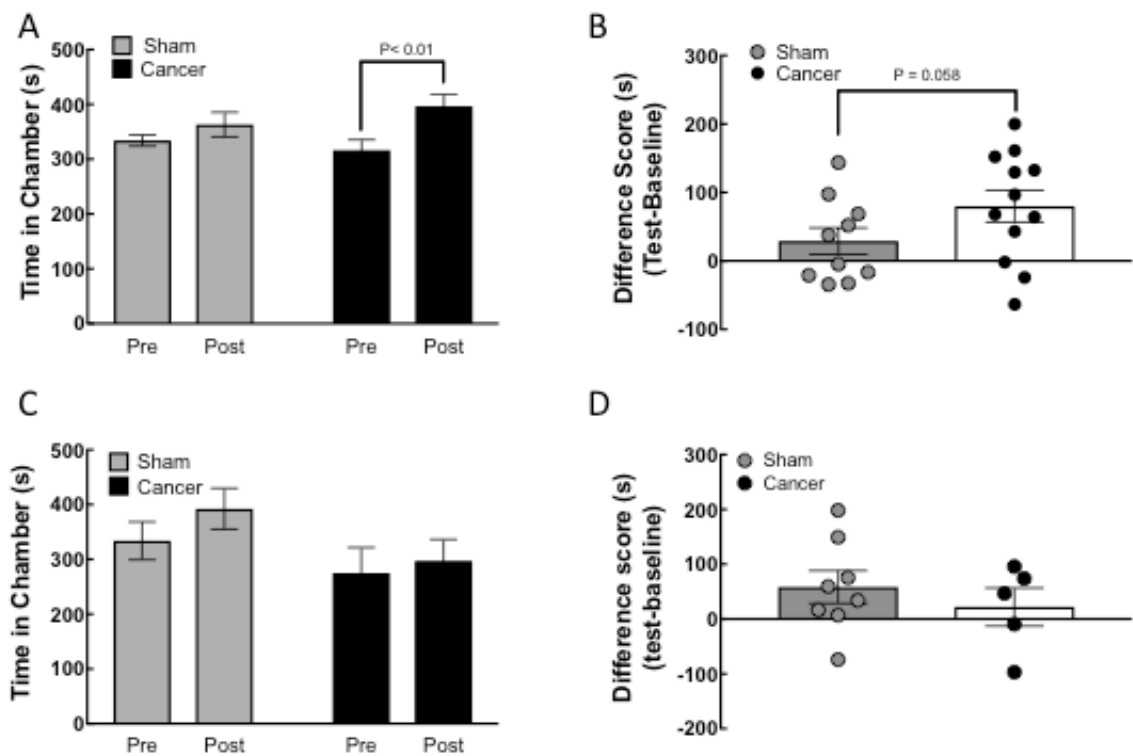


Figure 3.7. Pharmacologically Induced Pain Relief of Cancer-Induced Pain by MOR Agonist DAMGO but not DOR Agonist Deltorphin II. Intravenous DAMGO delivered at a dose of 3 mg/kg results in blockade of ongoing pain, where as 3 mg/kg Deltorphin fails. **A)** Animals treated with cancer show an increase in the PM DAMGO paired chamber, $p < 0.01$ pre vs post conditioning in cancer animals. **B)** Difference scores indicate difference between the sham and cancer treated animals, $p = 0.058$. **C and D)** Pairing Deltorphin II with the afternoon conditioning chamber did not result in an increase in time spent in that chamber, and no difference was observed between sham and cancer treated animals.

3.3.3. Evaluation of Tdtomato Expression in MrgD^{CreER2} Mouse Line.

Visual inspection of immunohistochemical staining for CGRP and IB4 labeling of spinal cord slices and cells within L4 DRG revealed no notable overlap of CGRP and MrgD-tdtomato signal in either tissue as seen in Figures 3.8G and Figure 3.8H. Whereas IB4 labeling with the IB4-AF647 conjugate and MrgD-tdtomato positive signals showed significant overlap in both spinal cord slices and cell bodies of L4 DRG (Figure 3.8C and Figure 3.8D). This labeling shows that the tamoxifen protocol used was successful in activation of cre in MrgD and IB4-binding cells, but not CGRP positive cells. Images displayed in Figure 3.8 have been pseudo colored for ease of consistency within this dissertation. Figure 3.8 panels, A, C, D, E, G, and H tdtomato is displayed in green, panel B, C and D IB4-AF647 signal is blue, panel F, G and H CGRP signal from Secondary AF647 is red.

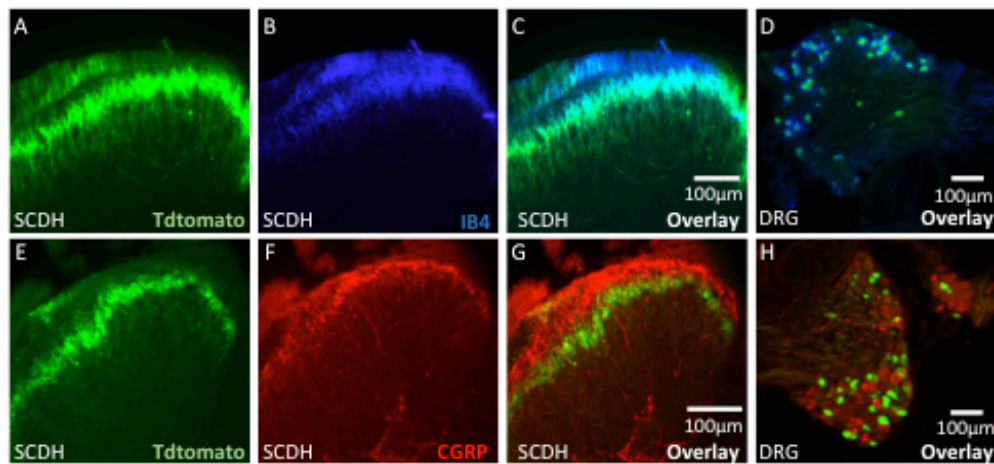


Figure 3.8. Representative Immunohistochemical Screening of MrgD-tdtomato Animals. Staining in spinal cord dorsal horn (SCDH) and cell bodies within L4 dorsal root ganglia (DRG) reveal overlap of MrgD and IB4 signal in lamina II of the SCDH, and distinct lack of overlap between MrgD-tdtomato in lamina II and CGRP signal in lamina I of the SCDH. **A-D)** Staining to confirm overlap of tdtomato signal [pseudo colored in green in panel A] with IB4-AF647. **E-H)** IHC staining to verify lack of overlap between MrgD-tdtomato [pseudo colored in green in panel H] with staining for CGRP with AF647 tagged secondary.

3.3.4. Evaluation of Delivery and Activation of Undiluted AAV2/8 ArchT Viral Vector in MrgD-tdtomato Positive Cells.

Delivery of the viral vector containing the ArchT-eGFP cassette at postnatal day 5 resulted in robust expression of ArchT-eGFP in MrgD-tdtomato positive spinal cord slices and cells within the L4 DRG. Figure 3.9 displays a representative image of lumbar spinal cord slices and L4 DRG where MrgD-tdtomato signal overlaps robustly with virally delivered ArchT-eGFP. In this image greater than ~70% of the cells expressing tdtomato also express ArchT-eGFP, and signal in the spinal cord dorsal horn show robust overlap. These results were a large improvement from previous attempts to administer a 1:10 dilution of the stock viral vector (data not shown). In Figure 3.9 tdtomato is displayed in red, ArchT-eGFP fusion protein is visualized in green.

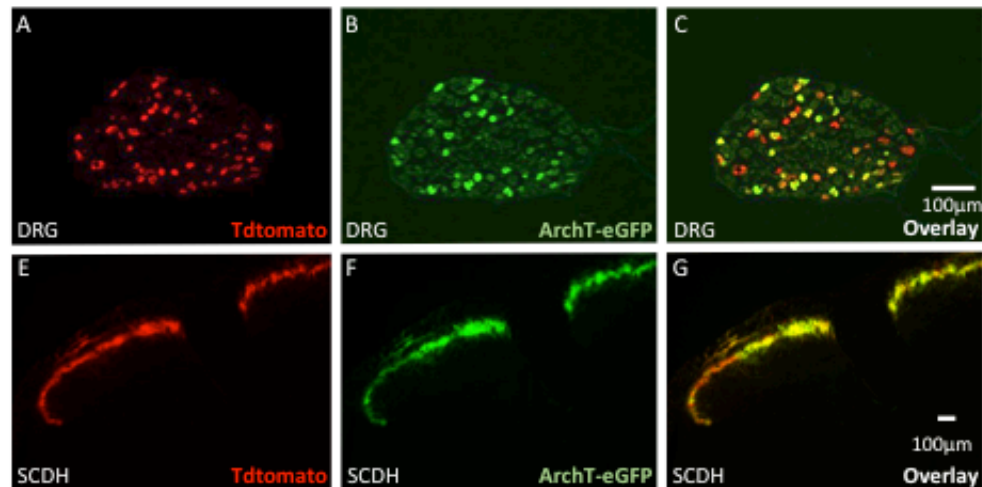


Figure 3.9. Successful Transfection of MrgD Cell Bodies with ArchT-eGFP Flex Virus and Trafficking to Afferent Terminals in the Spinal Cord Dorsal Horn. Fluorescent microscopy reveals successful induction of both floxed stop tdtomato fluorescent reporter protein and ArchT-eGFP fusion protein from flex virus injected into pups on postnatal day 5. Overlap of signal in both cell bodies within the L4 DRG and lamina II within the SCDH. **A-C)** Representative images taken from L4 DRG, tdtomato pseudo colored in red, ArchT-eGFP pseudo colored in green. **E-G)** Representative images taken from the SCDH, tdtomato pseudo colored in red, ArchT-eGFP pseudo colored in green.

3.3.5. Fiber Optic Implant Quality Assurance and Surgical Implant Challenges.

Following hand polishing of each individual fiber optic implant, fibers were individually tested for adequate light transmission compared to raw output from the laser patch cord. As seen in Figure 3.1, similar output efficiencies, roughly 50-80%, were measured at 2 separate power outputs from the laser source (30mA and 60mA) indicating no change in light emission efficiency between the two laser power settings. Relative distribution of power efficiency between fibers indicated consistent results from production of implants. Measured efficiencies were also consistent with reports from collaborators at Laval University from Dr. Yves DeKonick's lab, where I was trained. Of note, later batches of fiber production, such as those reported in Figure 3.12, had reduced transmission efficiency, we believe as a result of production differences in lots of fiber optics. A representative image of challenges resulting from implanting the fiber optic using previously described surgical procedures is displayed in Figure 3.1. After adequate practice it was estimated that < ~20% of surgeries resulted in incorrectly placed fiber implants, whereas paralysis of animals following surgery occurred independent of this.

3.3.6. Successful Optogenetic Blockade of AITC Induced Nocifensive Behaviors in Nav1.8 and MrgD Expressing Fibers.

Injection of a 1% AITC solution into the hind paw of mice induced robust licking and flinching behaviors in wildtype mice with no fiber optic implant, as well as animals with incorrectly implanted fiber optic implants expressing virally delivered ArchT in Nav1.8 or MrgD expressing cells displayed in Figure 3.10. Animals expressing virally delivered ArchT in either Nav1.8 or MrgD expressing cells with correctly placed fiber optic implants displayed a nearly

complete blockade of nocifensive behaviors. Although not statistically analyzed this data demonstrates that not only did our optogenetic approach to silence nociceptive fibers at the level of the spinal cord dorsal horn prove effective, but silencing either Nav1.8 or MrgD expressing fibers is sufficient to block AITC induced nociceptive behaviors (n = 6 wildtype vehicle treated animals with no fiber, 8 wildtype 1% AITC treated animals with no fiber, 2 Nav1.8 virally delivered ArchT animals with incorrectly implanted fiber optics, 2 Nav1.8 virally delivered ArchT animals with correctly implanted fiber optics, 3 MrgD virally delivered ArchT animals with incorrectly implanted fiber optics, 3 MrgD virally delivered ArchT animals with correctly implanted fiber optics).

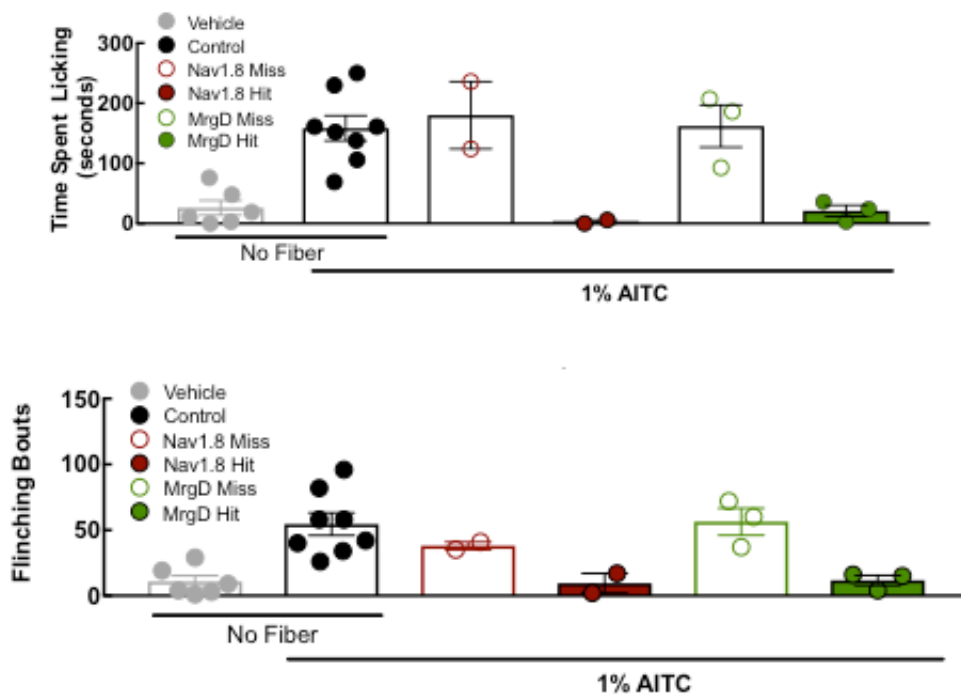


Figure 3.10. Activation of Virally Delivered ArchT in Both Nav1.8 and MrgD Afferents Blocks AITC-Induced Nocifensive Behaviors. Delivering green light to the SCDH to transiently silence either Nav1.8 or MrgD nociceptive fibers results in a reduction of nocifensive behaviors caused by 1% AITC injected into the hind paw. Data was not analyzed for statistical significance due to small n size of some groups. Groups labeled as “Miss” were animals that received improperly placed fiber optic implants that resulted in light not being delivered to the SCDH, whereas groups labeled with “Hit” received properly implanted fibers.

3.3.7. ArchT Expression in Animals from Nav1.8 and MrgD cre Mouse Lines Crossed with Ai40D

ArchT Transgenic Animals.

Representative images of spinal cord dorsal horn near the lumbar section of the spinal cord in Nav1.8 and MrgD animals crossed with the transgenic ArchT mice revealed differential expression patterns of ArchT-eGFP displayed in Figure 3.11. Microscopic evaluation of tissue taken from either Nav1.8-ArchT or MrgD-ArchT animals demonstrated robust eGFP expression in expected lamina of the spinal cord dorsal horn and robust expression of eGFP in L4 DRG. Incomplete activation of Cre in an MrgD-ArchT animal resulted in tissue found in representative images in panels G and H. This was relatively uncommon in animals and if detected, animals were removed from behavioral studies. DRG tissue was not used for ArchT-eGFP verification as MrgD positive cells are likely not homogenously distributed throughout the DRG and attempting to use IHC or staining methods to verify percent activation of IB4 to MrgD cells would have been labor intensive and ultimately inconclusive as no arbitrary percentage of cells required to be activated was established. Additionally, as light was being delivered to the spinal cord dorsal horn, spinal cord tissue was more relevant to verify ArchT-eGFP expression. ArchT-eGFP is displayed in green.

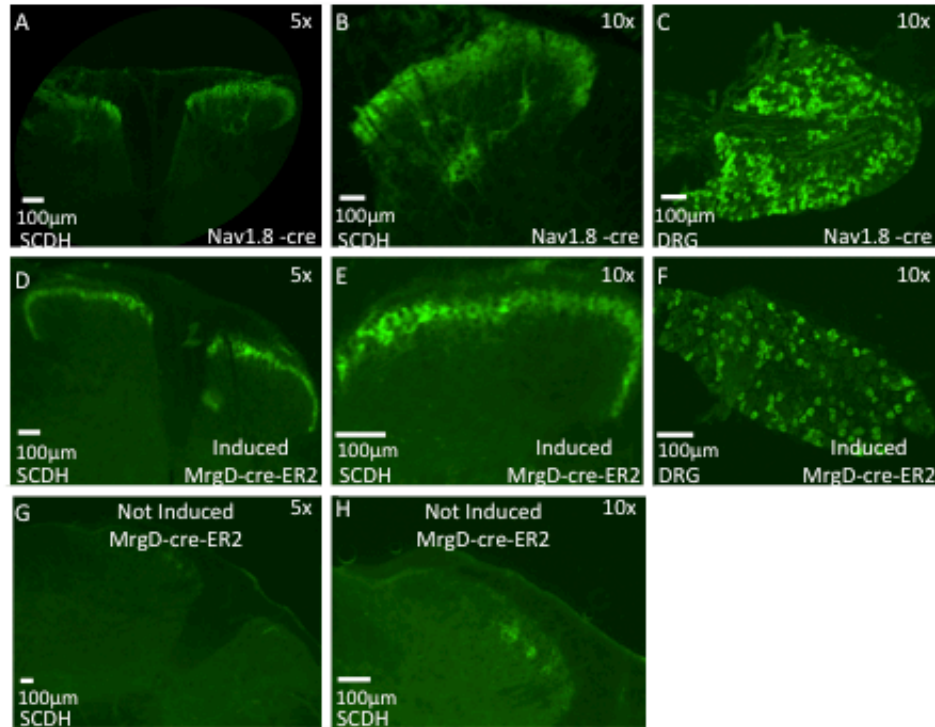


Figure 3.11. Expression Patterns of Cre-activated ArchT-eGFP from Ai40D Transgenic Mice. Differing expression patterns of ArchT-eGFP fusion protein in SCDH and DRG of the two cre lines of mice used. **A-C)** ArchT-eGFP expression in the superficial lamina of the SCDH with some lingering projections into deeper lamina of the spinal cord and robust expression of ArchT in cell bodies of the L4 DRG from Nav1.8-ArchT animals. **D-F)** Representative images of successful cre activation and subsequent ArchT-eGFP expression in the SCDH and cell bodies within DRG from MrgD-ArchT animals. **G-H)** Representative images of incomplete cre activation and lack of ArchT-eGFP expression in the SCDH of MrgD-ArchT animals, animals with ArchT-eGFP expression patterns such as this were removed from behavioral data.

3.3.8. ArchT Induced Silencing of Nav1.8 fibers Relieves Cancer-induced Ongoing Pain, and ArchT Induced Silencing of MrgD Fibers in Animals with Cancer Induces CPP.

Activation of ArchT in Nav1.8-ArchT animals with cancer resulted in an increase in time spent in the laser paired chamber post-conditioning, whereas no increase in time spent in the laser paired chamber was observed in Nav1.8-ArchT sham treated animals displayed in Figure 3.12A ($p < 0.01$, $n = 7$ Nav1.8-ArchT sham treated animals, 9 Nav1.8-ArchT cancer treated animals). MrgD-ArchT animals that underwent cancer implantation spent an increase in time in the laser paired chamber post-conditioning, indicating a preference to the chamber ArchT

induced silencing of MrgD-fibers occurred in ($p < 0.01$, $n = 11$ MrgD-ArchT cancer treated animals). Analysis of “different scores” between the 3 groups of animals demonstrated a significant difference between Nav1.8-ArchT sham treated animals and Nav1.8-ArchT cancer treated and MrgD-ArchT cancer treated animals, Figure 3.12B ($p < 0.05$, $n = 7$ Nav1.8-ArchT sham treated animals, 9 Nav1.8-ArchT cancer treated animals, 11 MrgD-ArchT cancer treated animals). This indicates cancer treated animals that express ArchT either on Nav1.8 or MrgD fibers showed a significant preference compared to Nav1.8-ArchT sham animals. A lack of additional animals restricted our ability to add and compare a group of sham treated MrgD-ArchT animals. We conclude that silencing Nav1.8 expressing fibers induce CPP indicating blockade of ongoing pain, and the same is likely true as a result of silencing MrgD fibers. Once MrgD-Cre-ArchT mice are regenerated, we will rerun a replication that includes shams to 1) provide a replication of this novel and exciting finding and 2) include the appropriate MrgD-Cre-ArchT sham group for publication purposes.

Comparing the “difference score” in Nav1.8-ArchT animals that underwent sham surgery or cancer surgery and MrgD-ArchT cancer treated animals with the measured fiber optic implant efficiency does not reveal a convincing linear correlation between an animals preference and the amount of light exposure to their spinal cord dorsal horn Figure 3.12C (R^2 values = 0.11 in Nav1.8-ArchT sham treated animals, 0.25 in Nav1.8-ArchT cancer treated animals, and 0.06 in MrgD-ArchT cancer treated animals). This indicates that there is likely a threshold for light-induced ArchT activation required to silence fibers resulting in CPP (on-off scenario), rather than a linear relation between ArchT activation and pain relief. We note that CPP may not have sufficient resolution to detect potential subtle changes in intensity of pain relief.

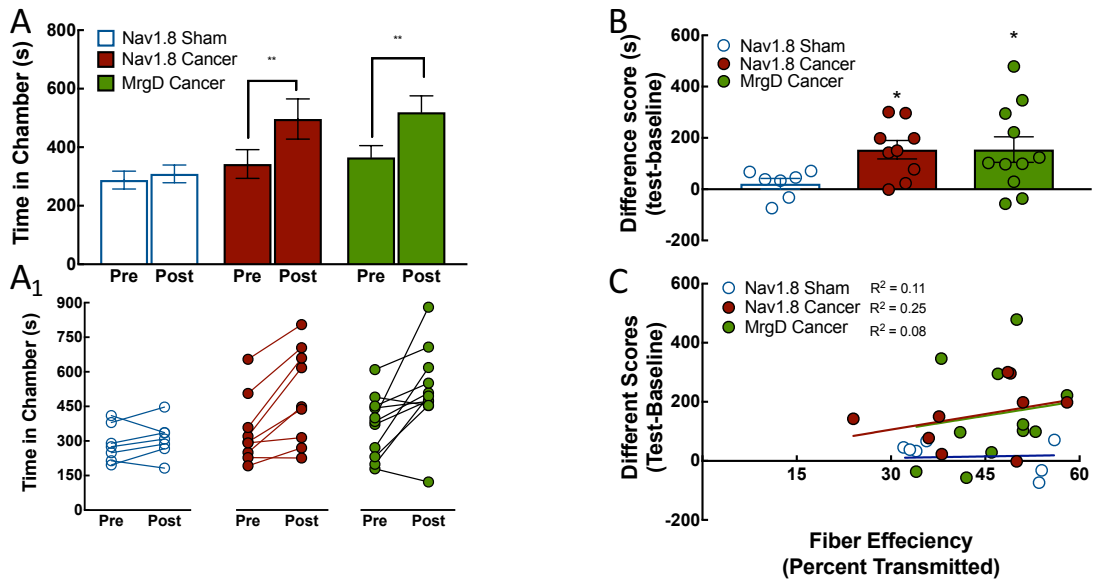


Figure 3.12. ArchT Induced Silencing of Nav1.8 Fibers Causes Relief of Ongoing Pain and ArchT Induced Silencing of MrgD Fibers in Cancer Animals Results in CPP. In Nav1.8-ArchT animals with cancer activation of ArchT paired with the PM chamber results in conditioned place preference, but fails to do so in sham treated Nav1.8-ArchT animals, indicating relief of ongoing pain from the bone. MrgD-ArchT animals with cancer also demonstrate a conditioned place preference for the PM chamber paired with ArchT activation, however no sham animals were run limiting the interpretation of these results. **A)** Both Nav1.8-ArchT and MrgD-ArchT animals with cancer demonstrated an increase in time spent with the laser paired PM chamber, ** $p < 0.01$ pre vs post conditioning. **A₁)** Scatter plots demonstrating individual animals change in behavior following conditioning paradigm. **B)** Comparison of “different scores” reveals that both Nav1.8-ArchT and MrgD-ArchT animals with cancer but not Nav1.8-ArchT sham treated animals developed a change in time spent in the PM chamber. **C)** Linear regression analysis of “different score” compared to measured power output of fiber optic implant reveals no correlation between power output and preference or aversion to the PM/laser paired conditioning chamber

3.3.9. Failure to Induce CPA to Hind Paw Movement in Cancer Treated Animals, and Alternative Behavioral Measures Affected by Hind Paw Movement.

Movement of the hind limb for 2-minutes failed to induce conditioned place aversion in either sham or cancer treated mice, a finding that differs from our published observations in the rat (Havelin, Imbert et al. 2017). Conditioned place aversion to hind paw movement failed in both male and female mice that underwent cancer cell implantation in the femur Figure 3.13A and Figure 3.13B (n = 13 sham treated male mice, 20 cancer treated male mice, 12 sham treated female mice, 12 cancer treated female mice). In an effort to measure alternative behaviors to conditioned place aversion, animals underwent a 2-minute hind limb movement paradigm

followed by measurement of distance traveled and rearing behaviors, 2 measures previously demonstrated to decrease in animals with cancer-afflicted hind limbs (Majuta, Guedon et al. 2017). Consistent with previous findings, animals with cancer travelled and reared less than their sham counter parts Figure 3.14 ($p < 0.01$ and $p < 0.01$ respectively). No statistically significant difference in distance travelled or rearing behavior was observed between sham animals who did not receive 2-minute hind limb movement and those that did ($p > 0.05$ and $p > 0.05$). Animals with cancer that received movement of their cancer-afflicted hind limb travelled less distance compared to cancer animals that did not receive hind limb movement, however no statistical difference between groups was found in rearing behavior ($p < 0.05$). These results indicate that hind limb movement in cancer treated animals but not sham treated animals causes a decrease in movement over the 45-minute observation period (n = 5 sham treated no movement animals, 6 sham treated hind limb movement animals, 5 cancer treated no movement animals, 6 cancer treated hind limb movement animals).

Other behaviors that were monitored were time spent and distance travelled in the margin and center of the LMA chambers, as well as number of center entries (Figure 3.15). Animals with cancer spent less time in the margin, while hind limb movement in animals with cancer decreased the distance travelled in the margin Figures 3.15A1 and Figure 3.15A ($p < 0.05$, n = 5 sham no-movement, 6 sham movement, 6 cancer no-movement, 5 cancer movement and $p < 0.05$, n = 5 sham no-movement, 5 sham movement, 6 cancer no-movement, 5 cancer movement respectively). Tumor bearing animals travelled less, spent less time and entered the center of the LMA chambers less than sham controls Figures 3.15B, 3.15B1 and Figure 3.15C respectively ($p < 0.01$; n = 6 sham no-movement, 6 sham movement, 6 cancer no-movement, 5 cancer movement; $p < 0.05$ n = 5 sham no-movement, 5 sham movement, 6 cancer no-

movement, 5 cancer movement; and $p < 0.05$ $n = 5$ sham no-movement, 5 sham movement, 6 cancer no-movement, 6 cancer movement, respectively).

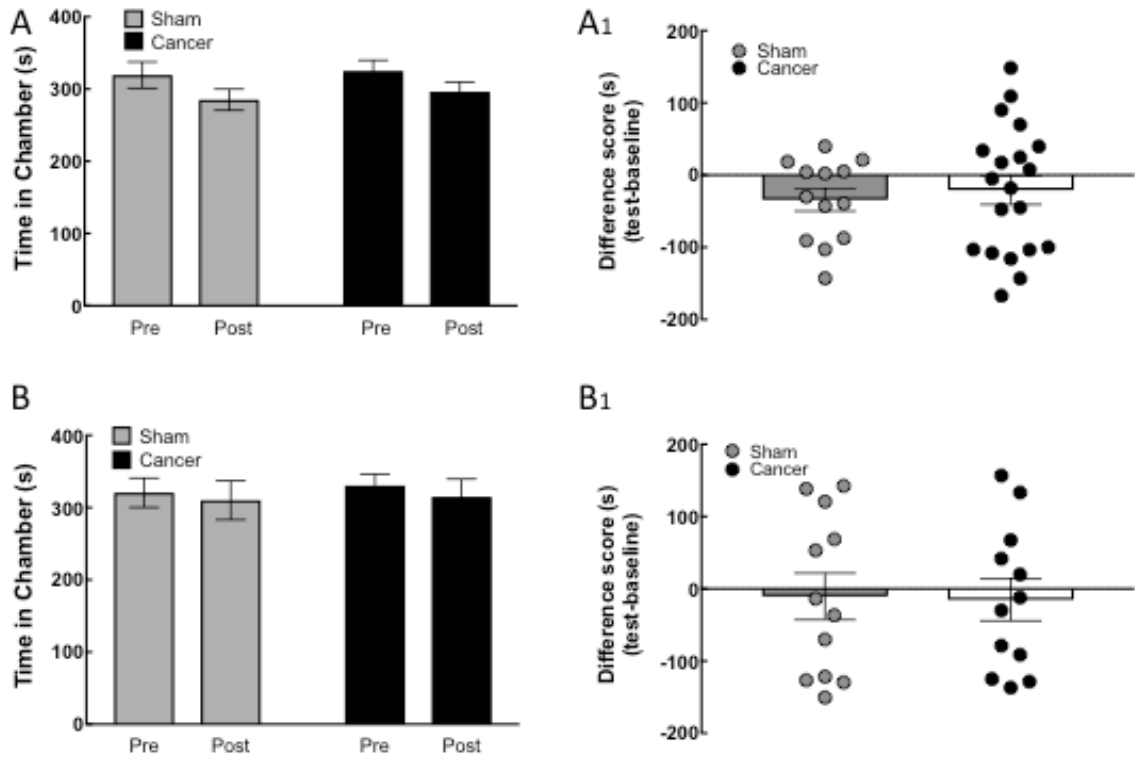


Figure 3.13. Failure of Hind Limb Movement to Induce CPA in Cancer Afflicted C57BL/6 Wild Type Mice. Pairing the PM chamber with a 2-minute hind limb movement fails to induce CPA in both sham and cancer treated animals. (A Males and B Females) No difference in time spent in the hind limb movement paired chamber in either sham or cancer treated animals of either sex. **A1 Males and B1 Females)** No difference between “different scores” of sham and cancer treated animals.

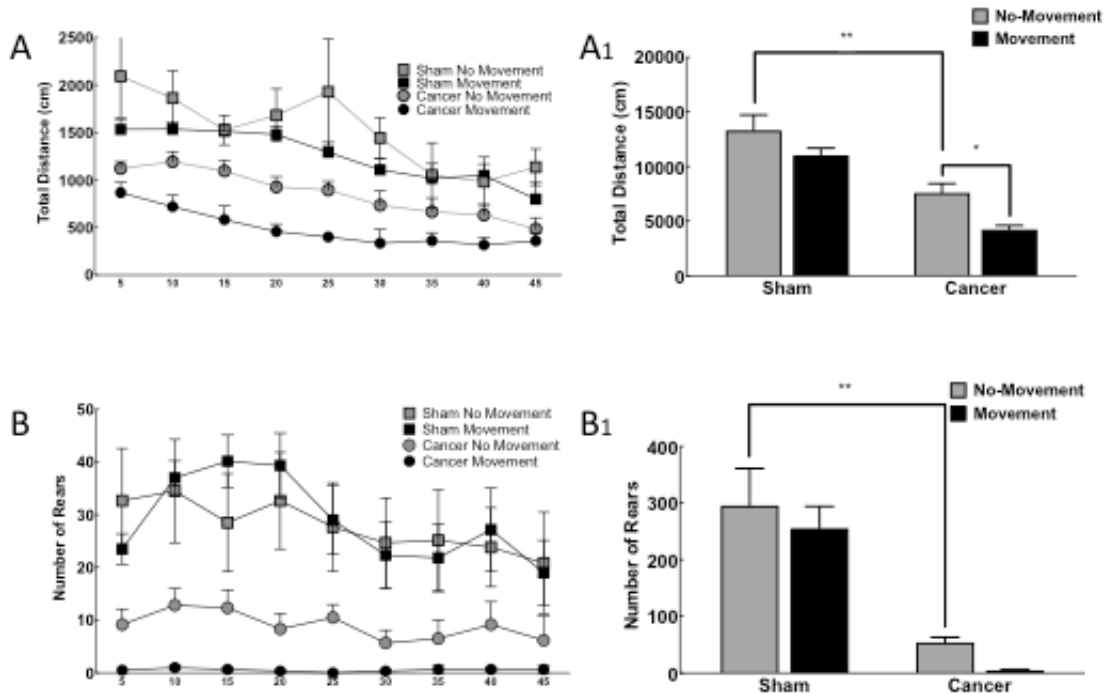


Figure 3.14. Hind Limb Movement Induced Decrease in Distance Travelled and Rearing Behavior. Movement of the cancer-afflicted hind limb in C57BL/6 mice resulted in a decrease in total distance travelled and a decrease in rearing episodes over a 45 minute observation period. **A and A₁**) 5 minute bins of time course of distance travelled by each group of treated mice, and an AUC comparison between groups. Cancer treated animals travelled less distance than sham controls, and movement of the hind limb resulted in a decrease in movement in cancer treated animals but not shams. *,**,**** designates $p < 0.05$, 0.01 and 0.0001 respectively between denoted groups. **B and B₁**) 5 minute bins of time course of rearing episodes over 45 minute observation period and AUC comparison between groups. Animals with cancer reared fewer times than sham controls and hind limb movement reduced the number of rears further, although not statistically significantly. ** and *** designate $p < 0.01$ and 0.001 respectively between denoted groups.

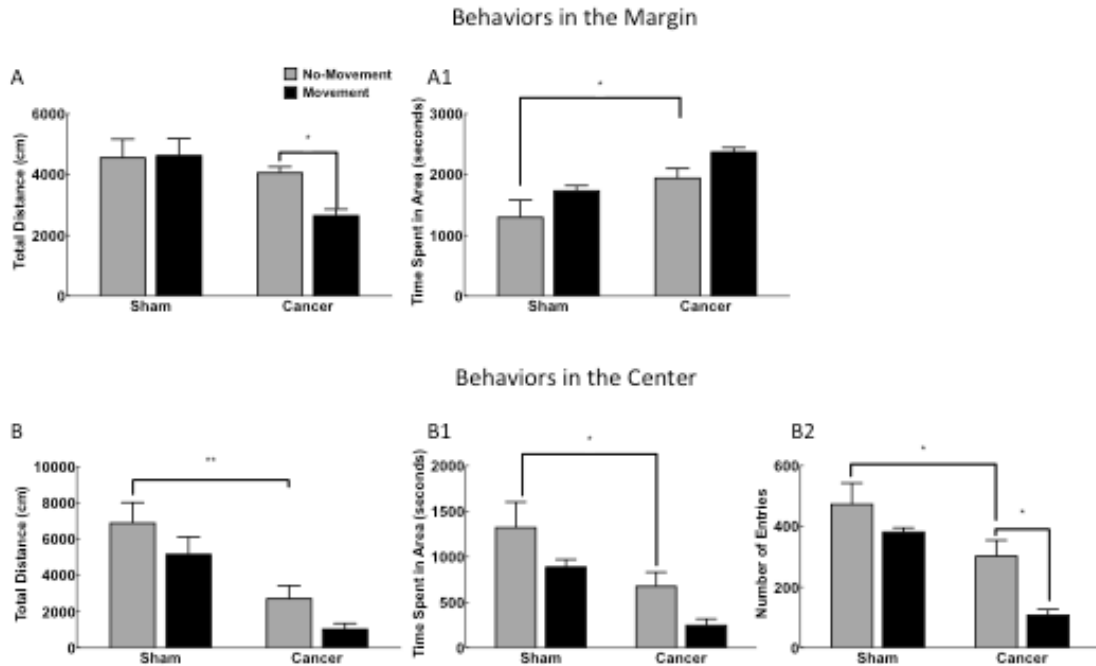


Figure 3.15. Altered Locomotor Behaviors from Cancer and Movement of the Cancer Afflicted Hind Limb. Cancer treatment and movement of the cancer-afflicted hind limb in C57BL/6 mice resulted in a change in behaviors consistent with measures of anxiety like behaviors in the LMA chambers over a 45 minute observation period. **A)** Hind limb movement of the cancer afflicted limb decreases distance traveled in the margin **A₁)** Cancer treated animals spent more time in the margin than sham treated. **B and B₁)** Cancer treated animals traveled and spent less time in the center of the chamber. **B₂)** Cancer treated animals entered the center of the chamber fewer times than sham treated animals, and movement of the cancer-afflicted hind limb resulted in a decrease in the number of times animals entered the center of the chamber. * and ** designate $p < 0.05$ and 0.01 respectively between denoted groups.

3.4. Discussion

We have developed a novel approach to measuring ongoing cancer-induced bone pain and demonstrated that Nav1.8 and MrgD expressing sensory fibers play a critical role in transducing pain in this model of CIBP in the mouse. Further, we have expanded the utility of previously published methods to investigate the role of afferent fibers in transducing pain with intervention to block pain signals at the level of the spinal cord dorsal horn (Bonin, Wang et al. 2016). Moreover, we adapted new measures of movement-induced pain that may serve as a foundation for further development of a measure of BTP in the mouse by monitoring previously

described behavioral changes that arise as a result of CIBP (Guedon, Longo et al. 2016, Majuta, Guedon et al. 2017). We demonstrate that hind limb movement induced changes in several behaviors, distance traveled, rearing and movement in the margin and center of an LMA chamber, that may prove useful in developing a model of breakthrough pain in the mouse.

3.4.1. Classical Measures of CIBP.

Time course data displayed in Figures 3.5 and 3.6 demonstrate that in our hands we have replicated previous reports within the CIBP literature. In both female and male C57BL/6 mice as tumor growth progresses within the femur, mice develop classical tactile hypersensitivity, decreased limb use and an increase in flinching behaviors, consistent with previous reports (Jimenez-Andrade, Bloom et al. 2010, Guedon, Longo et al. 2016, Majuta, Guedon et al. 2017). Female mice also demonstrated classical increase in hind limb guarding behavior and decrease in rearing, consistent with work by others (Honore, Luger et al. 2000, Guedon, Longo et al. 2016, Majuta, Guedon et al. 2017). While these measures have been used consistently over the past 20 years in animal models of CIBP, we wanted to expand and utilize novel measures of pain that rely on the affective components of pain, and the ability to condition animals to pain relief in a paradigm of conditioned place preference in mice where previous work has focused on the rat (King, Vera-Portocarrero et al. 2009, Remeniuk, Sukhtankar et al. 2015, Havelin, Imbert et al. 2017, Remeniuk, King et al. 2018). Additionally transferring focus to the mouse would allow us access to use novel tools such as optogenetics to investigate the role of ongoing afferent activity in CIBP.

3.4.2. Efficacy of the MOR agonist DAMGO to Alleviate Ongoing CIBP.

Previous work by Scherrer et al. 2009 has demonstrated distinct overlap of the MOR with peptidergic nociceptive afferents and the DOR with non-peptidergic afferents. This work also demonstrated a unique delineation of pain modalities between the two nociceptive populations, namely that peptidergic fibers respond to MOR agonists and transduce thermal nociception and that non-peptidergic fibers respond to DOR agonists and transduce mechanical nociception (Scherrer, Imamachi et al. 2009). These findings interest our group as we have previously published evidence that IB4-binding nociceptors (i.e. the non-peptidergic population) but not TRPV1 expressing (i.e. the peptidergic population) fibers plays a critical role in the transduction of hind limb movement induced BTP, a traditionally mechanical pain experience. However, our previous work did not investigate the role of these two fiber populations in ongoing pain from the cancer-afflicted hind limb. The observations that these fiber populations and receptors have overlap gave us the opportunity to attempt to evaluate the role of these fiber types in ongoing pain in the mouse. Previously our group has demonstrated the ability for systemic morphine to alleviate ongoing pain in a model of CIBP in the rat that mimics findings in the clinic (Remeniuk, Sukhtankar et al. 2015). Our attempts to use systemic morphine delivery via morphine pellets in mice led to too many complications to accurately test antinociception in mice (data not shown). Unlike work in the rat where analgesia without hyperlocomotion or sedation at 24 hrs post pellet implantation was observed, implantation of a single morphine pellet (25 mg, s.c.) resulted in hyperlocomotion that persisted through the 24-hour time-point which interfered with our ability to accurately measure behaviors (data not shown). Therefore, we moved to a strategy implementing peptidergic opioid agonists.

We tested the hypothesis that the peptidergic MOR agonist DAMGO but not the peptidergic DOR agonist Deltorphin II could alleviate ongoing pain in the mouse. The basis for

this hypothesis following previous work by Patrick Mantyh demonstrating the peptidergic population of fibers plays a critical role in transducing ongoing pain from the cancer-afflicted limb, and the non-peptidergic fiber did not (Jimenez-Andrade, Bloom et al. 2010). In addition to this, work in that rat ablating TRPV1 expressing (peptidergic population) fibers demonstrated these fibers play a critical role in transducing ongoing pain (King, Qu et al. 2011). Our results demonstrate that systemic injection and activation of the MOR with DAMGO does alleviate ongoing pain, consistent with our hypothesis and with previous findings and clinical observations that MOR agonists manage cancer-induced ongoing pain (Remeniuk, Sukhtankar et al. 2015, Guedon, Longo et al. 2016, Havelin, Imbert et al. 2017). However, at a dose of 3 mg/kg Deltorphan II failed to induce conditioned place preference in mice, again consistent with our hypothesis and previous work (Scherrer, Imamachi et al. 2009, King, Qu et al. 2011). It is possible that this dose of Deltorphan II was too low to effectively block ongoing pain, this dose was chosen based on preliminary results from colleagues to reverse other pain behaviors. These findings indirectly demonstrate a role for peptidergic nociceptors in transducing ongoing pain in preclinical models of CIBP, and add to both preclinical and clinical evidence that MOR agonists are capable of alleviating ongoing CIBP.

3.4.3. Efficacy of Virally Delivered ArchT to Block AITC Induced Nociceptive Behaviors.

In an attempt to verify the efficacy of our approach to target the Nav1.8 and MrgD populations of nociceptive fibers we chose to use an acute robust model of nociception using an injection of 1% AITC solution into the hind paw of mice. After verifying expression of virally delivered ArchT-eGFP in both the spinal cord dorsal horn and cell bodies of the dorsal root ganglion we sought to block nociceptive input from both populations of fibers. AITC activates the TRPA1 channel, which is critically involved MIA induced osteoarthritic pain blocked with

TRPA1 antagonists (Eid, Crown et al. 2008, Okun, Liu et al. 2012). Given their role in transducing nociceptive stimuli we believed that inhibition of Nav1.8 fibers would block the nocifensive response typically observed by activating TRPA1. Beyond this, mining the Usoskin 2016 database revealed that Nav1.8 and MrgD RNA transcripts are present at relatively high levels in the same cell types that express TRPA1, leading us to believe that inhibition of MrgD expressing fibers may also block AITC induced nocifensive behaviors.

Robust nocifensive responses in wild type mice were indeed observed following hind paw injection of 1% AITC, consistent with previous reports (Eid, Crown et al. 2008). Much to our excitement, laser induced activation of ArchT on Nav1.8 fibers nearly completely blocked nocifensive behaviors in mice with correctly implanted fiber optics that allowed for light delivery to the afferent terminals within the spinal cord dorsal horn. A similar blockade of nocifensive behaviors was observed by inhibiting MrgD afferents with ArchT, a most exciting finding indeed. Due to the overwhelming evidence that Nav1.8 expressing fibers play a critical role in nociceptive transduction, a recent benefit of the development of optogenetic technology, we were not surprised to see a blockade of these behaviors in mice (Daou, Tuttle et al. 2013, Bonin, Wang et al. 2016, Daou, Beaudry et al. 2016). However, previous to this work no published evidence has demonstrated a transient and direct role of the MrgD fibers in transducing nociceptive stimuli. Beyond our work in the rat implicating IB4-binding afferents in transducing BTP, evidence for the non-peptidergic fibers in playing a role for transducing nociceptive stimuli comes from ablating these neurons and demonstrating a critical role in transducing mechanical stimuli and tactile hypersensitivity by Cavanaugh et al. 2009. Indeed previous studies demonstrated that whereas optogenetic activation of TRPV1 and Nav1.8 expressing fibers results in robust nociceptive behaviors and conditioned place aversion, activation of MrgD fibers by channel rhodopsin resulted in paw lifting but failed to produce an aversive role (Daou, Tuttle

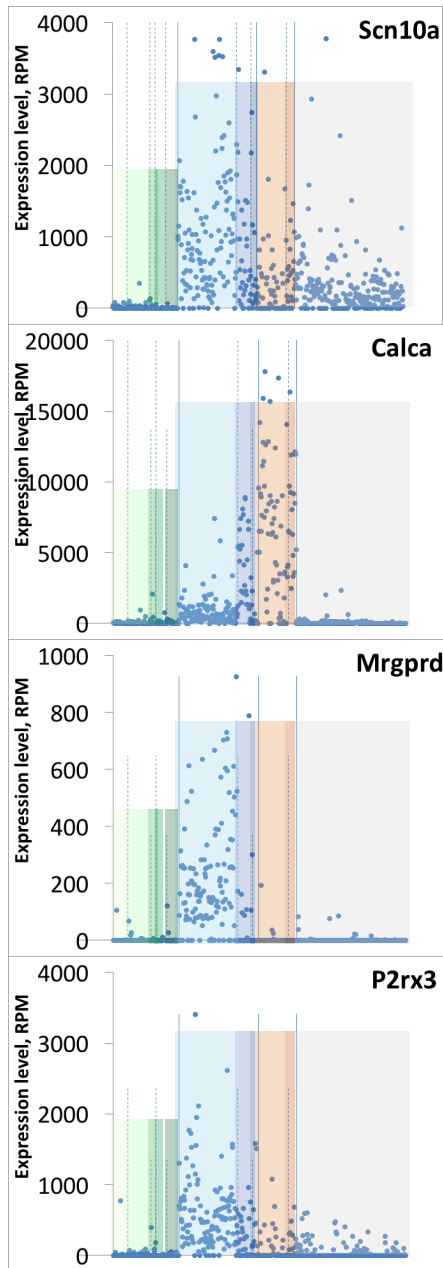
et al. 2013, Bonin, Wang et al. 2016, Daou, Beaudry et al. 2016, Beaudry, Daou et al. 2017, Uhelski, Bruce et al. 2017). Interestingly as reported by Beaudry et al. 2017, activation of TRPV1 fibers by channel rhodopsin resulted in paw withdrawal and paw licking, but not lifting, whereas activation of MrgD fibers resulted in withdrawal and lifting but not licking. Our results indicate that inhibition of MrgD fibers blocks afferent input that leads to licking responses, a finding that we intend to verify by repeating this study with adequate numbers for statistical analysis. We note that these observations may indicate that whereas direct stimulation of these afferents does not induce a response sufficient to induce nociception or pain, inactivation of these fibers in a state of acute pain is sufficient to produce pain relief. Nevertheless we demonstrate a unique role for MrgD fibers in transducing AITC induced TRPA1 activated nociception, and add evidence to the field that Nav1.8 fibers transduce a variety of nociceptive input. While technically cumbersome, these results also demonstrate the powerful efficacy this approach to selectively silence sensory afferents at the level of the spinal cord dorsal horn can have in the pain field.

3.4.4. The Role of Subsets of Nociceptive Fibers in Cancer-Induced Ongoing Pain.

The stimulation paradigm was chosen based on the possibility of repetitive activation induced exhaustion of the ArchT proton pump. There are few reported methods of relatively long term laser exposures within behavioral paradigms investigating pain, especially with regards to ArchT-induced CPP. Therefore, we estimated a recovery period for the ArchT proton pump of 60 seconds. Thus we selected a 2 minute on, 1 minute off laser activation paradigm, that would result in a total of 20 out of 30 minutes of potential inhibition of fibers.

Expanding on the use of conditioned place preference to pain relief we sought to demonstrate the role of Nav1.8 fibers in transducing CIBP by silencing them with the light

sensitive proton pump ArchT. We have demonstrated that ArchT-induced inhibition of Nav1.8 fibers in animals treated with cancer but not shams results in CPP to pain relief with our ArchT activation paradigm. These results demonstrate that ongoing pain from the cancer-afflicted limb is transduced by Nav1.8 expressing fibers. This observation is consistent with other work demonstrating that these channels are expressed on a broad population of sensory fibers including peptidergic and non-peptidergic fibers (Figure 3.16) which have previously been implicated in ongoing pain and other pain behaviors in models of CIBP (Jimenez-Andrade, Bloom et al. 2010, Bloom, Jimenez-Andrade et al. 2011, King, Qu et al. 2011). While work by Shields et al. has demonstrated that Nav1.8 is likely not restricted to C-fibers, optogenetic activation of Nav1.8 fibers has been demonstrated to convey nociceptive information (Daou, Tuttle et al. 2013, Daou, Beaudry et al. 2016, Uhelski, Bruce et al. 2017). We also believe this to be the first reported evidence of optogenetically silenced Nav1.8 fibers resulting in CPP to pain relief, demonstrating a paradigm of ArchT induced silencing of fibers that can be used in future experiments. These results also serve as a positive control for our work in silencing MrgD expressing fibers to measure their role in cancer-induced ongoing pain.



NP1	NP2	NP3	PEP1	PEP2	TH
PLXNC1 ^{high}	PLXNC1 ^{high}	PLXNC1 ^{high}	TRKA	TRKA	PIEZO2 ^{high}
P2X3	P2X3	P2X3	CGRP	CGRP	VGLUT3
GFRA2	TRKA	SST	KIT	KIT	GFRA2
MRGPRD	CGRP		TAC1	CNTNAP2	
	MRGPRA3		PLXNC1 ^{low}	FAM19A1	
Nonpeptidergic			Peptidergic		C-LTMRs
Unmyelinated				Myel.	Unmyel.
RET	RET	RET		NEFH	RET
TRPA1	TRPV1	TRPV1	TRPV1		TRPA1
TRPC3	TRPA1	TRPA1			
NAV1.8/9	TRPC3	TRPC3			
	NAV1.8/9	NAV1.8/9	NAV1.8/9	NAV1.8/9	NAV1.8/9

Taken from Bonin et al. 2016

Figure 3.16. Demonstrable Overlap in RNAseq Data of Sensory Neurons. Single Cell RNAseq demonstrating subpopulations of sensory fibers. Scn10A, Nav1.8 fibers; Calca, CGRP; Mrgprd, MrgD; P2rx3, P2X3. Colored table taken from Usoskin et al. 2016. Data mined from Linnarsson Lab website, (<http://linnarssonlab.org/drg/>). Figure adapted with color scheme by Joshua Havelin for ease of visualization. Note Y-axis change between graphs.

Interestingly, our results also demonstrate that ArchT-induced inhibition of MrgD fibers in animals with ongoing pain from the femur causes CPP. Initially the construction of our experiment was based on the hypothesis that we would not see conditioned place preference in MrgD-ArchT sham let alone cancer treated animals, and thus we needed to compare MrgD-ArchT cancer animals to a group we were confident that would have a positive outcome in the study. This group was run side by side with the positive control group, Nav1.8-ArchT cancer treated animals. Nevertheless this group of animals showed robust conditioned place preference to the PM laser paired chamber. Prior to this a lack of evidence suggested that MrgD, non-peptidergic, fibers would not play a role in transducing ongoing CIBP (Jimenez-Andrade, Bloom et al. 2010, Guedon, Longo et al. 2016). Several possible explanations do exist for this outcome. The first namely being that MrgD fibers do in fact play a role in transducing ongoing pain from the cancer-afflicted bone. This would require as previously mentioned the inclusion of an MrgD-ArchT sham group to demonstrate that inhibition of MrgD fibers is not inherently rewarding for some strange reason.

Alternatively, as there is evidence that MrgD fibers play a critical role in transducing mechanical nociception (Cavanaugh, Lee et al. 2009, Scherrer, Imamachi et al. 2009), It is possible that inhibition of these fibers blocks the occurrence of tactile hypersensitivity that the mice may be chronically experiencing while applying weight to the skin on their hind paws. Many times over in CIBP models, measurements of tactile hypersensitivity from the skin of the hind paw have been demonstrated (Honore, Luger et al. 2000, Jimenez-Andrade, Bloom et al. 2010, Guedon, Longo et al. 2016, Edwards, Havelin et al. 2018). Inhibition of this experience may result in a rewarding affective experience to the mice, which could result in conditioned place preference to the inhibition of MrgD fibers. However, the initial paper characterizing CPP to pain

relief (King, Vera-Portocarrero et al. 2009) demonstrated relief of tactile hypersensitivity was not sufficient to induce CPP, making the likelihood of this justification small.

Additionally, previous evidence by our group has implicated IB4-binding sensory neurons (“non-peptidergic”) in being critically involved in transducing BTP following manual manipulation of the cancer-afflicted hind limb in rats (Havelin, Imbert et al. 2017). As CIBP is a heterogeneous and complicated pain pathology, further muddled by the fact that movement may induce additional pain episodes as reported from the clinic, it is possible that transient inhibition of MrgD fibers may have blocked the induction of BTP episodes caused by normal movement of the mice throughout the PM conditioning phase. Which if in the mouse is as painful as reported by patients in the clinic, could likely induce a drastically rewarding effect when removed from animals with cancer. A potential method to examine this would be the use of ambulatory movement on a rot-a-rod apparatus with a similar optogenetic stimulation paradigm to that used in our hands, or wheel running behaviors. Work by Pat Mantyh in the past has used the rot-a-rod apparatus to investigate the effects of ambulatory movement on CIBP and demonstrated some interventions reverse CIBP induced deficits (Luger, Honore et al. 2001, Sabino, Ghilardi et al. 2002, Peters, Ghilardi et al. 2005). However this method has not been established or characterized as a model of BTP in the mouse. Additionally the measures proposed later in this body of work could be used (Figures 3.13 and 3.14).

To confirm any of these possibilities would take additional work that would require the introduction of additional pain measures, potentially some that currently don’t exist (i.e. a measure of BTP in the mouse).

3.4.5. Inability to Establish CPA to Hind Paw Movement in the Mouse and Potential Alternative Measures of Hind Paw Movement-Induced Pain.

The failure to translate hind limb movement induced conditioned place aversion in the mouse was surprising. The robustness of aversion observed in the rat convincingly conveys that movement of the cancer-afflicted hind limb induces an unpleasant experience in animals (Havelin, Imbert et al. 2017). Moreover, previous work published by Patrick Mantyh has also demonstrated that movement of the cancer-afflicted hind limb induces exacerbation of pain measurements and neurochemical markers of nociception in the spinal cord in mice (Luger, Honore et al. 2001, Sabino, Luger et al. 2003, Peters, Ghilardi et al. 2005). Experimenter notes from our group during hind limb movement of the cancer-afflicted limb also demonstrate that even in our hands mice appear to be in an exacerbated pain state, within increased limb guarding and decreased limb use immediately following limb movement. These observations make it is unlikely that an inter-technician variance is causing some sort of non-painful experience during hind limb movement in our hands that did not occur in others. Another possibility is that while rats and mice differ in some ways in their temperament, the experience may be more stressful or anxiety inducing in the mouse compared to the rat which may impart a detriment to the mice's ability to learn and "remember" to avoid the hind limb movement paired chamber on test day. This challenge would implicate that the conditioned place aversion approach would not be feasible with mice. More likely and surmountable would be that mice might require additional exposure to the hind limb movement paired chamber, i.e. multiple days of pairing, however, due to the nature of the pain state the mice are in and that in order to test this hypothesis the animals would need to be put in what may be excruciating pain more than once with no intervention to diminish or manage this pain, ethical considerations may need to be discussed before such an approach could be used.

As a result of our inability to observe aversion to the hind limb movement paired chamber, we performed an experiment to observe several other behaviors that have been previously described to be altered as a result of tumor growth within the femur, and orofacial cancer. Rearing behavior and total distance traveled has been reported as potential measures of pain that decrease in animals with cancer, and orofacial pain has been demonstrated to induce measures of anxiety in rats (Gambeta, Kopruszinski et al. 2016, Gambeta, Kopruszinski et al. 2017, Majuta, Guedon et al. 2017). These two behaviors have not, to our knowledge, been monitored following hind limb movement of the cancer-afflicted femur with the intent to examine changes that may present as a result of movement induced pain. We have replicated the finding that cancer animals rear and travel less than sham treated controls, as was reported by (Majuta, Guedon et al. 2017). Interestingly, a 2-minute movement of the hind limb did not significantly alter either rearing or distance traveled in sham treated animals, but did decrease both behaviors in cancer treated animals. A significant difference was observed in the amount of distance traveled over the course of 45 minutes, where as a difference, albeit not statistically, was observed in rearing episodes over the 45 minute observation period. We note that there is likely a floor effect for rearing at the time-point that we tested the behaviors. Testing for these behaviors at earlier time-points may allow for a larger, and more measureable change in behavior.

Our intent was to monitor whether ArchT induced inhibition of Nav1.8 or MrgD fibers could block this effect in cancer bearing animals. Due to restrictions within our animal colony and larger animal attrition than anticipated due to the technically difficult procedure of epidural implantation of optic fibers for the epigenetic studies, this work has not been completed. The colony of MrgD-ArchT mice used in the previous studies will be re-established in Dr. King's lab to complete this work. A pharmacological intervention could be performed in a timelier manner

than experiments requiring transgenic animals, however morphine administration in mice can result in hyperlocomotion. We have observed this and this is well reported in the past (Lowery, Raymond et al. 2011). The hyperlocomotion in cancer treated animals inevitably confounds the use of “distance travelled” and rearing episodes as a measure of hind limb movement induced suppression of this behavior that would have to be demonstrated to classify this as a measure of BTP. It is likely that other paradigms of MOR agonist administration could be used, we have not at this time characterized this work. Also, without a current pharmacological agent that effectively blocks BTP, screening of compounds using this approach would have no pharmacological positive control to compare to.

3.5. Conclusion

In conclusion, we have implemented a novel approach to investigate CIBP utilizing cutting edge optogenetic approaches, both through viral transfection of peripheral neurons and transgenic delivery of light sensitive proteins. Work presented here also lends evidence to a novel role of MrgD expressing or non-peptidergic nociceptive fibers may play in transducing CIBP. We have demonstrated and implicated Nav1.8 expressing fibers in transducing cancer-induced ongoing pain, and utilized a novel approach using optogenetically silenced peripheral neurons to induce conditioned place preference to pain relief in the mouse. Lastly, work presented here may allow for the development of a measure of BTP in the mouse.

CHAPTER 4

DISCUSSION OF FINDINGS

4.1. Summary of Results

In this body of work, we put forth new and exciting data that suggests a unique role for subpopulations of sensory neurons in mediating CIBP. While this work is not exhaustive down to the electrophysiological level, it is the first to investigate the role for subpopulations of sensory neurons using a paradigm of pain relief that involves the affective components of pain relief and pain induction, rather than reflexive and evoked measures of pain. Work by myself and colleagues have produced a model of BTP that can be evoked by manipulating the hind limb of a cancer bearing rat, which results in the production of an aversive state that “breaks through” onboard morphine, which can be blocked with a peripheral nerve block prior to induction of pain. Interestingly peripheral nerve block after the induction of pain fails to block this aversive pain state. We further demonstrate that the establishment of this pain state relies on the involvement of IB4-binding fibers (non-peptidergic), but not TRPV1 expressing fibers (peptidergic), an observation contrary to a number of previous theories of CIBP. Additionally, work reported here demonstrates that in the mouse, activation of the MOR, believed to be targeting peptidergic sensory neurons, alleviates ongoing CIBP, whereas activation of the DOR may not. Interestingly, optogenetic induced silencing of Nav1.8 sensory fibers also relieves ongoing pain in our mouse model of CIBP, and silencing MrgD (non-peptidergic) expressing sensory fibers in cancer bearing animals induces conditioned place preference. This culmination of work demonstrates and implicates a potentially unique role for the IB4-binding/MrgD-expressing/non-peptidergic populations of sensory neurons in conveying CIBP, contrary to the

majority of published work demonstrating evidence for a lack of involvement of these fibers in preclinical models of CIBP.

4.2. Major Findings

Classical measures of Cancer-Induced Bone Pain in the Rat and Mouse. As previously demonstrated by others in the field, we demonstrate that implantation of the MATB3 cell line into the tibia of rats, and the implantation of the LLC cell line into the femur of mice results in dramatic bone degradation accompanied by behaviors associated with preclinical models of CIBP. In both species of animals, mechanical tactile thresholds decreased as tumor growth and bone destruction progressed, consistent with original findings in both species (Schwei, Honore et al. 1999, Medhurst, Walker et al. 2002). Limb use in both species also decreased over time, a finding that is consistently reported and coincides with decreased motor activity by the animals, and decreased weight bearing to the affected hind limb, and hind limbs as a result of decreased rearing (Medhurst, Walker et al. 2002, Remeniuk, Sukhtankar et al. 2015, Guedon, Longo et al. 2016, Majuta, Guedon et al. 2017, Remeniuk, King et al. 2018). These behaviors have been demonstrated to coincide and likely be driven by pathological sprouting of peptidergic and sympathetic nerve fibers in both the periosteum and marrow space within the bone.

Several papers have examined the effects of an anti-NGF primary antibody and its ability to blunt the pathological sprouting observed in the mouse model of CIBP (Jimenez-Andrade, Bloom et al. 2010, Mantyh, Jimenez-Andrade et al. 2010, Bloom, Jimenez-Andrade et al. 2011, McCaffrey, Thompson et al. 2014, Guedon, Longo et al. 2016). Interestingly while this antibody does effectively block pathological sprouting of peptidergic and sympathetic fibers, along with the accompanying measures of pain, whether or not it blunts bone remodeling may depend on the cell line, surgical preparation, and immune system integrity as varying reports by the same

group have been published (Bloom, Jimenez-Andrade et al. 2011, McCaffrey, Thompson et al. 2014). These observations coincide with additional work by Patrick Mantyh and colleagues examining models of pathological bone fracture and the nerve sprouting that accompanies incomplete or pathological healing (Chartier, Thompson et al. 2014). Measures of spontaneous pain as well as measures of movement in this model of bone fracture pain are also attenuated by anti-NFG therapy, highlighting the role NGF plays in pain associated with pathological pain from the bone (Majuta, Guedon et al. 2017, Majuta, Mitchell et al. 2018).

While not as extensively analyzed as it has been in the mouse, it appears that in similar models of bone and joint pain, anti-NGF therapy appears to be effective in the rat, dogs, cats, and human (Xu, Nwosu et al. 2016, Suzuki, Millecamps et al. 2018, Enomoto, Mantyh et al. 2019). Fuseya et al 2016 targeted TRPV1 expressing neurons with qx-314 in mice and demonstrated reversal of spontaneous flinches but not scores of limb use, highlighting a differential role of peripheral fiber types and the role they play in CIBP (Fuseya, Yamamoto et al. 2016). Interestingly, in our hands capsaicin induced ablation of TRPV1 expressing sensory neurons (peptidergic) failed to block the development of cancer-induced mechanical tactile hypersensitivity in the rat (Havelin, Imbert et al. 2017). This observation may be result of specie differences, or perhaps anatomical location of the cancer-afflicted bone (femur in the mouse, tibia in the rat). While other treatments that are effective at blocking cancer-induced bone remodeling such as Denosumab/OPG and bisphosphonates, also appear to block classical measures of CIBP, it is unclear as to their effects on whether blocking pathological bone remodeling simultaneously blocks pathological sprouting. However, therapies that diminish bone degradation in the clinic are also reported to slow development of pain (Steger and Bartsch 2011).

While approaches to selectively target the peptidergic population of sensory neurons appear to be wholly efficacious in blocking the development of classical CIBP behaviors, agents targeting the non-peptidergic population seem to have more varying effects. In the mouse, targeting the P2X3 receptor with a primary antibody only resulted in reversal of tactile hypersensitivity and not other measures of bone pain such as shifted weight bearing and decreased rearing, indicating potential differential mechanisms mediating tactile hypersensitivity and other kinds of pain such as ongoing pain (Guedon, Longo et al. 2016). While in the rat, antagonism of the P2X3 receptor resulted in a reversal of tactile hypersensitivity in 2 separate studies, and offset weight bearing (Kaan, Yip et al. 2010, Wu, Xu et al. 2012), an observation that did not occur in the mouse (Guedon, Longo et al. 2016). In our hands, spinal administration of IB4-saporin induced ablation of IB4-binding fibers (non-peptidergic) and resulted in blockade of tactile hypersensitivity in the rat (Havelin, Imbert et al. 2017). The combination of these results undeniably suggests a critical role for non-peptidergic sensory fibers in the development and transduction of mechanical tactile hypersensitivity. To the best of my knowledge, no alternate approaches have been attempted in the mouse in a model of CIBP, although work investigating the effects of oral cancer pain has used an ablative approach similar to our rat work (Ye, Bae et al. 2014).

While work presented here aligns with literature within the field, and adds interesting new pieces that warrant further investigation, these classical measures of pain, i.e. flinching, guarding, limb use, referred tactile hypersensitivity, weight bearing, don't necessarily examine our main questions regarding fiber types and their involvement in driving ongoing and movement evoked breakthrough pain. Paramount to the justification to investigate alternative behavioral paradigms King et al. 2009 demonstrated that alleviation of tactile hypersensitivity in a model of neuropathic pain did not equate to alleviation of ongoing pain. That is to say,

alleviation of tactile hypersensitivity does not mean that alleviation of ongoing pain has been achieved, a clinical and preclinical observation (King, Vera-Portocarrero et al. 2009). Observations such as this placed the focus and priority of our work on examining behavioral paradigms of pain that include the affective motivation to seek out pain relief or avoid the induction or association of pain. Namely, by using conditioned place pairing paradigms that allow an animal to freely seek out pain relief, or avoid painful stimuli.

Role of Subsets of Peripheral Neurons in Cancer-induced Ongoing Pain. Building on our observations that different fiber types mediate different aspects of cancer-induced bone pain (Havelin, Imbert et al. 2017), we examined the role of MrgD vs Nav1.8 expressing fibers in mediating ongoing pain in the mouse. Our investigation into the role that subsets of fibers play in cancer-induced ongoing pain revealed an unsurprising role for the Nav1.8 expressing population of fibers and a potentially unique role for MrgD expressing fibers. Previous work used CPP to pain relief in a model of CIBP in the rat, demonstrating novel findings for mechanisms critical to the transduction of ongoing pain. Namely that ongoing pain in the rat requires input from peripheral neurons that innervate the tibia, which can be blocked by peripheral nerve block with 4% lidocaine, and that the same paradigm that results in CPP to pain relief results in release of dopamine in the Nucleus Accumbens, a hallmark of the rewarding factor of pain relief (Remeniuk, Sukhtankar et al. 2015). In addition to this Remeniuk et al. 2015 also demonstrated that whereas the NSAID diclofenac fails to alleviate ongoing pain, morphine successfully does so. This being a direct translation from bed to bench of investigating CIBP using CPP to pain relief. Remeniuk et al. 2018 also demonstrated that the inflammatory mediator IL-6 plays a critical role in the development and establishment of cancer-induced ongoing pain (Remeniuk, King et al. 2018). To my knowledge these are the only two papers using conditioned place preference to pain relief in the CIBP literature, however work investigating

orofacial cancer pain has also demonstrated CPP to pain relief in animals with cancer (Gambeta, Kopruszinski et al. 2017).

Work presented here solidifies the expected role that Nav1.8 expressing fibers play in transducing ongoing CIBP. As in many other models investigating the role of Nav1.8 fibers in models of pain we demonstrate that using a novel paradigm of Nav1.8 fiber inhibition, we can successfully induce CPP to pain relief in mice bearing tumors in their femur. The observation that inhibition of Nav1.8 fibers in cancer bearing but not sham animals induces CPP diminishes the likelihood that inhibition of Nav1.8 fibers itself is rewarding, implying the likelihood that these fibers are quiet under “normal” conditions. Silencing these fibers at the level of the spinal cord dorsal horn in cancer-bearing animals blocks the transduction of nociceptive signals from the periphery, similar to a peripheral nerve block which has been previously demonstrated to induce CPP to pain relief (Remeniuk, Sukhtankar et al. 2015). This is an intuitive interpretation of these results as it is well described and known that as a result of tumor growth and tumor-induced destruction of the bone, fibers in this tissue are constantly being bombarded with a slew of inflammatory mediators that can directly activate and drive signals in Nav1.8 expressing fibers (Mantyh 2014, Mantyh 2014). As the Nav1.8 fiber population includes the peptidergic population of nociceptive neurons, which have been previously demonstrated to be critical in transducing nociceptive stimuli, it is very likely Nav1.8 fibers are present in the bone and periosteum and undergo changes similar to those described in the peptidergic fibers described by others (Mach, Rogers et al. 2002, Jimenez-Andrade, Bloom et al. 2010, Bloom, Jimenez-Andrade et al. 2011, Castaneda-Corral, Jimenez-Andrade et al. 2011). These observations contribute to the body of work using optogenetics to investigate the theory that Nav1.8 fibers are critical in transducing painful stimuli from the periphery.

Perhaps the most intriguing results included in this body of work is the demonstration that ArchT induced silencing of MrgD expressing fibers in animals bearing tumors results in conditioned place preference. These data indicate that blockade of MrgD expressing sensory fibers likely blocks ongoing CIBP as no previous interventions have induced CPP in sham animals. Additional studies are planned once the colony is re-established to verify/replicate this observation in a study with a larger sample size and include MrgD sham controls as the initial study only included Nav1.8 sham controls. As mentioned previously, only correlative evidence exists using IHC methods staining for P2X3, staining with fluorescent IB4-conjugates, and transgenic reporter animals that demonstrates a lack of the presence of these fibers in the naïve and cancer-afflicted femur (Mach, Rogers et al. 2002, Jimenez-Andrade, Mantyh et al. 2010). Additionally, blockade or antagonism of P2X3 with antibody or antagonist has been demonstrated to play a role in measures of CIBP such as tactile hypersensitivity. Notably, these measures do not necessarily measure ongoing pain (Kaan, Yip et al. 2010, Wu, Xu et al. 2012, Guedon, Longo et al. 2016).

In addition, blocking a single channel on a fiber differs from blocking the activity of the entire neuron as we do by stimulating ArchT in the MrgD expressing neurons. Therefore, this may account for differential effects observed between our studies and those selectively blocking the P2X3 channel. As such, whether MrgD fibers play a role in ongoing pain was an open question. Our work indicates that blocking MrgD fibers blocks ongoing pain both in acute/transient pain states as indicated by our AITC findings and likely in CIBP. We note that others have demonstrated that driving MrgD fibers fails to induce pain-like behaviors indicating that driving these fibers alone may not be sufficient to induce pain (Beaudry, Daou et al. 2017). One limitation of previous imaging studies examining whether MrgD expressing or IB4-binding fibers innervate the bone is that identification, imaging and the treatment of decalcified tissue

as well as the periosteum can cause loss of antigen and general abuse to the tissue, resulting in a very challenging endeavor, and potentially leading to a false negative result (Mach, Rogers et al. 2002, Akkiraju, Bonor et al. 2016). These reservations of previous work lend some in the field to believe there may yet be a subpopulation of non-peptidergic fibers that does exist in the bone but has not been discovered or reported.

There are alternative explanations that would explain CPP to inhibition of MrgD fibers in tumor bearing animals. Due to the rapid nature of how quickly optogenetic tools can inhibit neurons, and how quickly this electrochemical effect wears off, it is unlikely that ArchT mediated inhibition of MrgD fibers results in a proteomic or genetic shift in cellular activity that could produce CPP. This begins the conundrum of interpreting and discussing these results if, as the field currently reports, MrgD fibers do not innervate the cancer afflicted femur or periosteum. The question becomes how does inhibiting this class of fibers that do not innervate the site of ongoing tumor pathology, result in a positive affective condition for the animals? I propose that the pain signal maintaining and generating ongoing pain originates from fibers either in the bone or the periosteum surrounding the bone, rather than a secondary site such as the skin. This does leave the possibility that sensitization of fibers in surrounding or anatomically relevant tissue can occur (i.e. peripheral and central sensitization) which may result in pathological pain originating from fibers other than those in the bone.

One attractive hypothesis is that if indeed MrgD expressing fibers do not innervate the bone or periosteum, perhaps activation of nociceptive fibers that do innervate the bone in one way or another lead to the generation of an antidromic signal from the spinal cord that leads to the sensitization of MrgD expressing fibers. Ferrari et al. 2015, elegantly describes just such a situation where hyperalgesic priming induced at the level of the spinal cord generates an antidromic signal, potentially CPEB mRNA, that induced hyperalgesia in peripheral sensory

fibers, and may be unique to the non-peptidergic population of nociceptors (Ferrari, Araldi et al. 2015). Origin of this signal is likely beyond the scope of this body of work, but may result as a cause of cancer-induced hypertrophy of astrocytes within the spinal cord as reported by others (Sabino, Luger et al. 2003). Interestingly in a side by side comparison of the effects of different cancer cell lines, out of the sarcoma, melanoma, and colon tumors compared, melanoma cells didn't induce drastic bone degradation, did not result in ambulatory movement induced pain, and did not induce astrocyte hypertrophy in the spinal cord (Sabino, Luger et al. 2003). Potentially indicating a necessary role of astrocyte hypertrophy in driving measures of ongoing and ambulatory movement-induced pain. Interestingly, recent work using optogenetic activation of astrocytes in the spinal cord, believed to induce release of ATP (an activator of the P2X3 receptor found on non-peptidergic fibers) has been shown to induce measures of nociception from the hind paw (Nam, Kim et al. 2016). Perhaps astrocytes within the spinal cord are producing a signal that causes changes in the MrgD expressing population of neurons in an antidromic fashion. To date no one has reported whether or not the induction of hyperalgesic priming results in a prolonged ongoing pain state that can be assessed by using CPP to pain relief. However, work by Okun et al. 2011 has demonstrated that while mechanical hypersensitivity persists, the ongoing pain from CFA injection into the hind paw does diminish, and previous work has demonstrated that CFA can induce hyperalgesic priming in the periphery.

This observation does not entirely exclude the possibility that astrocytes are inducing some form of sensitization that results in hyperalgesia, or some form of activity that leads to an ongoing pain signal from the MrgD expressing neurons. Not only are mechanisms of induction from the periphery different than signals from the spinal cord, cancer-induced activation of nociceptors is a chronic and increasingly intense stimulus. If this is driving pathology capable of

causing sensitization, it is likely different in effect compared to a single priming stimulus, not to mention different in nature to the second hyperalgesia precipitating stimulus.

4.3. Limitations and Lingering Questions

Role of TRPV1 and IB4-binding neurons in Ongoing Pain in the Rat. While the objective of our work in the rat was to establish a model of BTP and investigate primary nociceptor populations in said model, it would have been exciting to examine whether or not ablation of TRPV1 or IB4-binding fibers had a differential effect on ongoing pain. Based on the literature at the time, with the overwhelmingly demonstrated role for peptidergic fibers in classic measures of CIBP pain we hypothesized that ablation of TRPV1 expressing fibers would eliminate ongoing pain, whereas ablation of IB4-binding fibers would not. With the addition of our paper, Havelin et al. 2017, and the work provided here in the mouse, it is possible we would have observed something different. One limitation to consider during this approach is that in the rat, the classical “peptidergic” and “non-peptidergic” populations of nociceptive fibers have been demonstrated to be more overlapping than what is observed in the mouse, and in the rat small numbers of fibers both bind IB4 and express markers of peptidergic fibers (Price and Flores 2007). This can confound the translatability of results between the mouse and rat, where the ablation of IB4-binding fibers (non-peptidergic) actually results in ablation of some peptidergic fibers, and vice versa. While the minutia of this does not ultimately change the results of ablating “all” fibers of one category or the other, it could hinder steps towards isolating these populations and searching for targets for pharmacological compounds. Second, the approach of ablating fibers can inevitably lead to the development of compensatory effects of the nervous system. Whether this be fiber populations growing into areas they were previously restricted from, or perhaps compensatory signaling where fiber terminals once were, not to mention the

potential for altered signaling properties as a result of degenerated neurons both in the spinal cord and in the dorsal root ganglion.

Definitive Role of MrgD Expressing Fibers in Ongoing Pain in the Mouse. While inhibition of Nav1.8 fibers in the sham group did not result in CPP, it is worth examining the effects of inhibiting just the MrgD population in naïve or sham treated animals. Inhibition of Nav1.8 fibers likely results in the simultaneous inhibition of both the peptidergic and non-peptidergic fibers, which has been demonstrated here to be neither inherently aversive nor rewarding. However it is beyond this body of work to hypothesize the differences that may occur during simultaneous inhibition of both, or inhibition of singular populations, this contributes to the necessity to test the effects of independent inhibition of the MrgD population.

It would also be very interesting to utilize the recently published CGRP-cre mouse that would allow for inhibition of the peptidergic population in our approach (Cowie, Moehring et al. 2018). Based solely on the literature surrounding CIBP, I hypothesize we would also see CPP to pain relief by inhibiting the peptidergic population of fibers. If this were to end up being true, many, many grants could be written proposing ideas to investigate signaling at the level of the spinal cord and DRG examining converging or diverging roles for these populations.

Steps to Investigate Rearing and Movement as Measures of BTP in the Mouse and Utilizing Optogenetics to Tease out Fibers' Roles in BTP. We provide here at least 2 measures of behaviors that are altered in cancer bearing animals that are not in sham animals, and several others that may reflect anxiety behaviors in cancer-bearing mice. There are many more parameters and behaviors that can be observed and measured using locomotor chambers. The telltale examination to prove that rearing and distance traveled may be used as measures of BTP would be to demonstrate that hind limb movement induced decrease in behaviors persists while a MOR agonist is onboard. We did in fact try this using 25mg morphine pellets, however 24

hours post morphine pellet implantation our wildtype mice still exhibited stereotypical signs of high dose MOR agonists, i.e. straub tail, hyperlocomotion and circling patterns. Specifically, hyperlocomotion and circling patterned behavior resulted in an inability to use distance travelled or rearing as a measure of behavior, the mice treated with morphine demonstrated an immense increase in movement, and in addition to this they spent very little time rearing.

We also began to investigate whether or not inhibition of Nav1.8 or MrgD fibers blocked hind limb movement decreases in distance travelled and rearing, however, we met several technical challenges that stopped these results from being completed and included in this body of work. The approach we took while doing this was by inhibiting either population of neurons for 2 minutes prior to hind limb movement, the 2 minutes during hind limb movement and then were placed into a chamber with laser activation of 2 minutes ON and 1 minute OFF for the 30-minute duration of testing. The first challenge in doing this is restraining the animal while it has a laser cord attached to its head. This occasionally resulted in abrupt disruption of the fiber implant rendering it useless, blocking our ability to successfully expose neuron populations to our 520nm laser, and inhibiting them. In the animals we did successfully expose to our laser paradigm we did not see a reversal of behaviors. This could be the result of any number of things. A few thoughts and examples I have had are that pre-exposure to the laser may not have been long enough to inhibit or outcompete signals being generated in the periphery, or that unavoidable complications persist with our approach to having the mice attached to the laser source. The implementation of wireless optogenetics may allow for a path around some of these potential complications.

4.4. Future Directions

Complexities of the fiber implant surgery, timing of CIBP with the health of the mice, and mouse colony challenges stopped us from investigating whether transient inhibition of MrgD fibers blocks tactile hypersensitivity. It will be interesting to investigate this when the MrgD-ArchT colony of mice is reestablished. If reversal of tactile hypersensitivity is observed it would emphasize a role of the MrgD (non-peptidergic) fibers in transducing mechanical modality of nociception.

Investigating GABAergic signaling in the lumbar spinal cord in BTP. Current work in the laboratory is investigating the role for GABAergic signaling in the lumbar spinal cord both utilizing pharmacological and optogenetic interventions. This direction follows the observation that lidocaine before hind limb movement blocks BTP while, lidocaine post hind limb movement fails to do so. This dichotomy raises interesting questions about what may be occurring at the level of the spinal cord or supraspinal in terms of maintaining the experience of BTP. It would also be interesting to investigate the role the rACC or RVM may be playing in maintaining the unpleasant affective component of hind limb induced BTP.

Immunohistochemical Analysis of Tissues. Current work in the lab is investigating of the effects cancer-induced bone remodeling and pain has on peripheral nerves in the bone and periosteum, as well as sensory nerve terminals in the spinal cord dorsal horn. We are currently performing a number of comparisons between naïve, sham treated and cancer treated animals.

The first investigation we are performing is to identify whether Nav1.8 or MrgD fibers are undergoing sprouting in the bone or periosteum. Although several publications have already investigated fiber sprouting in the bone, we have collected bones from animals that expressed tdTomato in either Nav1.8 expressing or MrgD expressing cells, with the goal of identifying their

location in the bone, and what changes they may undergo during cancer. We expect to see pathological sprouting of Nav1.8 fibers in animals that have tumor growth within their bones, while observing relatively normal morphology of fiber endings in naïve and sham treated animals. This would replicate previous work by Pat Mantyh as the Nav1.8 fibers should contain peptidergic fibers that have been extensively demonstrated to undergo pathological growth in the presence of cancer. Given our results that demonstrated CPP to inhibition of MrgD fibers, we aren't sure if we will see MrgD-tdtomato fibers undergo pathological sprouting into the bone. Presumably based on the literature, there will be no MrgD-tdtomato fibers in the bone or periosteum of naïve or sham animals. Despite results published in the mouse, there is always the slight possibility that different cancer lines and different strains of mice respond differently to this procedure. Most of the previous work in mice has been with immunocompromised mice, C3H mice or BalbC strains of mice, and different cell lines than the LLC line we used.

Secondly we are investigating the correlation between ATF3 expression and fiber subtypes in L2 and L4 DRG in naïve, sham and cancer treated animals. Previous reports by Peters et al. 2005 and King et. Al 2007 demonstrated increased ATF3 expression in cancer bearing animals to differing degrees. We would like to understand if ATF3 expression occurs to a higher degree in Nav1.8+ cells than Nav1.8- negative cells, or if ATF3 is induced evenly amongst different cell types. If ATF3 is selectively, or at least correlated to be expressed more so in Nav1.8 cells, it might mean that nerve injury may be driving some degree of neuropathic pain in this model. We ask the same question in MrgD expressing cells. ATF3 expression in MrgD-tdtomato+ cells may mean that cancer-induced bone remodeling or pain is somehow causing nerve damage to this cell population that has classically been demonstrated to innervate the skin.

4.5 Concluding Remarks

In conclusion, this body of work contains novel implications of the role of subpopulations of sensory neurons contributing to cancer-induced bone pain. Additionally this body of work contributes to the body of work emphasizing the heterogeneity, and therefore difficulty of uncovering critical mechanisms driving cancer-induced bone pain. Work here also supports the differential roles of subpopulations of sensory fibers, and demonstrates a unique role for the non-peptidergic, specifically MrgD expressing, fibers in transducing cancer-induced bone pain. Future work involving the study of cancer-induced bone pain should not discount and continue to study the potentially critical role that MrgD expressing fibers may be playing in cancer-induced bone pain, as work in the field has and likely currently is being done. It is my hope that these novel findings contribute to the future work and discovery of more optimal treatments for those who are unfortunate enough to suffer from cancer pain, and cancer-induced bone pain.

BIBLIOGRAPHY

- Abraira, V. E. and D. D. Ginty (2013). "The Sensory Neurons of Touch." Neuron **79**(4): 10.1016/j.neuron.2013.1007.1051.
- Abraira, V. E., E. D. Kuehn, A. M. Chirila, M. W. Springel, A. A. Toliver, A. L. Zimmerman, L. L. Orefice, K. A. Boyle, L. Bai, B. J. Song, K. A. Bashista, T. G. O'Neill, J. Zhuo, C. Tsan, J. Hoynoski, M. Rutlin, L. Kus, V. Niederkofler, M. Watanabe, S. M. Dymecki, S. B. Nelson, N. Heintz, D. I. Hughes and D. D. Ginty (2017). "The Cellular and Synaptic Architecture of the Mechanosensory Dorsal Horn." Cell **168**(1-2): 295-310 e219.
- Akkiraju, H., J. Bonor and A. Nohe (2016). "An Improved Immunostaining and Imaging Methodology to Determine Cell and Protein Distributions within the Bone Environment." J Histochem Cytochem **64**(3): 168-178.
- Akopian, A. N., V. Souslova, S. England, K. Okuse, N. Ogata, J. Ure, A. Smith, B. J. Kerr, S. B. McMahon, S. Boyce, R. Hill, L. C. Stanfa, A. H. Dickenson and J. N. Wood (1999). "The tetrodotoxin-resistant sodium channel SNS has a specialized function in pain pathways." Nat Neurosci **2**(6): 541-548.
- Alliston, T., C. J. Hernandez, D. M. Findlay, D. T. Felson and O. D. Kennedy (2017). "Bone Marrow Lesions in Osteoarthritis: What Lies Beneath." J Orthop Res.
- Aoki, Y., S. Ohtori, K. Takahashi, H. Ino, H. Douya, T. Ozawa, T. Saito and H. Moriya (2005). "Expression and co-expression of VR1, CGRP, and IB4-binding glycoprotein in dorsal root ganglion neurons in rats: differences between the disc afferents and the cutaneous afferents." Spine (Phila Pa 1976) **30**(13): 1496-1500.
- Apkarian, A. V., Y. Sosa, B. R. Krauss, P. S. Thomas, B. E. Fredrickson, R. E. Levy, R. N. Harden and D. R. Chialvo (2004). "Chronic pain patients are impaired on an emotional decision-making task." Pain **108**(1-2): 129-136.
- Arendt-Nielsen, L., L. L. Egsgaard, K. K. Petersen, T. N. Eskehave, T. Graven-Nielsen, H. C. Hoeck and O. Simonsen (2015). "A mechanism-based pain sensitivity index to characterize knee osteoarthritis patients with different disease stages and pain levels." Eur J Pain **19**(10): 1406-1417.
- Bajic, D., M. M. Craig, C. R. L. Mongerson, D. Borsook and L. Becerra (2017). "Identifying Rodent Resting-State Brain Networks with Independent Component Analysis." Front Neurosci **11**: 685.

Bannister, K., C. Qu, E. Navratilova, J. Oyarzo, J. Y. Xie, T. King, A. H. Dickenson and F. Porreca (2017). "Multiple sites and actions of gabapentin-induced relief of ongoing experimental neuropathic pain." Pain **158**(12): 2386-2395.

Bao, L. (2015). "Trafficking regulates the subcellular distribution of voltage-gated sodium channels in primary sensory neurons." Mol Pain **11**: 61.

Barabas, M. E., E. A. Kossyeva and C. L. Stucky (2012). "TRPA1 is functionally expressed primarily by IB4-binding, non-peptidergic mouse and rat sensory neurons." PLoS One **7**(10): e47988.

Basbaum, A. I., D. M. Bautista, G. Scherrer and D. Julius (2009). "Cellular and molecular mechanisms of pain." Cell **139**(2): 267-284.

Beaudry, H., I. Daou, A. R. Ase, A. Ribeiro-da-Silva and P. Seguela (2017). "Distinct behavioral responses evoked by selective optogenetic stimulation of the major TRPV1+ and MrgD+ subsets of C-fibers." Pain **158**(12): 2329-2339.

Beggs, S. and M. W. Salter (2013). "The known knowns of microglia-neuronal signalling in neuropathic pain." Neurosci Lett **557 Pt A**: 37-42.

Bennett, G. J. and Y. K. Xie (1988). "A peripheral mononeuropathy in rat that produces disorders of pain sensation like those seen in man." Pain **33**(1): 87-107.

Bennett, M. I. (2010). "Cancer pain terminology: time to develop a taxonomy that promotes good clinical practice and allows research to progress." Pain **149**(3): 426-427.

Bloom, A. P., J. M. Jimenez-Andrade, R. N. Taylor, G. Castaneda-Corral, M. J. Kaczmarek, K. T. Freeman, K. A. Coughlin, J. R. Ghilardi, M. A. Kuskowski and P. W. Mantyh (2011). "Breast cancer-induced bone remodeling, skeletal pain, and sprouting of sensory nerve fibers." J Pain **12**(6): 698-711.

Bonin, R. P., F. Wang, M. Desrochers-Couture, A. Ga Secka, M. E. Boulanger, D. C. Cote and Y. De Koninck (2016). "Epidural optogenetics for controlled analgesia." Mol Pain **12**.

Borsook, D., R. Hargreaves and L. Becerra (2011). "Can Functional Magnetic Resonance Imaging Improve Success Rates in CNS Drug Discovery?" Expert Opin Drug Discov **6**(6): 597-617.

Bourane, S., B. Duan, S. C. Koch, A. Dalet, O. Britz, L. Garcia-Campmany, E. Kim, L. Cheng, A. Ghosh, Q. Ma and M. Goulding (2015). "Gate control of mechanical itch by a subpopulation of spinal cord interneurons." Science **350**(6260): 550-554.

Braun, T. and G. Schett (2012). "Pathways for bone loss in inflammatory disease." Curr Osteoporos Rep **10**(2): 101-108.

Braz, J. M., M. A. Nassar, J. N. Wood and A. I. Basbaum (2005). "Parallel "pain" pathways arise from subpopulations of primary afferent nociceptor." Neuron **47**(6): 787-793.

Breivik, H., N. Cherny, B. Collett, F. de Conno, M. Filbet, A. J. Foubert, R. Cohen and L. Dow (2009). "Cancer-related pain: a pan-European survey of prevalence, treatment, and patient attitudes." Ann Oncol **20**(8): 1420-1433.

Brown, D. C., K. Agnello and M. J. Iadarola (2015). "Intrathecal resiniferatoxin in a dog model: efficacy in bone cancer pain." Pain **156**(6): 1018-1024.

Browne, L. E., A. Latremoliere, B. P. Lehnert, A. Grantham, C. Ward, C. Alexandre, M. Costigan, F. Michoud, D. P. Roberson, D. D. Ginty and C. J. Woolf (2017). "Time-Resolved Fast Mammalian Behavior Reveals the Complexity of Protective Pain Responses." Cell Rep **20**(1): 89-98.

Bruera, E. and J. A. Paice (2015). "Cancer pain management: safe and effective use of opioids." Am Soc Clin Oncol Educ Book: e593-599.

Burgess, S. E., L. R. Gardell, M. H. Ossipov, T. P. Malan, Jr., T. W. Vanderah, J. Lai and F. Porreca (2002). "Time-dependent descending facilitation from the rostral ventromedial medulla maintains, but does not initiate, neuropathic pain." J Neurosci **22**(12): 5129-5136.

Castaneda-Corral, G., J. M. Jimenez-Andrade, A. P. Bloom, R. N. Taylor, W. G. Mantyh, M. J. Kaczmarek, J. R. Ghilardi and P. W. Mantyh (2011). "The majority of myelinated and unmyelinated sensory nerve fibers that innervate bone express the tropomyosin receptor kinase A." Neuroscience **178**: 196-207.

Cavanaugh, D. J., H. Lee, L. Lo, S. D. Shields, M. J. Zylka, A. I. Basbaum and D. J. Anderson (2009). "Distinct subsets of unmyelinated primary sensory fibers mediate behavioral responses to noxious thermal and mechanical stimuli." Proc Natl Acad Sci U S A **106**(22): 9075-9080.

Chang, D. S., E. Hsu, D. G. Hottinger and S. P. Cohen (2016). "Anti-nerve growth factor in pain management: current evidence." J Pain Res **9**: 373-383.

Chaplan, S. R., F. W. Bach, J. W. Pogrel, J. M. Chung and T. L. Yaksh (1994). "Quantitative assessment of tactile allodynia in the rat paw." J Neurosci Methods **53**(1): 55-63.

Chartier, S. R., M. L. Thompson, G. Longo, M. N. Fealk, L. A. Majuta and P. W. Mantyh (2014). "Exuberant sprouting of sensory and sympathetic nerve fibers in nonhealed bone fractures and the generation and maintenance of chronic skeletal pain." Pain **155**(11): 2323-2336.

Clark, A. K., E. A. Old and M. Malcangio (2013). "Neuropathic pain and cytokines: current perspectives." J Pain Res **6**: 803-814.

Clohisy, D. R., C. M. Ogilvie, R. J. Carpenter and M. L. Ramnaraine (1996). "Localized, tumor-associated osteolysis involves the recruitment and activation of osteoclasts." J Orthop Res **14**(1): 2-6.

Clohisy, D. R., C. M. Ogilvie and M. L. Ramnaraine (1995). "Tumor osteolysis in osteopetrotic mice." J Orthop Res **13**(6): 892-897.

Clohisy, D. R., D. Palkert, M. L. Ramnaraine, I. Pekurovsky and M. J. Oursler (1996). "Human breast cancer induces osteoclast activation and increases the number of osteoclasts at sites of tumor osteolysis." J Orthop Res **14**(3): 396-402.

Clohisy, D. R. and M. L. Ramnaraine (1998). "Osteoclasts are required for bone tumors to grow and destroy bone." J Orthop Res **16**(6): 660-666.

Clohisy, D. R., M. L. Ramnaraine, S. Scully, M. Qi, G. Van, H. L. Tan and D. L. Lacey (2000). "Osteoprotegerin inhibits tumor-induced osteoclastogenesis and bone tumor growth in osteopetrotic mice." J Orthop Res **18**(6): 967-976.

Coggeshall, R. E., K. A. Hong, L. A. Langford, H. G. Schaible and R. F. Schmidt (1983). "Discharge characteristics of fine medial articular afferents at rest and during passive movements of inflamed knee joints." Brain Res **272**(1): 185-188.

Coleman, R. E. (2006). "Clinical features of metastatic bone disease and risk of skeletal morbidity." Clin Cancer Res **12**(20 Pt 2): 6243s-6249s.

Coleman, R. E. (2008). "Risks and benefits of bisphosphonates." Br J Cancer **98**(11): 1736-1740.

Colon, E., E. A. Bittner, B. Kussman, M. E. McCann, S. Soriano and D. Borsook (2017). "Anesthesia, brain changes, and behavior: Insights from neural systems biology." Prog Neurobiol **153**: 121-160.

Cook, A. D., A. D. Christensen, D. Tewari, S. B. McMahon and J. A. Hamilton (2018). "Immune Cytokines and Their Receptors in Inflammatory Pain." Trends Immunol **39**(3): 240-255.

Copits, B. A., M. Y. Pullen and R. W. t. Gereau (2016). "Spotlight on pain: optogenetic approaches for interrogating somatosensory circuits." Pain **157**(11): 2424-2433.

Coull, J. A., S. Beggs, D. Boudreau, D. Boivin, M. Tsuda, K. Inoue, C. Gravel, M. W. Salter and Y. De Koninck (2005). "BDNF from microglia causes the shift in neuronal anion gradient underlying neuropathic pain." Nature **438**(7070): 1017-1021.

Cowie, A. M., F. Moehring, C. O'Hara and C. L. Stucky (2018). "Optogenetic Inhibition of CGRPalpha Sensory Neurons Reveals Their Distinct Roles in Neuropathic and Incisional Pain." J Neurosci **38**(25): 5807-5825.

Csont, T., E. Berezki, P. Bencsik, G. Fodor, A. Gorbe, A. Zvara, C. Csonka, L. G. Puskas, M. Santha and P. Ferdinandy (2007). "Hypercholesterolemia increases myocardial oxidative and nitrosative stress thereby leading to cardiac dysfunction in apoB-100 transgenic mice." Cardiovasc Res **76**(1): 100-109.

Daou, I., H. Beaudry, A. R. Ase, J. S. Wieskopf, A. Ribeiro-da-Silva, J. S. Mogil and P. Seguela (2016). "Optogenetic Silencing of Nav1.8-Positive Afferents Alleviates Inflammatory and Neuropathic Pain." eNeuro **3**(1).

Daou, I., A. H. Tuttle, G. Longo, J. S. Wieskopf, R. P. Bonin, A. R. Ase, J. N. Wood, Y. De Koninck, A. Ribeiro-da-Silva, J. S. Mogil and P. Seguela (2013). "Remote optogenetic activation and sensitization of pain pathways in freely moving mice." J Neurosci **33**(47): 18631-18640.

Davis, K. D. and D. A. Seminowicz (2017). "Insights for Clinicians From Brain Imaging Studies of Pain." The Clinical Journal of Pain **33**(4): 291-294.

De Koninck, Y. (2007). "Altered chloride homeostasis in neurological disorders: a new target." Curr Opin Pharmacol **7**(1): 93-99.

Denk, F., D. L. Bennett and S. B. McMahon (2017). "Nerve Growth Factor and Pain Mechanisms." Annual Review of Neuroscience **40**(1): 307-325.

Devor, M. (2006). "Sodium channels and mechanisms of neuropathic pain." J Pain **7**(1 Suppl 1): S3-S12.

Devor, M. (2009). "Ectopic discharge in Abeta afferents as a source of neuropathic pain." Exp Brain Res **196**(1): 115-128.

Dong, X., S. Han, M. J. Zylka, M. I. Simon and D. J. Anderson (2001). "A diverse family of GPCRs expressed in specific subsets of nociceptive sensory neurons." Cell **106**(5): 619-632.

Drake, M. T., B. L. Clarke and S. Khosla (2008). "Bisphosphonates: mechanism of action and role in clinical practice." Mayo Clin Proc **83**(9): 1032-1045.

Duan, B., L. Cheng, S. Bourane, O. Britz, C. Padilla, L. Garcia-Campmany, M. Krashes, W. Knowlton, T. Velasquez, X. Ren, S. Ross, B. B. Lowell, Y. Wang, M. Goulding and Q. Ma (2014). "Identification of spinal circuits transmitting and gating mechanical pain." Cell **159**(6): 1417-1432.

Duan, B., L. Cheng and Q. Ma (2017). "Spinal Circuits Transmitting Mechanical Pain and Itch." Neurosci Bull.

Dussor, G., M. J. Zylka, D. J. Anderson and E. W. McCleskey (2008). "Cutaneous sensory neurons expressing the Mrgprd receptor sense extracellular ATP and are putative nociceptors." J Neurophysiol **99**(4): 1581-1589.

Edwards, K. A., J. J. Havelin, M. I. McIntosh, H. A. Ciccone, K. Pangilinan, I. Imbert, T. M. Largent-Milnes, T. King, T. W. Vanderah and J. M. Streicher (2018). "A Kappa Opioid Receptor Agonist Blocks Bone Cancer Pain Without Altering Bone Loss, Tumor Size, or Cancer Cell Proliferation in a Mouse Model of Cancer-Induced Bone Pain." J Pain **19**(6): 612-625.

Eid, S. R., E. D. Crown, E. L. Moore, H. A. Liang, K. C. Choong, S. Dima, D. A. Henze, S. A. Kane and M. O. Urban (2008). "HC-030031, a TRPA1 selective antagonist, attenuates inflammatory- and neuropathy-induced mechanical hypersensitivity." Mol Pain **4**: 48.

Eitner, A., G. O. Hofmann and H. G. Schaible (2017). "Mechanisms of Osteoarthritic Pain. Studies in Humans and Experimental Models." Front Mol Neurosci **10**: 349.

Enomoto, M., P. W. Mantyh, J. Murrell, J. F. Innes and B. D. X. Lascelles (2019). "Anti-nerve growth factor monoclonal antibodies for the control of pain in dogs and cats." Vet Rec **184**(1): 23.

Falk, S., K. Bannister and A. H. Dickenson (2014). "Cancer pain physiology." Br J Pain **8**(4): 154-162.

Falk, S. and A. H. Dickenson (2014). "Pain and Nociception: Mechanisms of Cancer-Induced Bone Pain." J Clin Oncol.

Falk, S. and A. H. Dickenson (2014). "Pain and nociception: mechanisms of cancer-induced bone pain." J Clin Oncol **32**(16): 1647-1654.

Felson, D. T. (2005). "The sources of pain in knee osteoarthritis." Curr Opin Rheumatol **17**(5): 624-628.

Ferrari, L. F., D. Araldi and J. D. Levine (2015). "Distinct terminal and cell body mechanisms in the nociceptor mediate hyperalgesic priming." J Neurosci **35**(15): 6107-6116.

Fields, H. (2004). "State-dependent opioid control of pain." Nat Rev Neurosci **5**(7): 565-575.

Fields, H. L. (1999). "Pain: an unpleasant topic." Pain Suppl **6**: S61-69.

Fuseya, S., K. Yamamoto, H. Minemura, S. Yamaori, T. Kawamata and M. Kawamata (2016). "Systemic QX-314 Reduces Bone Cancer Pain through Selective Inhibition of Transient Receptor Potential Vanilloid Subfamily 1-expressing Primary Afferents in Mice." Anesthesiology **125**(1): 204-218.

Gambeta, E., C. M. Kopruszinski, R. C. Dos Reis, J. M. Zanoveli and J. G. Chichorro (2016). "Evaluation of heat hyperalgesia and anxiety like-behaviors in a rat model of orofacial cancer." Neurosci Lett **619**: 100-105.

Gambeta, E., C. M. Kopruszinski, R. C. Dos Reis, J. M. Zanoveli and J. G. Chichorro (2017). "Facial pain and anxiety-like behavior are reduced by pregabalin in a model of facial carcinoma in rats." Neuropharmacology **125**: 263-271.

Gao, Y. J. and R. R. Ji (2010). "Chemokines, neuronal-glia interactions, and central processing of neuropathic pain." Pharmacol Ther **126**(1): 56-68.

Ghilardi, J. R., K. T. Freeman, J. M. Jimenez-Andrade, W. G. Mantyh, A. P. Bloom, K. S. Bouhana, D. Trollinger, J. Winkler, P. Lee, S. W. Andrews, M. A. Kuskowski and P. W. Mantyh (2011). "Sustained blockade of neurotrophin receptors TrkA, TrkB and TrkC reduces non-malignant

skeletal pain but not the maintenance of sensory and sympathetic nerve fibers." Bone **48**(2): 389-398.

Gracely, R. H., S. A. Lynch and G. J. Bennett (1992). "Painful neuropathy: altered central processing maintained dynamically by peripheral input." Pain **51**(2): 175-194.

Gradinaru, V., F. Zhang, C. Ramakrishnan, J. Mattis, R. Prakash, I. Diester, I. Goshen, K. R. Thompson and K. Deisseroth (2010). "Molecular and cellular approaches for diversifying and extending optogenetics." Cell **141**(1): 154-165.

Grigg, P., H. G. Schaible and R. F. Schmidt (1986). "Mechanical sensitivity of group III and IV afferents from posterior articular nerve in normal and inflamed cat knee." J Neurophysiol **55**(4): 635-643.

Guedon, J. M., G. Longo, L. A. Majuta, M. L. Thomspson, M. N. Fealk and P. W. Mantyh (2016). "Dissociation between the relief of skeletal pain behaviors and skin hypersensitivity in a model of bone cancer pain." Pain **157**(6): 1239-1247.

Gul, G., M. A. Sendur, S. Aksoy, A. R. Sever and K. Altundag (2016). "A comprehensive review of denosumab for bone metastasis in patients with solid tumors." Curr Med Res Opin **32**(1): 133-145.

Halvorson, K. G., K. Kubota, M. A. Sevcik, T. H. Lindsay, J. E. Sotillo, J. R. Ghilardi, T. J. Rosol, L. Boustany, D. L. Shelton and P. W. Mantyh (2005). "A blocking antibody to nerve growth factor attenuates skeletal pain induced by prostate tumor cells growing in bone." Cancer Res **65**(20): 9426-9435.

Han, C., J. Huang and S. G. Waxman (2016). "Sodium channel Nav1.8: Emerging links to human disease." Neurology **86**(5): 473-483.

Han, X., B. Y. Chow, H. Zhou, N. C. Klapoetke, A. Chuong, R. Rajimehr, A. Yang, M. V. Baratta, J. Winkle, R. Desimone and E. S. Boyden (2011). "A high-light sensitivity optical neural silencer: development and application to optogenetic control of non-human primate cortex." Front Syst Neurosci **5**: 18.

Haugen, D. F., M. J. Hjermstad, N. Hagen, A. Caraceni and S. Kaasa (2010). "Assessment and classification of cancer breakthrough pain: a systematic literature review." Pain **149**(3): 476-482.

Havelin, J., I. Imbert, J. Cormier, J. Allen, F. Porreca and T. King (2016). "Central Sensitization and Neuropathic Features of Ongoing Pain in a Rat Model of Advanced Osteoarthritis." J Pain **17**(3): 374-382.

Havelin, J., I. Imbert, D. Sukhtankar, B. Remeniuk, I. Pelletier, J. Gentry, A. Okun, T. Tiutan, F. Porreca and T. E. King (2017). "Mediation of Movement-Induced Breakthrough Cancer Pain by IB4-Binding Nociceptors in Rats." J Neurosci **37**(20): 5111-5122.

Havelin, J. and T. King (2018). "Mechanisms Underlying Bone and Joint Pain." Curr Osteoporos Rep **16**(6): 763-771.

Hawker, G. A. and I. Stanaitis (2014). "Osteoarthritis year in review 2014: clinical." Osteoarthritis Cartilage **22**(12): 1953-1957.

Hawker, G. A., L. Stewart, M. R. French, J. Cibere, J. M. Jordan, L. March, M. Suarez-Almazor and R. Gooberman-Hill (2008). "Understanding the pain experience in hip and knee osteoarthritis--an OARSI/OMERACT initiative." Osteoarthritis Cartilage **16**(4): 415-422.

Helsby, M. A., P. M. Leader, J. R. Fenn, T. Gulsen, C. Bryant, G. Doughton, B. Sharpe, P. Whitley, C. J. Caunt, K. James, A. D. Pope, D. H. Kelly and A. D. Chalmers (2014). "CiteAb: a searchable antibody database that ranks antibodies by the number of times they have been cited." BMC Cell Biology **15**: 6-6.

Honore, P., N. M. Luger, M. A. Sabino, M. J. Schwei, S. D. Rogers, D. B. Mach, F. O'Keefe P, M. L. Ramnaraine, D. R. Clohisy and P. W. Mantyh (2000). "Osteoprotegerin blocks bone cancer-induced skeletal destruction, skeletal pain and pain-related neurochemical reorganization of the spinal cord." Nat Med **6**(5): 521-528.

Honore, P., S. D. Rogers, M. J. Schwei, J. L. Salak-Johnson, N. M. Luger, M. C. Sabino, D. R. Clohisy and P. W. Mantyh (2000). "Murine models of inflammatory, neuropathic and cancer pain each generates a unique set of neurochemical changes in the spinal cord and sensory neurons." Neuroscience **98**(3): 585-598.

Hunt, S. P. and J. Rossi (1985). "Peptide- and non-peptide-containing unmyelinated primary afferents: the parallel processing of nociceptive information." Philos Trans R Soc Lond B Biol Sci **308**(1136): 283-289.

Hwang, S. J., J. M. Oh and J. G. Valtschanoff (2005). "The majority of bladder sensory afferents to the rat lumbosacral spinal cord are both IB4- and CGRP-positive." Brain Research **1062**(1-2): 86-91.

Isensee, J., C. Wenzel, R. Buschow, R. Weissmann, A. W. Kuss and T. Hucho (2014). "Subgroup-elimination transcriptomics identifies signaling proteins that define subclasses of TRPV1-positive neurons and a novel paracrine circuit." PLoS One **9**(12): e115731.

Isono, M., T. Suzuki, K. Hosono, I. Hayashi, H. Sakagami, S. Uematsu, S. Akira, Y. A. DeClerck, H. Okamoto and M. Majima (2011). "Microsomal prostaglandin E synthase-1 enhances bone cancer growth and bone cancer-related pain behaviors in mice." Life Sci **88**(15-16): 693-700.

Ivanusic, J. J. (2007). "The evidence for the spinal segmental innervation of bone." Clin Anat **20**(8): 956-960.

Ivanusic, J. J. (2009). "Size, neurochemistry, and segmental distribution of sensory neurons innervating the rat tibia." The Journal of Comparative Neurology **517**(3): 276-283.

Ivanusic, J. J. (2017). "Molecular Mechanisms That Contribute to Bone Marrow Pain." Front Neurol **8**: 458.

Jeon, O. H., N. David, J. Campisi and J. H. Elisseeff (2018). "Senescent cells and osteoarthritis: a painful connection." J Clin Invest **128**(4): 1229-1237.

Ji, R. R., T. Berta and M. Nedergaard (2013). "Glia and pain: is chronic pain a gliopathy?" Pain **154 Suppl 1**: S10-28.

Jimenez-Andrade, J. M., A. P. Bloom, J. I. Stake, W. G. Mantyh, R. N. Taylor, K. T. Freeman, J. R. Ghilardi, M. A. Kuskowski and P. W. Mantyh (2010). "Pathological sprouting of adult nociceptors in chronic prostate cancer-induced bone pain." J Neurosci **30**(44): 14649-14656.

Jimenez-Andrade, J. M., W. G. Mantyh, A. P. Bloom, A. S. Ferng, C. P. Geffre and P. W. Mantyh (2010). "Bone cancer pain." Ann N Y Acad Sci **1198**: 173-181.

Jimenez-Andrade, J. M., W. G. Mantyh, A. P. Bloom, K. T. Freeman, J. R. Ghilardi, M. A. Kuskowski and P. W. Mantyh (2012). "The effect of aging on the density of the sensory nerve fiber innervation of bone and acute skeletal pain." Neurobiol Aging **33**(5): 921-932.

Jimenez-Andrade, J. M., W. G. Mantyh, A. P. Bloom, H. Xu, A. S. Ferng, G. Dussor, T. W. Vanderah and P. W. Mantyh (2010). "A phenotypically restricted set of primary afferent nerve fibers innervate the bone versus skin: therapeutic opportunity for treating skeletal pain." Bone **46**(2): 306-313.

Jimenez-Andrade, J. M., C. D. Martin, N. J. Koewler, K. T. Freeman, L. J. Sullivan, K. G. Halvorson, C. M. Barthold, C. M. Peters, R. J. Buus, J. R. Ghilardi, J. L. Lewis, M. A. Kuskowski and P. W. Mantyh (2007). "Nerve growth factor sequestering therapy attenuates non-malignant skeletal pain following fracture." Pain **133**(1-3): 183-196.

Joseph, E. K., X. Chen, O. Bogen and J. D. Levine (2008). "Oxaliplatin acts on IB4-positive nociceptors to induce an oxidative stress-dependent acute painful peripheral neuropathy." J Pain **9**(5): 463-472.

Kaan, T. K., P. K. Yip, S. Patel, M. Davies, F. Marchand, D. A. Cockayne, P. A. Nunn, A. H. Dickenson, A. P. Ford, Y. Zhong, M. Malcangio and S. B. McMahon (2010). "Systemic blockade of P2X3 and P2X2/3 receptors attenuates bone cancer pain behaviour in rats." Brain : a journal of neurology **133**(9): 2549-2564.

Kaan, T. K., P. K. Yip, S. Patel, M. Davies, F. Marchand, D. A. Cockayne, P. A. Nunn, A. H. Dickenson, A. P. Ford, Y. Zhong, M. Malcangio and S. B. McMahon (2010). "Systemic blockade of P2X3 and P2X2/3 receptors attenuates bone cancer pain behaviour in rats." Brain **133**(9): 2549-2564.

Kane, C. M., P. Hoskin and M. I. Bennett (2015). "Cancer induced bone pain." BMJ **350**: h315.

Kennel, K. A. and M. T. Drake (2009). "Adverse effects of bisphosphonates: implications for osteoporosis management." Mayo Clin Proc **84**(7): 632-637; quiz 638.

King, T., C. Qu, A. Okun, O. K. Melemedjian, E. K. Mandell, I. Y. Maskaykina, E. Navratilova, G. O. Dussor, S. Ghosh, T. J. Price and F. Porreca (2012). "Contribution of PKMzeta-dependent and independent amplification to components of experimental neuropathic pain." Pain **153**(6): 1263-1273.

King, T., C. Qu, A. Okun, R. Mercado, J. Ren, T. Brion, J. Lai and F. Porreca (2011). "Contribution of afferent pathways to nerve injury-induced spontaneous pain and evoked hypersensitivity." Pain **152**(9): 1997-2005.

King, T., A. Vardanyan, L. Majuta, O. Melemedjian, R. Nagle, A. E. Cress, T. W. Vanderah, J. Lai and F. Porreca (2007). "Morphine treatment accelerates sarcoma-induced bone pain, bone loss, and spontaneous fracture in a murine model of bone cancer." Pain **132**(1-2): 154-168.

King, T., L. Vera-Portocarrero, T. Gutierrez, T. W. Vanderah, G. Dussor, J. Lai, H. L. Fields and F. Porreca (2009). "Unmasking the tonic-aversive state in neuropathic pain." Nat Neurosci **12**(11): 1364-1366.

Koch, S. C., D. Acton and M. Goulding (2018). "Spinal Circuits for Touch, Pain, and Itch." Annu Rev Physiol **80**: 189-217.

Krustev, E., D. Rioux and J. J. McDougall (2015). "Mechanisms and Mediators That Drive Arthritis Pain." Curr Osteoporos Rep **13**(4): 216-224.

Kuner, R. and H. Flor (2016). "Structural plasticity and reorganisation in chronic pain." Nature Reviews Neuroscience **18**: 20.

Laedermann, C. J., M. Pertin, M. R. Suter and I. Decosterd (2014). "Voltage-gated sodium channel expression in mouse DRG after SNI leads to re-evaluation of projections of injured fibers." Mol Pain **10**: 19.

Lai, J., M. C. Luo, Q. Chen and F. Porreca (2008). "Pronociceptive actions of dynorphin via bradykinin receptors." Neurosci Lett **437**(3): 175-179.

Langford, L. A. and R. F. Schmidt (1983). "Afferent and efferent axons in the medial and posterior articular nerves of the cat." Anat Rec **206**(1): 71-78.

Latremoliere, A. and C. J. Woolf (2009). "Central sensitization: a generator of pain hypersensitivity by central neural plasticity." J Pain **10**(9): 895-926.

Lee, A., M. B. Ellman, D. Yan, J. S. Kroin, B. J. Cole, A. J. van Wijnen and H.-J. Im (2013). "A Current Review of Molecular Mechanisms Regarding Osteoarthritis and Pain." Gene **527**(2): 440-447.

Lima, D. and A. Almeida (2002). "The medullary dorsal reticular nucleus as a pronociceptive centre of the pain control system." Progress in neurobiology **66**(2): 81-108.

Link, C. L., S. J. Pulliam, P. M. Hanno, S. A. Hall, P. W. Eggers, J. W. Kusek and J. B. McKinlay (2008). "Prevalence and psychosocial correlates of symptoms suggestive of painful bladder syndrome: results from the Boston area community health survey." J Urol **180**(2): 599-606.

Liu, Q., P. Sikand, C. Ma, Z. Tang, L. Han, Z. Li, S. Sun, R. H. LaMotte and X. Dong (2012). "Mechanisms of itch evoked by beta-alanine." J Neurosci **32**(42): 14532-14537.

Liu, X. D., J. J. Yang, D. Fang, J. Cai, Y. Wan and G. G. Xing (2014). "Functional upregulation of nav1.8 sodium channels on the membrane of dorsal root Ganglia neurons contributes to the development of cancer-induced bone pain." PLoS One **9**(12): e114623.

Lowery, J. J., T. J. Raymond, D. Giuvelis, J. M. Bidlack, R. Polt and E. J. Bilsky (2011). "In vivo characterization of MMP-2200, a mixed delta/mu opioid agonist, in mice." J Pharmacol Exp Ther **336**(3): 767-778.

Lozano-Ondoua, A. N., K. E. Hanlon, A. M. Symons-Liguori, T. M. Largent-Milnes, J. J. Havelin, H. L. Ferland, 3rd, A. Chandramouli, M. Owusu-Ankomah, T. Nikolich-Zugich, A. P. Bloom, J. M. Jimenez-Andrade, T. King, F. Porreca, M. A. Nelson, P. W. Mantyh and T. W. Vanderah (2013). "Disease modification of breast cancer-induced bone remodeling by cannabinoid 2 receptor agonists." J Bone Miner Res **28**(1): 92-107.

Lozano-Ondoua, A. N., A. M. Symons-Liguori and T. W. Vanderah (2013). "Cancer-induced bone pain: Mechanisms and models." Neurosci Lett **557 Pt A**: 52-59.

Luger, N. M., P. Honore, M. A. Sabino, M. J. Schwei, S. D. Rogers, D. B. Mach, D. R. Clohisy and P. W. Mantyh (2001). "Osteoprotegerin diminishes advanced bone cancer pain." Cancer research **61**(10): 4038-4047.

Luger, N. M., M. A. Sabino, M. J. Schwei, D. B. Mach, J. D. Pomonis, C. P. Keyser, M. Rathbun, D. R. Clohisy, P. Honore, T. L. Yaksh and P. W. Mantyh (2002). "Efficacy of systemic morphine suggests a fundamental difference in the mechanisms that generate bone cancer vs inflammatory pain." Pain **99**(3): 397-406.

Ma, Q. (2010). "Labeled lines meet and talk: population coding of somatic sensations." J Clin Invest **120**(11): 3773-3778.

Mach, D. B., S. D. Rogers, M. C. Sabino, N. M. Luger, M. J. Schwei, J. D. Pomonis, C. P. Keyser, D. R. Clohisy, D. J. Adams, P. O'Leary and P. W. Mantyh (2002). "Origins of skeletal pain: sensory and sympathetic innervation of the mouse femur." Neuroscience **113**(1): 155-166.

Majuta, L. A., J. G. Guedon, S. A. T. Mitchell, M. A. Kuskowski and P. W. Mantyh (2017). "Mice with cancer-induced bone pain show a marked decline in day/night activity." Pain Rep **2**(5): e614.

Majuta, L. A., S. A. T. Mitchell, M. A. Kuskowski and P. W. Mantyh (2018). "Anti-nerve growth factor does not change physical activity in normal young or aging mice but does increase activity in mice with skeletal pain." Pain **159**(11): 2285-2295.

Mansour, A. R., M. A. Farmer, M. N. Baliki and A. V. Apkarian (2014). "Chronic pain: The role of learning and brain plasticity." Restorative neurology and neuroscience **32**(1): 129-139.

Mantyh, P. (2013). "Bone cancer pain: causes, consequences, and therapeutic opportunities." PAIN® **154**: S54-S62.

Mantyh, P. W. (2002). "A mechanism based understanding of cancer pain." Pain **96**(1-2): 1-2.

Mantyh, P. W. (2006). "Cancer pain and its impact on diagnosis, survival and quality of life." Nat Rev Neurosci **7**(10): 797-809.

Mantyh, P. W. (2014). "Bone Cancer Pain: From Mechanism to Therapy." Current opinion in supportive and palliative care **8**(2): 83-90.

Mantyh, P. W. (2014). "The neurobiology of skeletal pain." Eur J Neurosci **39**(3): 508-519.

Mantyh, P. W., D. R. Clohisy, M. Koltzenburg and S. P. Hunt (2002). "Molecular mechanisms of cancer pain." Nat Rev Cancer **2**(3): 201-209.

Mantyh, W. G., J. M. Jimenez-Andrade, J. I. Stake, A. P. Bloom, M. J. Kaczmarek, R. N. Taylor, K. T. Freeman, J. R. Ghilardi, M. A. Kuskowski and P. W. Mantyh (2010). "Blockade of nerve sprouting and neuroma formation markedly attenuates the development of late stage cancer pain." Neuroscience **171**(2): 588-598.

Mapplebeck, J. C., S. Beggs and M. W. Salter (2016). "Sex differences in pain: a tale of two immune cells." Pain **157 Suppl 1**: S2-6.

McCaffrey, G., M. L. Thompson, L. Majuta, M. N. Fealk, S. Chartier, G. Longo and P. W. Mantyh (2014). "NGF blockade at early times during bone cancer development attenuates bone destruction and increases limb use." Cancer Res **74**(23): 7014-7023.

Medhurst, S. J., K. Walker, M. Bowes, B. L. Kidd, M. Glatt, M. Muller, M. Hattenberger, J. Vaxelaire, T. O'Reilly, G. Wotherspoon, J. Winter, J. Green and L. Urban (2002). "A rat model of bone cancer pain." Pain **96**(1-2): 129-140.

Mercadante, S. (2011). "Managing Breakthrough Pain." Current pain and headache reports.

Mercadante, S. (2012). "Pharmacotherapy for breakthrough cancer pain." Drugs **72**(2): 181-190.

Mercadante, S. (2015). "Breakthrough pain in cancer patients: prevalence, mechanisms and treatment options." Curr Opin Anaesthesiol **28**(5): 559-564.

Mercadante, S. (2018). "Non pharmacological interventions and non-fentanyl pharmacological treatments for breakthrough cancer pain: A systematic and critical review." Crit Rev Oncol Hematol **122**: 60-63.

Mercadante, S. and E. Bruera (2016). "Opioid switching in cancer pain: From the beginning to nowadays." Crit Rev Oncol Hematol **99**: 241-248.

Molliver, D. C., M. J. Radeke, S. C. Feinstein and W. D. Snider (1995). "Presence or absence of TrkA protein distinguishes subsets of small sensory neurons with unique cytochemical characteristics and dorsal horn projections." J Comp Neurol **361**(3): 404-416.

Molliver, D. C. and W. D. Snider (1997). "Nerve growth factor receptor TrkA is down-regulated during postnatal development by a subset of dorsal root ganglion neurons." J Comp Neurol **381**(4): 428-438.

Molliver, D. C., D. E. Wright, M. L. Leitner, A. S. Parsadonian, K. Doster, D. Wen, Q. Yan and W. D. Snider (1997). "IB4-binding DRG neurons switch from NGF to GDNF dependence in early postnatal life." Neuron **19**(4): 849-861.

Molliver, D. C., D. E. Wright, M. L. Leitner, A. S. Parsadonian, K. Doster, D. Wen, Q. Yan and W. D. Snider (1997). "IB4-Binding DRG Neurons Switch from NGF to GDNF Dependence in Early Postnatal Life." Neuron **19**(4): 849-861.

Morgan, M., S. Nencini, J. Thai and J. J. Ivanusic (2019). "TRPV1 activation alters the function of Adelta and C fiber sensory neurons that innervate bone." Bone **123**: 168-175.

Morrone, L. A., D. Scuteri, L. Rombola, H. Mizoguchi and G. Bagetta (2017). "Opioids Resistance in Chronic Pain Management." Curr Neuropharmacol **15**(3): 444-456.

Nam, Y., J. H. Kim, J. H. Kim, M. K. Jha, J. Y. Jung, M. G. Lee, I. S. Choi, I. S. Jang, D. G. Lim, S. H. Hwang, H. J. Cho and K. Suk (2016). "Reversible Induction of Pain Hypersensitivity following Optogenetic Stimulation of Spinal Astrocytes." Cell Rep **17**(11): 3049-3061.

Nassar, M. A., L. C. Stirling, G. Forlani, M. D. Baker, E. A. Matthews, A. H. Dickenson and J. N. Wood (2004). "Nociceptor-specific gene deletion reveals a major role for Nav1.7 (PN1) in acute and inflammatory pain." Proc Natl Acad Sci U S A **101**(34): 12706-12711.

Navratilova, E., C. W. Atcherley and F. Porreca (2015). "Brain Circuits Encoding Reward from Pain Relief." Trends Neurosci **38**(11): 741-750.

Navratilova, E., K. Morimura, J. Y. Xie, C. W. Atcherley, M. H. Ossipov and F. Porreca (2016). "Positive emotions and brain reward circuits in chronic pain." J Comp Neurol **524**(8): 1646-1652.

Navratilova, E. and F. Porreca (2014). "Reward and motivation in pain and pain relief." Nat Neurosci **17**(10): 1304-1312.

Nitta, Y., S. Kawamoto, C. Halbert, A. Iwata, A. D. Miller, J. Miyazaki and M. D. Allen (2005). "A CMV-actin-globin hybrid promoter improves adeno-associated viral vector gene expression in the arterial wall in vivo." J Gene Med **7**(10): 1348-1355.

Okun, A., M. DeFelice, N. Eyde, J. Ren, R. Mercado, T. King and F. Porreca (2011). "Transient inflammation-induced ongoing pain is driven by TRPV1 sensitive afferents." Molecular pain **7**: 4.

Okun, A., P. Liu, P. Davis, J. Ren, B. Remeniuk, T. Brion, M. H. Ossipov, J. Xie, G. O. Dussor, T. King and F. Porreca (2012). "Afferent drive elicits ongoing pain in a model of advanced osteoarthritis." Pain **153**(4): 924-933.

Olson, W., I. Abdus-Saboor, L. Cui, J. Burdge, T. Raabe, M. Ma and W. Luo (2017). "Sparse genetic tracing reveals regionally specific functional organization of mammalian nociceptors." Elife **6**.

Ossipov, M. H., D. Bian, T. P. Malan, Jr., J. Lai and F. Porreca (1999). "Lack of involvement of capsaicin-sensitive primary afferents in nerve-ligation injury induced tactile allodynia in rats." Pain **79**(2-3): 127-133.

Ossipov, M. H., G. O. Dussor and F. Porreca (2010). "Central modulation of pain." J Clin Invest **120**(11): 3779-3787.

Paice, J. A. (2018). "Cancer pain management and the opioid crisis in America: How to preserve hard-earned gains in improving the quality of cancer pain management." Cancer **124**(12): 2491-2497.

Paice, J. A. (2018). "Navigating Cancer Pain Management in the Midst of the Opioid Epidemic." Oncology (Williston Park) **32**(8): 386-390, 403.

Paice, J. A. and B. Ferrell (2011). "The management of cancer pain." CA: A Cancer Journal for Clinicians **61**(3): 157-182.

Parks, E. L., P. Y. Geha, M. N. Baliki, J. Katz, T. J. Schnitzer and A. V. Apkarian (2011). "Brain activity for chronic knee osteoarthritis: dissociating evoked pain from spontaneous pain." Eur J Pain **15**(8): 843 e841-814.

Peng, K., S. C. Steele, L. Becerra and D. Borsook (2018). "Brodmann area 10: Collating, integrating and high level processing of nociception and pain." Prog Neurobiol **161**: 1-22.

Peters, C. M., J. R. Ghilardi, C. P. Keyser, K. Kubota, T. H. Lindsay, N. M. Luger, D. B. Mach, M. J. Schwei, M. A. Sevcik and P. W. Mantyh (2005). "Tumor-induced injury of primary afferent sensory nerve fibers in bone cancer pain." Exp Neurol **193**(1): 85-100.

Porreca, F. and E. Navratilova (2017). "Reward, motivation and emotion of pain and its relief." Pain **158**(Suppl 1): S43-S49.

Portenoy, R. K. and N. A. Hagen (1989). "Breakthrough pain: definition and management." Oncology (Williston Park) **3**(8 Suppl): 25-29.

Portenoy, R. K. and N. A. Hagen (1990). "Breakthrough pain: definition, prevalence and characteristics." Pain **41**(3): 273-281.

Prescott, S. A., Q. Ma and Y. De Koninck (2014). "Normal and abnormal coding of somatosensory stimuli causing pain." Nat Neurosci **17**(2): 183-191.

Price, T. J. and C. M. Flores (2007). "Critical evaluation of the colocalization between calcitonin gene-related peptide, substance P, transient receptor potential vanilloid subfamily type 1 immunoreactivities, and isolectin B4 binding in primary afferent neurons of the rat and mouse." J Pain **8**(3): 263-272.

Pujol, J., G. Martinez-Vilavella, J. Llorente-Onaindia, B. J. Harrison, M. Lopez-Sola, M. Lopez-Ruiz, L. Blanco-Hinojo, P. Benito, J. Deus and J. Monfort (2017). "Brain imaging of pain sensitization in patients with knee osteoarthritis." Pain **158**(9): 1831-1838.

Qu, C., T. King, A. Okun, J. Lai, H. L. Fields and F. Porreca (2011). "Lesion of the rostral anterior cingulate cortex eliminates the aversiveness of spontaneous neuropathic pain following partial or complete axotomy." Pain **152**(7): 1641-1648.

Raimondo, J. V., L. Kay, T. J. Ellender and C. J. Akerman (2012). "Optogenetic silencing strategies differ in their effects on inhibitory synaptic transmission." Nat Neurosci **15**(8): 1102-1104.

Rau, K. K., S. L. McIlwrath, H. Wang, J. J. Lawson, M. P. Jankowski, M. J. Zylka, D. J. Anderson and H. R. Koerber (2009). "Mrgprd enhances excitability in specific populations of cutaneous murine polymodal nociceptors." J Neurosci **29**(26): 8612-8619.

Remeniuk, B., T. King, D. Sukhtankar, A. Nippert, N. Li, F. Li, K. Cheng, K. C. Rice and F. Porreca (2018). "Disease modifying actions of interleukin-6 blockade in a rat model of bone cancer pain." Pain **159**(4): 684-698.

Remeniuk, B., D. Sukhtankar, A. Okun, E. Navratilova, J. Y. Xie, T. King and F. Porreca (2015). "Behavioral and Neurochemical Analysis of Ongoing Bone Cancer Pain in Rats." Pain.

Remeniuk, B., D. Sukhtankar, A. Okun, E. Navratilova, J. Y. Xie, T. King and F. Porreca (2015). "Behavioral and neurochemical analysis of ongoing bone cancer pain in rats." Pain **156**(10): 1864-1873.

Rutlin, M., C. Y. Ho, V. E. Abaira, C. Cassidy, L. Bai, C. J. Woodbury and D. D. Ginty (2014). "The cellular and molecular basis of direction selectivity of Adelta-LTMRs." Cell **159**(7): 1640-1651.

Sabino, M. A., J. R. Ghilardi, J. L. Jongen, C. P. Keyser, N. M. Luger, D. B. Mach, C. M. Peters, S. D. Rogers, M. J. Schwei, C. de Felipe and P. W. Mantyh (2002). "Simultaneous reduction in cancer pain, bone destruction, and tumor growth by selective inhibition of cyclooxygenase-2." Cancer Res **62**(24): 7343-7349.

Sabino, M. A., N. M. Luger, D. B. Mach, S. D. Rogers, M. J. Schwei and P. W. Mantyh (2003). "Different tumors in bone each give rise to a distinct pattern of skeletal destruction, bone cancer-related pain behaviors and neurochemical changes in the central nervous system." Int J Cancer **104**(5): 550-558.

Sabino, M. A. and P. W. Mantyh (2005). "Pathophysiology of bone cancer pain." J Support Oncol **3**(1): 15-24.

Sabino, M. C., J. R. Ghilardi, K. J. Feia, J. L. Jongen, C. P. Keyser, N. M. Luger, D. B. Mach, C. M. Peters, S. D. Rogers, M. J. Schwei, C. De Filipe and P. W. Mantyh (2002). "The involvement of prostaglandins in tumorigenesis, tumor-induced osteolysis and bone cancer pain." J Musculoskelet Neuronal Interact **2**(6): 561-562.

Sang, C. N., R. H. Gracely, M. B. Max and G. J. Bennett (1996). "Capsaicin-evoked mechanical allodynia and hyperalgesia cross nerve territories. Evidence for a central mechanism." Anesthesiology **85**(3): 491-496.

Scarpi, E., D. Calistri, P. Klepstad, S. Kaasa, F. Skorpen, R. Habberstad, O. Nanni, D. Amadori and M. Maltoni (2014). "Clinical and genetic factors related to cancer-induced bone pain and bone pain relief." Oncologist **19**(12): 1276-1283.

Schaible, H. G. (2018). "Osteoarthritis pain. Recent advances and controversies." Curr Opin Support Palliat Care.

Schaible, H. G. and R. F. Schmidt (1983). "Activation of groups III and IV sensory units in medial articular nerve by local mechanical stimulation of knee joint." Journal of Neurophysiology **49**(1): 35-44.

Schaible, H. G. and R. F. Schmidt (1983). "Responses of fine medial articular nerve afferents to passive movements of knee joints." Journal of Neurophysiology **49**(5): 1118-1126.

Schaible, H. G. and R. F. Schmidt (1985). "Effects of an experimental arthritis on the sensory properties of fine articular afferent units." Journal of Neurophysiology **54**(5): 1109-1122.

Schaible, H. G., R. F. Schmidt and W. D. Willis (1987). "Enhancement of the responses of ascending tract cells in the cat spinal cord by acute inflammation of the knee joint." Exp Brain Res **66**(3): 489-499.

Scherrer, G., N. Imamachi, Y. Q. Cao, C. Contet, F. Mennicken, D. O'Donnell, B. L. Kieffer and A. I. Basbaum (2009). "Dissociation of the opioid receptor mechanisms that control mechanical and heat pain." Cell **137**(6): 1148-1159.

Schindelin, J., I. Arganda-Carreras, E. Frise, V. Kaynig, M. Longair, T. Pietzsch, S. Preibisch, C. Rueden, S. Saalfeld, B. Schmid, J. Y. Tinevez, D. J. White, V. Hartenstein, K. Eliceiri, P. Tomancak and A. Cardona (2012). "Fiji: an open-source platform for biological-image analysis." Nat Methods **9**(7): 676-682.

Schmidt, B. L. (2015). "The Neurobiology of Cancer Pain." J Oral Maxillofac Surg **73**(12 Suppl): S132-135.

Schwei, M. J., P. Honore, S. D. Rogers, J. L. Salak-Johnson, M. P. Finke, M. L. Ramnaraine, D. R. Clohisy and P. W. Mantyh (1999). "Neurochemical and cellular reorganization of the spinal cord in a murine model of bone cancer pain." J Neurosci **19**(24): 10886-10897.

Sevcik, M. A., N. M. Luger, D. B. Mach, M. A. Sabino, C. M. Peters, J. R. Ghilardi, M. J. Schwei, H. Rohrich, C. De Felipe, M. A. Kuskowski and P. W. Mantyh (2004). "Bone cancer pain: the effects

of the bisphosphonate alendronate on pain, skeletal remodeling, tumor growth and tumor necrosis." Pain **111**(1-2): 169-180.

Shields, S. D., H. S. Ahn, Y. Yang, C. Han, R. P. Seal, J. N. Wood, S. G. Waxman and S. D. Dib-Hajj (2012). "Nav1.8 expression is not restricted to nociceptors in mouse peripheral nervous system." Pain **153**(10): 2017-2030.

Shiers, S., G. Pradhan, J. Mwirigi, G. Mejia, A. Ahmad, S. Kroener and T. Price (2018). "Neuropathic Pain Creates an Enduring Prefrontal Cortex Dysfunction Corrected by the Type II Diabetic Drug Metformin But Not by Gabapentin." J Neurosci **38**(33): 7337-7350.

Shinohara, T., M. Harada, K. Ogi, M. Maruyama, R. Fujii, H. Tanaka, S. Fukusumi, H. Komatsu, M. Hosoya, Y. Noguchi, T. Watanabe, T. Moriya, Y. Itoh and S. Hinuma (2004). "Identification of a G protein-coupled receptor specifically responsive to beta-alanine." J Biol Chem **279**(22): 23559-23564.

Smith, A., M. López-Solà, K. McMahon, A. Pedler and M. Sterling (2017). "Multivariate pattern analysis utilizing structural or functional MRI in individuals with musculoskeletal pain and healthy controls: A systematic review." Seminars in Arthritis and Rheumatism **47**(3): 418-431.

Smith, T. J. and C. B. Saiki (2015). "Cancer Pain Management." Mayo Clin Proc **90**(10): 1428-1439.

Snider, W. D. and S. B. McMahon (1998). "Tackling Pain at the Source: New Ideas about Nociceptors." Neuron **20**(4): 629-632.

Sopata, M., N. Katz, W. Carey, M. D. Smith, D. Keller, K. M. Verburg, C. R. West, G. Wolfram and M. T. Brown (2015). "Efficacy and safety of tanezumab in the treatment of pain from bone metastases." Pain **156**(9): 1703-1713.

Sousa, A. M., J. de Santana Neto, G. M. Guimaraes, G. M. Cascudo, J. O. Neto and H. A. Ashmawi (2014). "Safety profile of intravenous patient-controlled analgesia for breakthrough pain in cancer patients: a case series study." Support Care Cancer **22**(3): 795-801.

Steger, G. G. and R. Bartsch (2011). "Denosumab for the treatment of bone metastases in breast cancer: evidence and opinion." Ther Adv Med Oncol **3**(5): 233-243.

Stucky, C. L. and G. R. Lewin (1999). "Isolectin B(4)-positive and -negative nociceptors are functionally distinct." J Neurosci **19**(15): 6497-6505.

Sukhtankar, D., A. Okun, A. Chandramouli, M. A. Nelson, T. W. Vanderah, A. E. Cress, F. Porreca and T. King (2011). "Inhibition of p38-MAPK signaling pathway attenuates breast cancer induced bone pain and disease progression in a murine model of cancer-induced bone pain." Mol Pain **7**: 81.

Suzuki, M., M. Millecamps, S. Ohtori, C. Mori and L. S. Stone (2018). "Anti-nerve growth factor therapy attenuates cutaneous hypersensitivity and musculoskeletal discomfort in mice with osteoporosis." Pain Rep **3**(3): e652.

Suzuki, R., W. Rahman, S. P. Hunt and A. H. Dickenson (2004). "Descending facilitatory control of mechanically evoked responses is enhanced in deep dorsal horn neurones following peripheral nerve injury." Brain Res **1019**(1-2): 68-76.

Syx, D., P. B. Tran, R. E. Miller and A. M. Malfait (2018). "Peripheral Mechanisms Contributing to Osteoarthritis Pain." Curr Rheumatol Rep **20**(2): 9.

Tetreault, P., A. Mansour, E. Vachon-Presseau, T. J. Schnitzer, A. V. Apkarian and M. N. Baliki (2016). "Brain Connectivity Predicts Placebo Response across Chronic Pain Clinical Trials." PLoS Biol **14**(10): e1002570.

Thakur, M., A. H. Dickenson and R. Baron (2014). "Osteoarthritis pain: nociceptive or neuropathic?" Nat Rev Rheumatol **10**(6): 374-380.

Thakur, M., W. Rahman, C. Hobbs, A. H. Dickenson and D. L. Bennett (2012). "Characterisation of a peripheral neuropathic component of the rat monoiodoacetate model of osteoarthritis." PLoS One **7**(3): e33730.

Todd, A. J. (2017). "Identifying functional populations among the interneurons in laminae I-III of the spinal dorsal horn." Mol Pain **13**: 1744806917693003.

Towne, C., M. Pertin, A. T. Beggah, P. Aebischer and I. Decosterd (2009). "Recombinant adeno-associated virus serotype 6 (rAAV2/6)-mediated gene transfer to nociceptive neurons through different routes of delivery." Mol Pain **5**: 52.

Tracey, I. (2017). "Neuroimaging mechanisms in pain: from discovery to translation." Pain **158 Suppl 1**: S115-S122.

Tran, P. B., R. E. Miller, S. Ishihara, R. J. Miller and A. M. Malfait (2017). "Spinal microglial activation in a murine surgical model of knee osteoarthritis." Osteoarthritis Cartilage **25**(5): 718-726.

Trang, T., S. Beggs and M. W. Salter (2011). "Brain-derived neurotrophic factor from microglia: a molecular substrate for neuropathic pain." Neuron Glia Biol **7**(1): 99-108.

Uhelski, M. L., D. J. Bruce, P. Seguela, G. L. Wilcox and D. A. Simone (2017). "In vivo optogenetic activation of Nav1.8(+) cutaneous nociceptors and their responses to natural stimuli." J Neurophysiol **117**(6): 2218-2223.

Urch, C. E., T. Donovan-Rodriguez and A. H. Dickenson (2003). "Alterations in dorsal horn neurones in a rat model of cancer-induced bone pain." Pain **106**(3): 347-356.

Urch, C. E., T. Donovan-Rodriguez, R. Gordon-Williams, L. A. Bee and A. H. Dickenson (2005). "Efficacy of chronic morphine in a rat model of cancer-induced bone pain: behavior and in dorsal horn pathophysiology." J Pain **6**(12): 837-845.

Usoskin, D., A. Furlan, S. Islam, H. Abdo, P. Lonnerberg, D. Lou, J. Hjerling-Leffler, J. Haeggstrom, O. Kharchenko, P. V. Kharchenko, S. Linnarsson and P. Ernfors (2015). "Unbiased classification of sensory neuron types by large-scale single-cell RNA sequencing." Nat Neurosci **18**(1): 145-153.

Vulchanova, L., T. H. Olson, L. S. Stone, M. S. Riedl, R. Elde and C. N. Honda (2001). "Cytotoxic targeting of isolectin IB4-binding sensory neurons." Neuroscience **108**(1): 143-155.

Wacnik, P. W., L. J. Kehl, T. M. Trempe, M. L. Ramnaraine, A. J. Beitz and G. L. Wilcox (2003). "Tumor implantation in mouse humerus evokes movement-related hyperalgesia exceeding that evoked by intramuscular carrageenan." Pain **101**(1-2): 175-186.

Wang, H. and M. J. Zylka (2009). "Mrgprd-expressing polymodal nociceptive neurons innervate most known classes of substantia gelatinosa neurons." The Journal of neuroscience : the official journal of the Society for Neuroscience **29**(42): 13202-13209.

Wang, T., D. C. Molliver, X. Jing, E. S. Schwartz, F. C. Yang, O. A. Samad, Q. Ma and B. M. Davis (2011). "Phenotypic switching of nonpeptidergic cutaneous sensory neurons following peripheral nerve injury." PLoS One **6**(12): e28908.

Woller, S. A., K. A. Eddinger, M. Corr and T. L. Yaksh (2018). "An overview of pathways encoding nociception." Clin Exp Rheumatol **36**(1): 172.

Woolf, C. J. (2011). "Central sensitization: implications for the diagnosis and treatment of pain." Pain **152**(3 Suppl): S2-15.

Wu, J. X., M. Y. Xu, X. R. Miao, Z. J. Lu, X. M. Yuan, X. Q. Li and W. F. Yu (2012). "Functional up-regulation of P2X3 receptors in dorsal root ganglion in a rat model of bone cancer pain." Eur J Pain **16**(10): 1378-1388.

Xie, Y. F., J. Wang and R. P. Bonin (2018). "Optogenetic exploration and modulation of pain processing." Exp Neurol **306**: 117-121.

Xu, L., L. N. Nwosu, J. J. Burston, P. J. Millns, D. R. Sagar, P. I. Mapp, P. Meesawatsom, L. Li, A. J. Bennett, D. A. Walsh and V. Chapman (2016). "The anti-NGF antibody muMab 911 both prevents and reverses pain behaviour and subchondral osteoclast numbers in a rat model of osteoarthritis pain." Osteoarthritis Cartilage **24**(9): 1587-1595.

Yaksh, T. L., D. H. Farb, S. E. Leeman and T. M. Jessell (1979). "Intrathecal capsaicin depletes substance P in the rat spinal cord and produces prolonged thermal analgesia." Science **206**(4417): 481-483.

Yaksh, T. L. and T. A. Rudy (1976). "Chronic catheterization of the spinal subarachnoid space." Physiol Behav **17**(6): 1031-1036.

Yanagisawa, Y., H. Furue, T. Kawamata, D. Uta, J. Yamamoto, S. Furuse, T. Katafuchi, K. Imoto, Y. Iwamoto and M. Yoshimura (2010). "Bone cancer induces a unique central sensitization through synaptic changes in a wide area of the spinal cord." Mol Pain **6**: 38.

Ye, Y., S. S. Bae, C. T. Viet, S. Troob, D. Bernabe and B. L. Schmidt (2014). "IB4(+) and TRPV1(+) sensory neurons mediate pain but not proliferation in a mouse model of squamous cell carcinoma." Behav Brain Funct **10**: 5.

Ye, Y., D. Dang, C. T. Viet, J. C. Dolan and B. L. Schmidt (2012). "Analgesia Targeting IB4-Positive Neurons in Cancer-Induced Mechanical Hypersensitivity." The Journal of Pain **13**(6): 524-531.

Zhang, L., N. Taylor, Y. Xie, R. Ford, J. Johnson, J. E. Paulsen and B. Bates (2005). "Cloning and expression of MRG receptors in macaque, mouse, and human." Brain Res Mol Brain Res **133**(2): 187-197.

Zhou, Y. Q., Z. Liu, H. Q. Liu, D. Q. Liu, S. P. Chen, D. W. Ye and Y. K. Tian (2016). "Targeting glia for bone cancer pain." Expert Opin Ther Targets **20**(11): 1365-1374.

Zimmerman, A., L. Bai and D. D. Ginty (2014). "The gentle touch receptors of mammalian skin." Science **346**(6212): 950-954.

Zylka, M. J., X. Dong, A. L. Southwell and D. J. Anderson (2003). "Atypical expansion in mice of the sensory neuron-specific Mrg G protein-coupled receptor family." Proc Natl Acad Sci U S A **100**(17): 10043-10048.

Zylka, M. J., F. L. Rice and D. J. Anderson (2005). "Topographically distinct epidermal nociceptive circuits revealed by axonal tracers targeted to Mrgprd." Neuron **45**(1): 17-25.

BIOGRAPHY OF THE AUTHOR

Joshua Havelin was born in Geneva, New York on December 31, 1988. He was raised in Seneca Falls, New York and graduated from Mynderse Academy in 2007. Joshua attended the University of New England in Biddeford, Maine and completed his Honors Thesis in the lab of Dr. Edward Bilsky investigating the effects of a mixed mu/delta opioid receptor agonist in a rat model of isovolumetric overactive bladder. In May 2011 he graduated cum laude receiving a Bachelor of Science degree in Biochemistry and Medical Biology. Joshua then built and managed two research labs at the University of New England until entering the Graduate School of Biomedical Science and Engineering at the University of Maine in 2014. Under the mentorship of Dr. Tamara King at the University of New England, he investigated the roles of subpopulations of sensory fibers in cancer-induced bone pain. Joshua has three first author publications and three supporting author publications in peer-reviewed journals; he is a member of the Society of Neuroscience, American Pain Society and the International Association for the Study of Pain. Joshua is a candidate for a Doctor of Philosophy degree in Biomedical Science from the University of Maine in August 2019.